INVESTIGATION OF CO HYDROGENATION CATALYSTS FOR DIRECT SYNTHESIS OF DIMETHYL ETHER

by

Çiğdem Ekmen

B.S., Chemical Engineering, Gazi University, 2011

Submitted to the Institute for Graduate Studies in
Science and Engineering in partial fulfillment of
the requirements for the degree of
Master of Science

Graduate Program in Chemical Engineering
Boğaziçi University
2014

INVESTIGATION OF CO HYDROGENATION CATALYSTS FOR DIRECT SYNTHESIS OF DIMETHYL ETHER

APPROVED BY:

Assoc. Prof. Ahmet Kerim Avcı (Thesis Supervisor)	....…….
Prof. Zeynep İlsen Önsan (Thesis Co-Supervisor)	……
Prof. Ayşe Nilgün Akın	.....……..
Prof. Ahmet Erhan Aksoylu	…….
Prof. Ramazan Yıldırım	…….

DATE OF APPROVAL: 13.08.2014

to my family

ACKNOWLEDGEMENTS

I would like to present my deep and sincere gratitude to my thesis supervisor Assoc. Prof. Ahmet Kerim Avcı for endless support and continuous encouragement. I also want to thank him for his understanding and kindly attitude in every aspect. I am very grateful to my co-supervisor Prof. Zeynep İlsen Önsan for her great help, motivation and suggestions not only for my research but also my future life. It was a privilege for me to work with Prof. Önsan and Assoc. Prof. Avcı.

I am very grateful to my thesis committee members, Prof. Ramazan Yıldırım, Prof. Ahmet Erhan Aksoylu and Prof. Ayşe Nilgün Akın sparing their valuable time for reading and commenting on my thesis.

I would like to present my sincere thanks to research colleague Didem Büşra Kabakçı for her support and friendship. I cannot pass without presenting my sincere thanks to Andrew Mussett of Autoclave Engineers for his great contribution during the start-up of this project.

Very special thanks to my friends Pınar Eribol, Hazal Bal and Gökçe Ezeroğlu for their everlasting help and encouragement on any matter. Their friendship is the biggest asset that I have gained in my life.

I would like to present thanks to Onur Kavaklı, Can Ekici and Sinan Koç, my lab mates in KB 404. Special thanks go to Elif Erdinç for their friendship. I was very lucky to work with CATREL team, especially Melek Selcen Başar, A. İpek Paksoy, Merve Eropak, Ali Uzun, Sezin Sezen, Çağla Odabaşı, Burcu Karagöz, Aybüke Leba, Serhat Erşahin, Emre Demirel and Özge Ertem.

Cordial thanks are for Bilgi Dedeoğlu and Yakup Bal for their technical assistance. I should also to thank Bilge Gedik Uluocak for her significant effort in SEM analyses conducted at Boğaziçi University Advanced Technologies Research and Development Center.

Heartfelt thanks goes to Ramazan Okutan for his tireless encouragement and emotional support. This thesis would not been possible without him.

Last but not least, I owe special thanks to my family. It is very difficult to express in words for all the support and encouragement they have given to me.

Boğaziçi Scientific Research Coordination is also acknowledged for the financial support with the research fund BAP-6188 (11A05S2). I would also like to acknowledge TUBITAK project 113M229, from which I got financial aid for actively working on the detailed design and construction of the reaction/analysis system, and synthesis and characterization of the catalysts used in the project.

ABSTRACT

INVESTIGATION OF CO HYDROGENATION CATALYSTS FOR DIRECT SYNTHESIS OF DIMETHYL ETHER

The aim of this work was to prepare and test bi-functional direct DME synthesis catalysts, including commercial ones, involving methanol synthesis and methanol dehydration functions. Catalyst beds were prepared by physical mixing of methanol synthesis catalysts ($Cu/ZnO/Al_2O_3$, commercial Cu–Zn based HiFUEL R120) with methanol dehydration catalysts (δ-Al_2O_3, MCM-41 type SiO_2/Al_2O_3, zeolite, phosphotungstic acid hydrate and 20wt%CeO_2/δ-Al_2O_3) except a case in which the bed was composed of only of 2wt%Pd-20wt%CeO_2/ γ-Al_2O_3, which included synthesis and dehydration functions. The Autoclave Engineers' BTRS-Jr-PC reaction system that can handle pressures up to 100 bar and temperatures up to 650 ^{0}C was used in the experiments. Parametric studies were first conducted on the bed configuration characterized by physical mixing of commercial Cu–Zn based catalyst, denoted as HiFUEL R120, with δ-Al_2O_3, methanol dehydration catalyst. The reaction temperature and pressure, feed composition, metal to acid catalyst weight ratio (=mass of methanol synthesis catalyst/mass of methanol dehydration catalyst) were the parameters used in activity and selectivity tests of this catalyst. In addition, the bi-functional catalyst prepared by physical mixing of an in-house, co-precipitated $CuO/ZnO/Al_2O_3$ catalyst, denoted as CZA, with δ-Al_2O_3 was also tested in the temperature range of 250-300 ^{0}C. Subsequent experiments were performed at 34 bar and 275 ^{0}C for a feed composition of $CO/H_2/N_2$=32/64/4. Highest DME selectivity (49.1%) was observed over the bed configuration involving the physical mixture of HiFUEL R120 with δ-Al_2O_3 catalysts operating at 34 bar and at 275 ^{0}C with a molar feed composition of $CO/H_2/N_2$=48/48/4. CZA/ δ-Al_2O_3 catalyst showed lower catalytic activity in comparison with HiFUEL R120/ δ-Al_2O_3 catalyst. Methane and CO_2 formation were observed significantly over SiO_2/Al_2O_3, zeolite, PTA and 2wt%Pd-20wt%CeO_2/ γ-Al_2O_3 catalysts. HiFUEL R120/ zeolite showed the lowest DME selectivity. The modified δ-Al_2O_3 with cerium oxide showed lower catalytic activity than unmodified one.

ÖZET

DOĞRUDAN DİMETİL ETER SENTEZİ İÇİN KARBON MONOKSİT HİDROJENASYON KATALİZÖRLERİNİN İNCELENMESİ

Bu çalışmanın amacı, iki aktif merkezli, metanol sentez ve metanol dehidrasyon fonksiyonlarını içeren, doğrudan dimetil eter sentez katalizörlerinin hazırlanması ve denenmesi olarak belirlendi. Katalizör yatakları, sentez ve dehidrasyon fonksiyonlarını içeren 2wt%Pd-20wt%CeO_2/γ-Al_2O_3 katalizörün dışında, metanol sentez katalizörleri (Cu/ZnO/Al_2O_3, ticari Cu–Zn bazlı HiFUEL R120) ile methanol dehidrasyon katalizörlerinin (γ-Al_2O_3, MCM- 41 tipi SiO_2/Al_2O_3, zeolit, fosfotungstik asit hidrat (PTA) and 20wt%CeO_2/δ-Al_2O_3) fiziksel olarak karıştırılmasıyla hazırlanmıştır. 650 ^{0}C sıcaklık ve 100 bar basıncına kadar çıkabilen Autoclave Engineers şirketinin BTRS-Jr-PC reaksiyon sistemi kullanılmıştır. Parametrik çalışmalar önce HiFUEL R120 ile δ-Al_2O_3 katalizörlerinin fiziksel karıstırılarak karakterize edilen yatak konfigürasyonu üzerinde gerçekleştirilmiştir. Bu katalizörün aktivite ve seçicilik deneylerinde kullanılan parametreler sıcaklık, basınç, besleme gazı kompozisyonu ve metal ve asit katalizörünün ağırlıkça oranı olarak seçilmiştir. Buna ek olarak, aynı anda çöktürme yöntemiyle hazırlanan CuO/ZnO/Al_2O_3 katalizörünün, δ-Al_2O_3 ile fiziksel olarak karıştırılmasıyla hazırlanan iki aktif merkezli katalizör 250 ve 300 ^{0}C sıcaklık aralığında test edilmiştir. İzleyen deneyler 34 bar basıncında, 275 ^{0}C sıcaklığında ve CO/H_2/N_2 =32/64/4 besleme gazı kompozisyonunda test edilmiştir. En yüksek DME seçiciliği (49.1%), HiFUEL R120 ile δ-Al_2O_3 katalizörlerinin fiziksel karıstırılarak hazırlanmış olan yatak konfigürasyonu üzerinde 34 bar , 275 ^{0}C ve CO/H_2/N_2 =48/48/4 besleme gazı kompozisyonunda yürütülen deneyler sonucunda elde edilmiştir. CZA/ δ-Al_2O_3 katalizörü HiFUEL R120/ δ-Al_2O_3 katalizöründen daha düşük aktivite göstermiştir. SiO_2/Al_2O_3, zeolit, PTA and 2wt%Pd-20wt%CeO_2/ γ-Al_2O_3 katalizörlerinin aktivite deneylerinde çoğunlukla metan and karbon dioksit oluşumu gözlenmiştir. En düşük DME seçiciliği HiFUEL R120/ zeolit deneylerinde saptanmıştır. Seryum oksitle ile modifiye edilmiş δ-Al_2O_3 katalizörü modifiye edilmeyen δ-Al_2O_3 katalizöründen daha düşük katalitik aktivite göstermiştir.

TABLE OF CONTENTS

ACKNOWLEDGEMENTS iv
ABSTRACT vi
ÖZET vii
LIST OF FIGURES xi
LIST OF TABLES xv
LIST OF ACRONYMS/ABBREVIATIONS xvii
1. INTRODUCTION 1
2. LITERATURE SURVEY 3
2.1. Dimethyl Ether (DME) as an Alternative Fuel and Energy Carrier 3
2.2. Catalytic Formation of Dimethyl Ether (DME) 7
2.2.1. Indirect Synthesis of Dimethyl ether 7
2.2.1.1. Catalytic Methanol Synthesis 7
2.2.1.2. Catalytic Methanol Dehydration to Dimethyl Ether 11
2.2.2. Direct Synthesis of Dimethyl Ether (The single-step DME synthesis) 15
3. EXPERIMENTAL 22
3.1. Materials 22
3.1.1. Chemicals 22
3.1.2. Gases 23
3.2. Experimental Systems 24
3.2.1. Catalyst Preparation Systems 24
3.2.1.1. Coprecipitation System 24
3.2.1.2. Impregnation System 25
3.2.2. Catalyst Characterization Systems 24
3.2.2.1. Scanning Electron Microscopy (SEM) 26
3.2.2.2. Energy Dispersive X-ray Spectroscopy (EDX). 26
3.2.3. Catalytic Reaction System 26
3.2.3.1. Reactant Preparation 30
3.2.3.2. Reactor 31
3.2.3.3. Gas Liquid Separator.. 31
3.2.3.4. Back Pressure Regulator 31

3.2.3.5. GC Sampling Valve (optional) 32
3.2.3.6. Transfer Line 32
3.2.3.7. BTRS Oven 32
3.2.4. Product Analysis System 33
3.3. Catalyst Preparation and Pretreatment 35
3.3.1. Preparation and Pretreatment of $CuO/ZnO/Al_2O_3$ 35
3.3.2. Preparation and Pretreatment of 20wt% ceria-modified δ -Al_2O_3 catalyst ... 37
3.3.3. Dry-Physical Mixing Catalysts 37
3.4. Reactor Tube Catalyst Packing 38
3.5. Catalytic Activity Experiments 39
3.5.1. Preliminary Work 39
3.5.1.1. Commissioning of the BTRS-Jr-PC Reactor System 39
3.5.1.2. Gas Chromatograph Calibration 41
3.5.2. Reaction Tests 42
4. RESULTS AND DISCUSSION. 46
4.1. Catalyst Characterization Results 46
4.2. Catalyst Activity Results 49
4.2.1. Catalytic Activity Results of HiFUEL R120/ δ-Al_2O_3 49
4.2.1.1. Effect of Temperature 49
4.2.1.2. Effect of Pressure 53
4.2.1.3. Effect of Feed Composition 56
4.2.1.4. Effect of Metal to Acid Catalyst Weight Ratio 58
4.2.2. Catalytic Activity Results of CZA/ δ-Al_2O_3 60
4.2.3. Catalytic Activity Results of HiFUEL R120 with Different Acid Catalysts . 63
4.2.3.1. HiFUEL R120-SiO_2/Al_2O_3 63
4.2.3.2. HiFUEL R120/Zeolite 64
4.2.3.3. HiFUEL R120/PTA 65
4.2.3.4. HiFUEL R120-20 wt%CeO_2/ δ-Al_2O_3 66
4.2.4. Catalytic Activity Results of 2wt%Pd-20wt%CeO_2/ γ-Al_2O_3 69
5. CONCLUSIONS AND RECOMMENDATIONS 71
5.1. Conclusions 71
5.2. Recommendations 72
APPENDIX A: SAMPLE CONVERSION AND SELECTIVITY CALCULATIONS 74

REFERENCES 77

LIST OF FIGURES

Figure 2.1.	Structure of dimethyl ether (DME). …….....	4
Figure 2.2.	DME production processes. ...……...……..	6
Figure 3.1.	Schematic diagram of co- precipitation system.	25
Figure 3.2.	Schematic diagram of the impregnation system. …….....	25
Figure 3.3.	The AE BTRS-Jr-PC System. …….....	27
Figure 3.4.	The AE BTRS-Jr-PC System inside open oven cabinet. …….....	28
Figure 3.5.	Schematic Diagram of the AE BTRS-Jr-PC. ….....	29
Figure 3.6.	Screenshot of software program used for controlling the BTRS Jr-PC. ……...	30
Figure 3.7.	GC Sampling Valve Connections. …….....	32
Figure 3.8.	Schematic diagram of preparation recipe. …….....	36
Figure 3.9.	5 ml reactor loading method. …….....	39
Figure 4.1.	HiFUEL R120 catalyst (a) SEM bright area image of freshly reduced catalyst(b) SEM bright area image of the spent catalyst for $CO/H_2/N_2$ =32/64/4, 34 bar, 275 ^{0}C (c) Cu-Zn-Al-O mapping of freshly reduced catalyst. ……..	47

Figure 4.2. CZA catalyst (a) SEM bright area image of freshly reduced catalyst (b) SEM bright area image of the spent catalyst for $CO/H_2/N_2$ =32/64/4, 34 bar, 275 ^{0}C (c) Cu-Zn-Al-O mapping of freshly reduced catalyst. ……. 48

Figure 4.3. Evolution with time on stream of CO conversion for HiFUEL R120/ δ-Al_2O_3 (CO/H2/N2 =32/64/4, 34 bar, metal to acid catalyst ratio: 1/1). ……... 50

Figure 4.4. Effect of temperature on CO conversion over HiFUEL R120/ δ-Al_2O_3 ($CO/H_2/N_2$ =32/64/4, 34 bar, metal to acid ratio: 1/1). .. 52

Figure 4.5. Effect of temperature on DME, CO2 and CH4 selectivities over HiFUEL R120/ δ-Al2O3 ($CO/H_2/N_2$ =32/64/4, 34 bar, metal to acid ratio: 1/1). ……...…. 53

Figure 4.6. Effect of pressure in the evolution with time-on-stream of CO conversion for HiFUEL R120/ δ-Al_2O_3 ($CO/H_2/N_2$ =32/64/4, 275 ^{0}C, metal to acid catalyst ratio: 1/1). …… 54

Figure 4.7. Effect of pressure on CO conversion over HiFUEL R120/ δ-Al_2O_3 ($CO/H_2/N_2$ =32/64/4, 275 ^{0}C, metal to acid catalyst ratio: 1/1). ……. 55

Figure 4.8. Effect of pressure on DME, CO_2 and CH_4 selectivities over HiFUEL R120/ δ-Al_2O_3 ($CO/H_2/N_2$ =32/64/4, 275 ^{0}C, metal to acid catalyst ratio: 1/1). ……..... 56

Figure 4.9. Effect of feed composition in the evolution with time-on-stream of CO conversion for HiFUEL R120/ δ-Al_2O_3 (275 ^{0}C, 34 bar, metal to acid catalyst ratio: 1/1). ……..... 56

Figure 4.10. Comparison of product distributions obtained over HiFUEL R120/ δ-Al2O3 for $CO/H_2/N_2$= 32/64/4 and $CO/H_2/N_2$= 48/48/4 (275 ^{0}C, 34 bar, metal to acid catalyst ratio: 1/1). ……. 57

Figure 4.11. Effect of metal to acid catalyst weight ratio in the evolution with time-on-stream of CO conversion for HiFUEL R120/ δ-Al2O3 ($CO/H_2/N_2$ =32/64/4, 275 ^{0}C, 34 bar). ……..… 58

Figure 4.12. Comparison of product distributions obtained over HiFUEL R120/ δ-Al2O3 for 1:1 and 2:1 ratios ($CO/H_2/N_2$ =32/64/4, 275 ^{0}C, 34 bar). ……..... 59

Figure 4.13. Effect of temperature in the evolution with time-on-stream of CO conversion for CZA/ δ-Al2O3 ($CO/H_2/N_2$ =32/64/4, 34 bar). ……. 60

Figure 4.14. Effect of temperature on DME, CO_2 and CH_4 selectivities over CZA/ δ-Al_2O_3 ($CO/H_2/N_2$ =32/64/4, 34 bar, metal to acid ratio: 1/1). ……..……... 61

Figure 4.15. Comparison of carbon monoxide conversions obtained over CZA/ δ-Al_2O_3 and HiFUEL R120/ δ-Al_2O_3 ($CO/H_2/N_2$ =32/64/4, 275 ^{0}C, 34 bar, metal to acid ratio: 1/1). ……. 62

Figure 4.16. Comparison of selectivities of the products obtained over CZA/ δ-Al_2O_3 and HiFUEL R120/ δ-Al_2O_3 ($CO/H_2/N_2$ =32/64/4, 275 ^{0}C, 34 bar, metal to acid ratio: 1/1). …… 62

Figure 4.17. Effect of temperature in the evolution with time-on-stream of CO conversion for HiFUEL R120-SiO_2/Al_2O_3 ($CO/H_2/N_2$ =32/64/4, 34 bar). …… 63

Figure 4.18. Effect of temperature on DME, CO_2 and CH_4 selectivities over HiFUEL R120-SiO_2/Al2O_3 (CO/H_2/N_2 =32/64/4, 34 bar, metal to acid ratio: 1/1). ……..…….. 64

Figure 4.19. Evolution with time on stream of CO conversion for HiFUEL R120/Zeolite (CO/H_2/N_2 =32/64/4, 275 ^{0}C, 34 bar, metal to acid ratio: 1/1). …… 65

Figure 4.20. Evolution with time on stream of CO conversion for HiFUEL R120/PTA (CO/H_2/N_2 =32/64/4, 275 ^{0}C, 34 bar, metal to acid ratio: 1/1). ……..... 66

Figure 4.21. Effect of temperature in the evolution with time-on-stream of CO conversion for HiFUEL R120-20 wt. % CeO_2/δ-Al_2O_3 (CO/H_2/N_2 =32/64/4, 34 bar). ……...…….. 67

Figure 4.22. Effect of temperature on DME, CO_2 and CH_4 selectivities over HiFUEL R120-20 wt. % CeO_2/ δ-Al_2O_3 (CO/H_2/N_2 =32/64/4, 34 bar, metal to acid ratio: 1/1). …….. 68

Figure 4.23. Comparison of selectivity of the products obtained over bi-functional catalyst made by combining HiFUEL R120 and various solid acid catalysts. …… 69

Figure 4.24. Evolution with time on stream of CO conversion for 2wt%Pd-20wt%CeO_2/ γ-Al_2O_3 (CO/H_2/N_2 =32/64/4, 275 ^{0}C, 34 bar, metal to acid ratio: 1/1). …….. 70

LIST OF TABLES

Table 2.1.	Comparison of dimethyl ether physical and thermo-physical properties to other alternative fuels. …….....	4
Table 2.2.	Reaction conditions of direct DME synthesis. ...…….....…..	16
Table 3.1.	Chemicals used for catalyst preparation. …….....	22
Table 3.2.	Applications and specifications of the liquids used. ……...	23
Table 3.3.	Specifications and applications of the gases used in the study. ..	23
Table 3.4.	Reactant and product gas analysis conditions for GC-2014. …..	33
Table 3.5.	Product gas analysis conditions for GCMS-QP2010. ….....	34
Table 3.6.	Contributions of various atoms to total ionization cross section.	42
Table 3.7.	The catalysts and the conditions used in the activity tests. …….	44
Table 4.1.	EDX analysis results of HiFUEL and CZA catalysts. ……...	49
Table 4.2.	The results obtained with HiFUEL R120/δ-Al_2O_3, which were calculated with respect to converted CO at temperature of 250, 275 and 300 ^{0}C for feed mixture of 32% CO, 64% H_2 and 4% N_2. ……..…….....	51

Table 4.3. The results obtained with HiFUEL R120/δ-Al_2O_3, which were calculated with respect to converted CO at pressure of 25, 30 and 34 bar for feed mixture of 32% CO, 64% H_2 and 4% N_2. 54

Table 4.4. Comparison of CO conversion and selectivity of the products values obtained with a feed gas composition of CO/H_2/N_2: 32/64/4 and CO/H_2/N_2:48/48/4. ……... 58

Table 4.5. Comparison of CO conversion and selectivity of the products values obtained with different metal to acid weight ratio of HiFUEL R120/δ-Al_2O_3. ……. 60

LIST OF ACRONYMS/ABBREVIATIONS

DME	Dimethyl Ether
PTA	Phosphotungstic Acid
TPA	Tungstophosphoric Acid
ZSM-5	Zeolite Socony Mobil–5
MCM-41	Mobil Composition of Matter-41
SBA-15	Santa Barbara Amorphous
LPG	Liquefied Petroleum Gases
XPS	X-Ray Photoelectron Spectroscopy
SEM	Scanning Electron Microscopy
EDX	Energy Dispersive X-Ray Spectroscopy
GC	Gas Chromatography
GC/MS	Gas Chromatography-Mass Spectrometry
WGS	Water Gas Shift
AE	Autoclave Engineers
PLC	Programmable Logic Controller
BPR	Back Pressure Regulator
GLS	Gas Liquid Separator

1. INTRODUCTION

Fast depletion of reserves due to the increased use of non-renewable fossil fuels, like petroleum and coal is expected to lead to the energy shortage in near future. Also, with the increasing rate of global warming, researchers are carrying out studies on the development of alternative transportation fuels and petrochemical feedstock with less greenhouse gas emissions. Alcohols and ethers are considered as potential transportation fuel alternatives or additives due to their good burning characteristics and environmentally friendly aspects. Among the alternative fuels, dimethyl ether (DME, CH_3OCH_3), is considered as a clean transportation fuel having excellent qualities as a diesel fuel alternate with very low NO_x emissions, no black smoke formation and with a significantly high cetane number (55-60) [1-3].

DME are produced from synthesis gas (mixture of CO and H_2) which can be obtained from not only from the fossil resources such as natural gas and coal, but also from the renewable resources such as biomass, waste and agricultural products. There are two process routes for the synthesis of DME. In the first route known as the ‘indirect method’, syngas is first converted to methanol, which is then converted to DME in a separate reactor. The second route, known as the ‘direct method’, syngas is converted to DME in the same reactor volume [4, 5].

Direct conversion of synthesis gas to DME requires hybrid catalysts with two kinds of active sites; one is responsible for methanol synthesis and the other for methanol dehydration. The use of $CuO\text{-}ZnO\text{-}Al_2O_3$ as the methanol synthesis catalyst is being investigated by many researchers and received industrial attention, while $\gamma\text{-}Al_2O_3$, HZSM-5 zeolites with high Si/Al ratio or partially sodium ones, microporous zeolites and silicoaluminophosphate (SAPO) are explored for use in methanol dehydration [4-5].

The objective of this study is to developed and test bi-functional catalysts for direct synthesis of DME by CO hydrogenation, using the Autoclave Engineers' BTRS-Jr-PC reaction system that can handle pressures up to 100 bar and temperatures up to 650 ^{0}C. The experimental work included a parametric study of CO hydrogenation reaction as a

function of temperature, pressure, feed composition and metal to acid catalyst weight ratio over the bi-functional catalyst prepared by physical mixing of commercial Cu–Zn based catalyst, namely HiFUEL R120, with δ-Al_2O_3 catalyst. Moreover, a parametric study of CZA/δ-Al_2O_3 as a function of temperature is performed. In addition to these bi-functional catalyst combinations, the activity of several other bi-functional configurations made by combining HiFUEL R120 with various solid acid catalysts including MCM-41 type SiO_2/Al_2O_3, microporous zeolite, phosphotungstic acid (PTA) and 20 wt. % CeO_2- δ-Al_2O_3 are tested at 34 bar and 275 ^{0}C with a molar feed gas composition of $CO/H_2/N_2$ =32/64/4. Finally, a 2wt%Pd-20wt%CeO_2/ γ-Al_2O_3 catalyst synthesized in our laboratory is tested standalone for direct synthesis of DME from syngas.

In Chapter 2, the physical and fuel properties of DME compared to specific conventional fuels are summarized. Information about the production routes and catalytic literature review are also given in Chapter 2. In Chapter 3, experimental systems used in this study, catalysts preparation methods, characterization techniques, the procedures used in the experiments are explained. High pressure experimental set-up (BTRS-Jr-PC) is also explained in detail in Chapter 3. In Chapter 4, catalyst characterization results are presented and activity results of synthesized and commercial catalysts are given. The conclusions and recommendations for future work are given in Chapter 5.

2. LITERATURE SURVEY

2.1. Dimethyl Ether (DME) as an Alternative Fuel and Energy Carrier

Starting with coal and afterwards petroleum oil and natural gas, the majority of energy needs has been provided with fossil fuels in the past two centuries. The world still depends on fossil fuels for its energy, but fossil fuels are finite resources and they are expected to run out if continued to be used excessively [6, 7]. Excessive use of fossil fuels leads to severe environmental issues. The combustion of oil, natural gas and coal generates large amounts of CO_2. Since CO_2 emission is the most important source of greenhouse gas contributing to global warming, alleviation of its harmful effects is a task that needs to be done for humankind [2, 6, 7].

Considering the above mentioned findings, there seems to be a consensus among the global community about finding non-petroleum based alternative fuels, along with more advanced energy technologies (e.g., fuel cells) to increase the efficiency of energy use. Among the alternative fuels, dimethyl ether (DME), in particular, has a huge potential for eliminating the dependency on petroleum [7].

Dimethyl ether, also known as methoxymethane, oxybismethane, methyl ether or wood ether is the simplest ether having a low carbon-to-hydrogen ratio (C:H) with a chemical formation of $CH_3–O–CH_3$ as shown in Figure 2.1 [3, 8]. DME is a colorless, nontoxic, non-carcinogenic, non-teratogenic, non-mutagenic and environmentally friendly alternative fuel [7, 9].

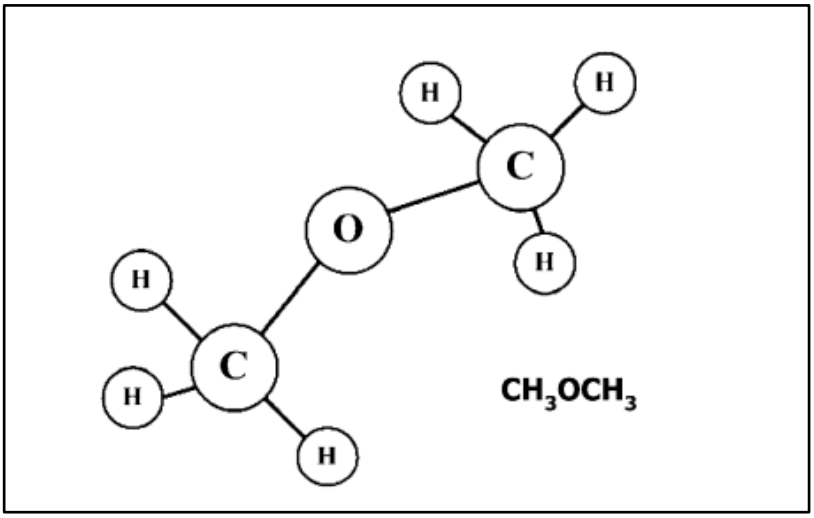

Figure 2.1. Structure of dimethyl ether (DME) [8].

DME exists in the gas form at standard temperature and pressure and can be liquefied by cooling at -25 °C under atmospheric pressure or by pressurizing at 6 atm at room temperature. Therefore, DME is easily liquefied and can be stored in pressurized tanks like liquefied petroleum gas (LPG) [1, 10-12]. DME and liquefied petroleum gases (LPG) have similar physical properties. Therefore, DME can be used as a substitute for LPG. According to the fuel properties, DME has a high cetane number of 55-60 indicating its excellent combustion characteristic so that DME can be used as diesel substitute. As DME has no carbon-carbon bonds, it does not produce particulate matter (PM) and low NO_x emission during the combustion of DME. In addition, synthesized DME has no sulfur content so that there is no SO_x emission. The negative environmental impact of DME is extremely small and it is also known as a clean energy carrier. The physical and fuel properties of DME compared to specific conventional fuels are listed in Table 2.1.

Table 2.1. Comparison of dimethyl ether physical and thermo-physical properties to other alternative fuels [7, 13].

Properties	**DME**	**Methane**	**Methanol**	**Ethanol**	**Propane**	**Gasoline**	**Diesel**
Chemical formula	CH_3OCH_3	CH_4	CH_3OH	C_2H_5OH	C_3H_8	C_7H_{16}	$C_{14}H_{30}$
Molecular weight (g mol^{-1})	46.07	16.04	32.04	46.07	-	100.2	198.4
Boiling point (^{0}C)	-24.9	-162	64	78	-42	38-204	125-400
Liquid density (g cm^{-3}) (@293 K)	0.661	0.00072	0.792	0.785	0.49	0.737	0.856
Specific gravity of gas (vs. air)	1.59	0.55	-	-	1.52	-	-
Heat of vaporization (kJ/kg)	467	1097	510	-	426	-	-
Vapor pressure (atm) (@293 K)	6.1	-	-	-	9.3	-	-
Ignition temperature (K)	623	905	743	-	777	-	-
Explosion limit	3.4-17	5-15	5.5-36	-	2.1-9.4	-	0.6-6.5
Cetane number	55-60	0	5	-	5	-	40-55
Net calorific value (10^6J/kg)	28.90	50.23	21.10	-	46.46	-	41.86
Carbon content (wt. %)	52.2	0.74	37.5	52.2	-	85.5	87
Sulfur content (ppm)	0	~7-25	0	0	-	~200	~250

DME (particularly, bio-DME including specific amounts of methanol and water) can be used as a diesel alternative for the transportation sector and the small-scale electric power generation sector, with almost smoke-free combustion. Use of DME in the diesel engines provides a number of significant benefits including significantly reduced engine noise, high thermal efficiency as well as decreased emissions of NO_x, hydrocarbons and CO compared with diesel fuel. Although use of DME in the diesel engine is more efficient than its use in a conventional diesel engine, some minor modifications including a new storage system and a new fuel delivery system are needed. The DME fuel storage tank needs nearly 2 times the volume of a diesel fuel storage tank due to the lower energy density of DME (27.6 MJ/kg) when compared to diesel fuel (42.5 MJ/kg) [1, 8]. Moreover, practical use of DME in the diesel engines leads to some problems resulting from the physical properties of DME. The viscosity of DME is lower than that of the conventional diesel by a factor of about 20, leading to the leakage in pumps and fuel injectors. DME easily vaporizes during injection due to its low boiling temperature of -25 ^{0}C which requires comparatively low fuel injection pressures. Lubrication problem is another drawback of DME. Solutions to lubrication problems are developed by using additives to increase the lubricity of DME and additives commonly used for the conventional diesel are also improved for DME [1].

DME can also be used as a blend fuel with LPG for domestic cooking and heating purposes (for containing up to 20 volume % of DME in LPG/DME blends, there is no need any modification to appliances); more than 90% of DME produced in China is blended with LPG [1, 3]. DME can use the existing LPG infrastructure for transport and storage with minor modifications to the pumps, seals, and gaskets [7].

DME as a gas turbine fuel demonstrates excellent performance in terms of emission levels, particularly those of NO_x, CO and unburned hydrocarbons. The resulting emission levels are comparable to those of natural gas and liquid naphtha. However, DME is not acceptable fuel for spark-ignition (SI) engines because of its high cetane number although the burning velocity is similar to hydrocarbon fuels [8].

DME is increasingly used as a propellant in aerosol products to replace chlorofluorocarbons, which contribute to destroy the ozone layer of the atmosphere. DME

offers exceptional advantages such as solvency power and water miscibility. It is an appreciated propellant in many aerosol products such as personal care (i.e., hairsprays, shave creams, foams, and antiperspirants), paint sprays, insect control and other technical aerosol products [14].

DME is also being used as chemical intermediate for producing olefins like propylene and ethylene or higher molecular weight compounds (i.e., gasoline) via various methanol-to-olefins (MTO) processes [1]. Methanol is first converted to DME and then DME is converted to the olefins as shown below:

$$CH_3OH \longrightarrow CH_3OCH_3 \longrightarrow C_2\text{-}C_4 \text{ Olefins} \qquad (2.1)$$

DME can be produced from wide range of energy resources; not only from the fossil resources such as natural gas and coal, but also from the renewable resources such as biomass, waste and agricultural products. There are two processes for the synthesis of DME, as shown in Figure 2.2. First, DME can be synthesized via the conventional route where synthesis gas (produced from several energy resources as mentioned above) is converted to methanol followed by a methanol dehydration step, which is also known as 'indirect method'. Second, DME can be obtained directly from synthesis gas (CO, H_2), which is also known as 'direct method' [12].

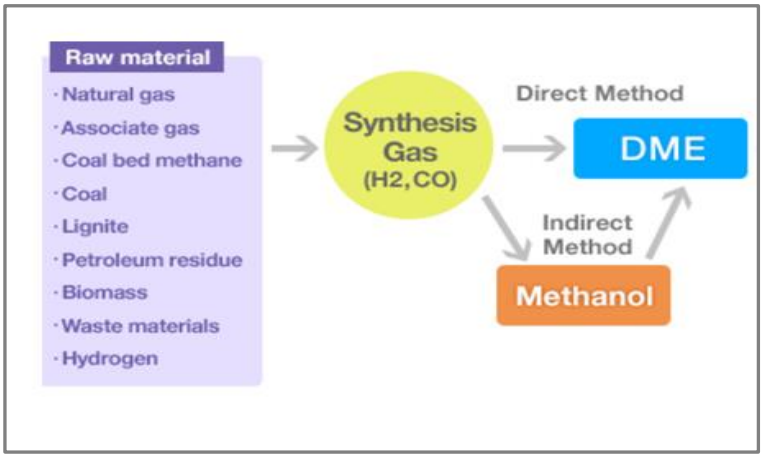

Figure 2.2. DME production processes [12].

2.2. Catalytic Formation of Dimethyl Ether (DME)

Up to now, there are two routes which are known as main processes for DME production from synthesis gas, the indirect and direct methods. Brief information about these methods as well as the catalysts involved in them is given in detail.

2.2.1. Indirect Synthesis of Dimethyl ether

In indirect method, there are two-step process, methanol synthesis and methanol dehydration. Methanol is firstly produced from synthesis gas (syngas) in one reactor and then followed by methanol dehydration to DME in another reactor.

2.2.1.1. Catalytic Methanol Synthesis. Pure methanol was first separated as a chemical form in 1661 by Robert Boyle by the distillation of boxwood, which is why it is frequently called wood alcohol or wood naphtha. However, commercial methanol was first produced by the destructive distillation of wood wastes dating back to the early 1900s [15].

In 1923, high-pressure methanol synthesis technology was developed by BASF over ZnO/Cr_2O_3 catalyst. This process was favorably conducted at a temperature range of 350 - 450°C and a pressure range of 250-300 bar. A number of industries have adopted high-pressure methanol process for nearly 50 years [15].

In 1963, Imperial Chemical Industries (ICI, now Synetix) developed a new methanol synthesis technology called as low-pressure methanol synthesis technology operating at a pressure range of 35 to 55 bar and a temperature range of 225 to 275 °C. In this process, Cu-based catalyst with Zn promoter was used. Zn was reported to be an important promoter since it enhanced the dispersion of copper and prevented agglomeration of it. A number of industries now utilize the low pressure methanol synthesis technology [15].

Methanol is mostly synthesized from synthesis gas (syngas) containing CO and H_2 along with a small amount of CO_2. Synthesis gas is mostly obtained from the steam reforming of methane to produce hydrogen and carbon monoxide in a molar ratio of H_2/CO=2-3. In the low pressure methanol synthesis, both the hydrogenation of carbon

oxides (CO and CO_2) and water gas shift reaction occur over the copper-based catalyst by the following reactions [16]:

$$CO + 2H_2 \leftrightarrow CH_3OH \qquad \Delta H_r^0 = -90.7 \text{ kJ/mol} \qquad (2.2)$$

$$CO_2 + 3H_2 \leftrightarrow CH_3OH + H_2O \qquad \Delta H_r^0 = -50.1 \text{ kJ/mol} \qquad (2.3)$$

$$CO + H_2O \leftrightarrow CO_2 + H_2 \qquad \Delta H_r^0 = -41.2 \text{ kJ/mol} \qquad (2.4)$$

Temperature is one of the most important operating parameter for the methanol synthesis reactions. These reactions are highly exothermic. Therefore, the equilibrium conversion is thermodynamically favored by low temperatures [16].

Among most of the low pressure methanol synthesis technologies, carbon dioxide must be present in the feed, which makes the water gas shift reaction proceed in the forward direction. The CO_2 content in the feed syngas changes from process to process, varying typically between 2% and 8% by volume. Furthermore, as reported in the literature, the absence of carbon dioxide makes the Boudouard reaction leading to carbon deposition on the surface of the catalyst [15]:

$$2\,CO \leftrightarrow CO_2 + C\,(s) \qquad (2.5)$$

A typical commercial catalyst used in low-pressure methanol synthesis is prepared by co-precipitation technique in which both CuO and ZnO are precipitated on alumina, Al_2O_3. However, the principal drawback of these catalysts is that they are readily deactivated. The reasons of deactivation are mostly based on thermal sintering (copper site clustering) or carbon deposition. Recently, low temperature/pressure catalysts and role of different metal oxides (e.g., Zr, Cr, Ce, Co or Ti) on the catalytic activity are extensively studied by researchers for methanol synthesis [17, 18].

Suh *et al.* [19] prepared Cu/ZnO catalysts modified with different contents of ZrO_2 for the hydrogenation of CO to methanol. They investigated the nature of active sites of $Cu/ZnO/ZrO_2$ catalysts and role of ZrO_2 on the catalytic activity via XPS. Catalytic activity tests were conducted in a fixed bed reactor operating at 250 ^{0}C and 34.5 bar with a molar feed ratio of $H_2/CO=4$. They reported that the $Cu/ZnO/ZrO_2$ catalyst with 15 wt. % of ZrO_2

exhibited the highest catalytic activity. It was seen that the addition of ZrO_2 enhanced the formation of Cu^+ ions. They claimed that Cu^+ ions formed the active sites for the methanol synthesis reaction and the ratio of Cu^+/Cu^0 was the key parameter to obtain high selectivity.

A study carried out by Arena *et al.* [20] gave similar results. They worked on methanol synthesis over Zr promoted Cu-ZnO type catalysts, which were prepared by the reverse co-precipitation under ultrasound field. Catalytic activity was tested in an Inconel micro-reactor operating at 10 bar and a temperature range of 160 to 200 ^{0}C. They reported that Cu^+/Cu^0 played a critical role to obtain high methanol yield and ZrO_2 modified Cu-ZnO catalysts showed higher catalytic performance than Cu-ZnO catalysts.

The addition of ceria to the copper zinc catalysts was investigated by Shen *et al.* [21] for low temperature methanol synthesis from synthesis gas. They prepared ceria supported copper catalysts by a co-precipitation method. Activity tests were carried out in a fixed-bed continuous flow reactor operating at a reaction temperature below 200 ^{0}C and 20 bar. The results showed that 10 wt. % Cu/CeO_2 increased the catalytic activity and also enhanced the dispersion of copper.

Pokrovski *et al.* [22] worked on the effects of cerium incorporation into the Cu/ZrO_2 methanol synthesis catalyst for the hydrogenation of CO to methanol. They found that the catalytic activity of $Cu/Ce\text{-}ZrO_2$ catalyst was four times higher than that of the Cu/ZrO_2 catalyst. The higher catalytic activity of Ce-containing catalyst was attributed to its higher adsorbed hydrogen content. In their another study, Pokrovski *et al.* [23] investigated methanol synthesis over Cu/ZrO_2 type catalysts with Mn and Pr additives. They concluded that the activity of the catalysts increased in the order of $Cu/ZrO_2 < Cu/Mn\text{-}ZrO_2 < Cu/Pr\text{-}ZrO_2 < Cu/Ce\text{-}ZrO_2$.

Sloczynski *et al.* [24] prepared $Cu/ZnO/ZrO_2$ catalysts with different oxide additives (B, Ga, In, Gd, Y, Mg and Mn) for methanol synthesis. They reported that the presence of these additives led to significant changes in the catalytic activity. They concluded that among the additives, Ga_2O_3-modified $Cu/ZnO/ZrO_2$ catalyst showed the highest catalytic

activity whereas In_2O_3-modified $Cu/ZnO/ZrO_2$ catalyst showed the lowest catalytic activity.

Meshkini *et al.* [17] studied the promoting effect of various metal oxide additives (Mn, Mg, Zr, Ce, Ba, Cr and W) on the catalytic properties of $Cu/ZnO/Al_2O_3$ for methanol synthesis from syngas. Catalytic activities tests were carried out in a stainless steel fixed bed reactor operating at 50 bar and 240 ^{0}C with a feed mixture of $CO/CO_2/H_2$=1/1/4.5. According to the experimental results, the addition of Mn and Zr together to $Cu/ZnO/Al_2O_3$ increased the copper surface area and the amount of exposed copper (Cu^0), and the Mn and Zr promoted with $Cu/ZnO/Al_2O_3$ catalysts showed the best catalytic activity.

Gao *et al.* [25] also investigated the effect of promoters including Mn, La, Ce, Zr and Y on the catalytic performance of Cu/Zn/Al catalyst for methanol synthesis. The prepared catalysts were tested in a continuous-flow fixed-bed reactor operating at 230-270 ^{0}C, 50 bar and at a gas hourly space velocity (GHSV) of 12,000 ml/ (g_{-cat} h). The experimental results showed that the presence of these promoters resulted in higher BET specific surface area, Cu surface area and Cu dispersion. They reported that the methanol selectivity decreased in the order of Cu/Zn/Al/Zr > Cu/Zn/Al/Y > Cu/Zn/Al/Ce > Cu/Zn/Al/La > Cu/Zn/Al/Mn >Cu/Zn/Al.

Zhang *et al.* [26] studied the role of TiO_2 over the catalytic performance of CuO-ZnO-Al_2O_3 for methanol synthesis by co-precipitation. Reaction conditions were 26 bar, 260 ^{0}C and space velocity of 3600 ml/(g. h). They reported that the optimum methanol selectivity was obtained with the sample of 4% TiO_2/CuO-ZnO-Al_2O_3. It was seen that moderate addition of TiO_2 improved the dispersion of CuO and ZnO in the catalyst and also changed the acidity on the surface of catalyst, which resulted in higher methanol yield.

Apart from the Cu-based ones, noble metal catalysts are recognized as hydrogenation catalysts and supported palladium catalysts have been found to be fairly active for methanol synthesis [27, 28]. Shen *et al.* [28] investigated the effect of a ceria-support on the activity of palladium for methanol synthesis from carbon monoxide and hydrogen. Catalytic activity tests were carried out in a fixed-bed continuous-flow reactor operating at

250 ^{0}C and 20 bar. According to the experimental results, the activity was increased by a strong contact between the palladium particles and the support. They found that Pd/CeO_2 catalyst was highly active for methanol synthesis. In their another work, Shen *et al.* [29] investigated the effect of the support on the activity and selectivity of Pd in CO hydrogenation. They prepared Pd supported on Al_2O_3, SiO_2, TiO_2, and ZrO_2 catalysts for methanol synthesis from CO hydrogenation. They reported that Pd/Al_2O_3 produced dimethyl ether as a major product and dimethyl ether selectivity was found as 76.3% and 50.2% at 200 ^{0}C and 250 ^{0}C, respectively. They also reported that significant amount of dimethyl ether formation over Pd/Al_2O_3 was attributed to the acidity of the support metal oxide. According to the experimental results, Pd/SiO_2 favored methanol formation whereas Pd/TiO_2 produced mostly CH_4. The high methanol yield was observed over Pd/ZrO_2 catalyst.

2.2.1.2. Catalytic Methanol Dehydration to Dimethyl Ether. Traditionally, DME is synthesized via methanol dehydration reaction in a catalytic dehydration reactor over a solid-acid catalyst. Catalytic activity tests are operated at a temperature range of 250–400 ^{0}C and pressures up to 18 bar by the following reaction [30]:

$$2CH_3OH \leftrightarrow CH_3OCH_3 + H_2O \qquad \Delta H_r^0 = -21.3 \text{ kJ/mol} \tag{2.6}$$

Several solid-acid catalysts such as γ-alumina, zeolites (HZSM-5 and HMCM-22), silica aluminas (SiO_2-Al_2O_3), mesoporous molecular sieves (mostly MCM-41 and SBA-15), mixed metal oxides and ion-exchange resins have been tested by many researchers for methanol dehydration reaction. Although these materials have been considered as good candidates, they are prone to produce undesired products (mostly hydrocarbons) and coke leading to catalyst deactivation [31]. In recent years, the properties of these solid-acid catalysts (e.g. Brönsted and/or Lewis acidity, the strength and number of these sites and the morphology of the support) have become more and more important in order to enhance catalyst activity as well as to obtain high DME selectivity [30, 32, 33].

The dehydration of crude methanol to dimethyl ether over Na-modified H-ZSM-5 catalysts was studied by Vishwanathan *et al.* [34]. Before a detailed study was made on the Na-modified H-ZSM-5 catalysts, they studied the dehydration of methanol over

commercial γ-alumina catalyst. According to their results, the dehydration reaction formed high amount of water, and both methanol and water were captured by the same sites of alumina. Lewis acid sites over γ-alumina catalysts were much more likely to capture water molecules than methanol. The captured water decreased the activity of the catalyst by blocking the acid sites. Therefore, they decided to study over the H-ZSM-5 type catalysts due to the hydrophobic nature of H-ZSM-5. They also reported that since H-ZSM-5 catalysts had strong surface acidity leading to increased hydrocarbon formations as by-products, sodium content varying from 0 to 80 mol% was added to H-ZSM-5 catalysts to prevent such products. The reaction was tested in a fixed-bed micro-reactor under normal atmospheric pressure and in the temperature range of 230 to 340°C. Na-modified H-ZSM-5 (Si/Al = 20) showed the highest catalytic activity and Na_{80}-H-ZSM-5 showed the highest methanol conversion, 100% selectivity for DME and highest resistance against the water.

Yaripour *et al.* [30] prepared various solid-acid catalysts including γ-alumina and modified γ-alumina with silica by co-precipitation (sol–gel) method and tested for catalytic dehydration of methanol to dimethyl ether (DME). The influence of silica addition to γ-alumina for methanol dehydration reaction and also the correlation of the activity results with surface acid properties of these catalysts were investigated. These catalysts were tested in a fixed bed reactor operating at a temperature of 300 ^{0}C under atmospheric pressure. They observed that DME selectivity depended heavily on sites with weak and medium acidity. They reported that silica-modified γ-alumina catalysts showed better performance compared to pure γ-alumina because silica-modified γ-alumina catalysts had much more weak and medium acid sites. The optimum methanol conversion to DME without any by-product was obtained with the sample with 6 wt. % silica loading.

Hassanpour *et al.* [32] worked on dehydration of methanol to dimethyl ether over different commercial zeolites and Na-modified H-ZSM-5 catalysts prepared by wet-impregnation method. Catalytic activity tests were carried out in a fixed bed reactor operating at reaction conditions of 300 °C and 16 bar. Temperature programmed desorption of ammonia (NH_3-TPD) was used to test the influence of acid strength and its distribution in zeolite samples. Based on the activity and NH_3 -TPD results, the H-form zeolite samples were much more active and selective than Na-form catalysts. Catalytic activities can be ordered as MDHC-1 (H-ZSM-5 structure) > MDHC-2 (H-Mordenite

structure) ≈ MDHC-3 (NH_4-Mordenite structure) > Na form Zeolite. Among the Na-modified H-ZSM-5 catalysts, Na_{100} MDHC-1 was found to be the best catalytic performance in terms of activity, selectivity and conversion.

Catalytic dehydration of methanol to dimethyl ether over commercial mordenite and ion-exchanged catalysts was investigated by Moradi *et al.* [35]. Five commercially available acidic mordenites with various SiO_2/Al_2O_3 ratios namely, MCDH-1, MCDH-2, MCDH-3, MCDH-4 and MCDH-5 were used in the experiments. These catalysts were tested in a vertical fixed-bed flow micro reactor operating at 300 °C under atmospheric pressure. According to the experimental results, the MCDH-1 was found to be the best catalyst for methanol dehydration reaction. After finding the most active catalyst, the effect of water on catalyst deactivation was investigated for two selected catalyst. They reported that the H-mordenite catalyst (MCDH-1) exhibited higher catalytic activity and stability than the H-mordenite catalyst MCDH-7 (ion exchanged of MCDH-4) for a feed involving 20 wt. % water.

Naik *et al.* [36] prepared various Al-MCM-41 catalysts, [SiO2]/ [Al2O3] = 30, for methanol dehydration to DME synthesis. They added aluminum to MCM-41 to improve the acidity of pure MCM-41. Therefore, they tried to generate acidity on its framework structure by the incorporation of metal ion. Catalytic activity tests were carried out in a in a tubular fixed-bed stainless steel reactor operating at between 250 and 400 ^{0}C and gas per hourly velocity (GHSV) of 14,000–80,000 ml $g^{-1}_{cat}\,h^{-1}$. They reported that with the increase in temperature range from 250 to 400 ^{0}C, the conversion of methanol increased for all catalysts. The methanol conversion of 73% and selectivity to DME of 97% was achieved at 400 ^{0}C and 14,000 ml $g^{-1}_{cat}\,h^{-1}$.

The conversion of methanol to dimethyl ether synthesis over alumina based catalysts was studied by Tokay *et al.* [37]. Alumina impregnated SBA-15 (mesoporous silica, Al@SBA-15), commercial γ-alumina (Al-T) and a mesoporous aluminosilicate ($AlSi_3$) catalyst were used as alumina based catalysts in the experiments. Catalytic activity was tested in a tubular reactor operating at 120-450 ^{0}C for a constant flow rate of 44.2 cm^3/ min. According to the reaction results, DME and formaldehyde (FA) were found as the reaction products and particularly formation of some formaldehyde was obtained at

temperatures lower than 300 ^{0}C. They reported that almost 100% DME selectivity was reached above 300 ^{0}C with Al@SBA-15 catalyst. They also observed that the optimum methanol conversion was reached to a value of 0.8 at 350 ^{0}C.

Fu *et al.* [38] worked on the effects of surface acidity on the dehydration of methanol to DME over H-ZSM-5, steam de-aluminated H-Y zeolite (SDY), γ-Al_2O_3 and $Ti(SO_4)_2$ modified γ-Al_2O_3 type catalytic materials by using microcalorimetric adsorption of ammonia and FT-IR spectra method. The dehydration of methanol was carried out in a fixed-bed micro-reactor involving 0.2 g of catalyst. Activity tests were conducted at different temperatures with gas hourly space velocity of 3400 ml g^{-1}_{cat} h^{-1} with a feed gas of methanol:N_2 =21:79. They found that H-ZSM-5 and SDY exhibited the best catalytic activity because of having strong Brönsted surface acidity at low temperatures, but at higher temperatures, the formation of hydrocarbons and coke was also observed. They reported that no significant deactivation was observed for $Ti(SO_4)_2$ modified γ-Al_2O_3 catalyst at high temperatures.

Ciftci *et al.* [39] prepared tungstophosphoric acid (TPA) incorporated silicate structured new mesoporous (MCM-41) via one-pot hydrothermal and impregnation procedures for dehydration of methanol to DME. As reported in the literature, although mesoporous silicate structures (M41S family) have high surface area and larger pore diameters than zeolites, these materials are quite inert and have low catalytic activity in pure form, for most catalytic applications. Since heteropolyacid (HPA) compounds like tungstophosphoric acid (TPA) had very strong Bronsted acidity with very high proton mobility, tungstophosphoric acid (TPA) was incorporated into MCM-41 for the improvement of the acidic characteristics of MCM-41. Catalytic activity tests were carried out in a temperature range of 200–400 ^{0}C with using 0.2 g of fresh catalyst. The experimental results showed that TPA impregnated MCM-41 catalyst had higher activity than pure TPA. They reported that DME selectivity values of about 1.0 were obtained in the temperature range of 200–300 ^{0}C. They also reported that at high temperatures, in particular above 300 ^{0}C, coke formation was observed.

2.2.2. Direct Synthesis of Dimethyl Ether (The single-step DME synthesis)

The direct synthesis of dimethyl ether (DME) process is becoming more and more attractive due to its greatly economical and thermodynamic properties. Until now, DME has been conventionally produced by methanol dehydration on industrial scale. However, the direct synthesis of DME from syngas has been achieved only in pilot scale [40, 41].

The direct synthesis of dimethyl ether (DME) from syngas is a combination of three reactions, including methanol synthesis, methanol dehydration and water-gas shift reactions taking place in the same reactor. DME can be produced directly from synthesis gas according to the following reactions [13]:

Methanol synthesis from synthesis gas:

$$2CO + 4\,H_2 \leftrightarrow 2CH_3OH \qquad \Delta H_r^0 = -182\ kJ/mol \qquad (2.2)$$

Methanol dehydration to dimethyl ether:

$$2\,CH_3OH \leftrightarrow CH_3OCH_3 + H_2O \qquad \Delta H_r^0 = -23\ kJ/mol \qquad (2.6)$$

Water gas shift reaction:

$$CO + H_2O \leftrightarrow CO_2 + H_2 \qquad \Delta H_r^0 = -41\ kJ/mol \qquad (2.4)$$

The combination of Equations 2.2, 2.6 and 2.4 gives the net reaction:

$$3CO + 3H_2 \leftrightarrow CH_3OCH_3 + CO_2 \qquad \Delta H_r^0 = -246\ kJ/mol \qquad (2.7)$$

Reactions 2.2 and 2.4 are performed by a methanol synthesis catalyst (e.g. Cu/Zn based catalysts) and Reaction 2.6 is performed by an acidic catalyst (e.g. γ-alumina). Reaction 2.7 is a combination of Reactions 2.1, 2.3 and 2.5 [13]. Reaction 2.4 is the water gas shift reaction which takes place very fast. Methanol synthesis is an equilibrium reaction that is thermodynamically limited. The synergy among the Reactions 2.2, 2.4 and 2.6 allows very high conversion of syngas in a single pass because of subsequent removal of methanol by dehydration. Furthermore, water produced in Reaction 2.6 is removed via the Reaction 2.4 to form hydrogen which kinetically favors the production of methanol, allowing the relief of the equilibrium limitation of methanol synthesis [42-46].

A wide range of different feed and operating conditions have been reported for the direct synthesis of DME [45]. Typical temperature, pressure, feed gas ratio (H_2/CO) and W/F ratios used for the direct synthesis of DME are listed in Table 2 [13].

Table 2.2. Reaction conditions of direct DME synthesis [13].

Reaction condition	Temperature (^{0}C)	Pressure (bar)	H_2 /CO ratio	W/F (kg-cat.h/ kg mol)
Experimental	240-280	30-70	0.5-2.0	3.0-8.0
Standard	260	50	1.0	4.0

A typical bi-functional catalyst involves two active sites, one for the first reaction step (methanol synthesis and water gas shift reactions) and another for the second reaction step (methanol dehydration). However, catalyst systems are subject to deactivation by sintering of active copper sites, coke deposition, poisoning by contaminants. Therefore, the design of bi-functional catalysts for the direct synthesis of DME is still on a research level [40, 41, 46-51].

In the literature, there are several studies related to the catalyst development including catalyst compositions and preparation conditions (i.e. pH, precipitation and calcination temperatures) in order to avoid the deactivation of the bi-functional catalysts. Stiefel *et al.* [46] studied DME synthesis directly from CO-rich synthesis gas (H_2/CO≤1) and focused on the effect of dehydration catalysts and operating conditions. Catalyst mixtures composed of a methanol catalyst (Cu/ZnO/Al_2O_3) and various methanol dehydration components (zeolites of the mordenite and ZSM-5 type as well as γ-alumina) were investigated. In addition, several reaction parameters such as temperature, H_2/CO, and space velocity were also studied. The influence of water and CO_2 in the gas feed was also tested using Cu/ZnO/Al_2O_3 as catalyst for methanol synthesis with γ-alumina as catalyst for methanol dehydration. Catalytic activities were tested in a stainless steel fixed-bed reactor in which 2 g of each catalyst system (wt.: wt. =1:1, particle size: 355-500 μm) was placed into the reactor. Activity tests were carried out at 200-260 ^{0}C, 51 bar, and at

three different H_2/CO ratios (H_2/CO=2, 1 and 0.67). They reported that the acidity of the dehydration component, i.e., its acid strength and number of acid sites in the catalytic system, was a crucial parameter for direct conversion of carbon-monoxide rich synthesis gas to DME. They claimed that if acidity is quite low, the amount of methanol produced cannot be dehydrated with adequate efficiency and if the acidity is remarkably high, further conversion of DME to hydrocarbons also occurs. γ-Al_2O_3 was identified to be a suitable dehydration component due to the comparatively low content of highly acidic sites and high selectivity towards DME. The results showed that high DME selectivity was reached at 250-260 ^{0}C and at H_2/CO ratio of 1 by using γ-Al_2O_3 as methanol dehydration catalyst. They observed that water content below 10% resulted in no deactivation on catalyst structure, and water content of 10% caused the rise in CO conversion. In the latter case, however, water gas shift reaction became dominating and CO_2 was found as the main product. They also found that the presence of 8% of CO_2 led to ca. 10% lower CO conversion and ca. 5% lower DME selectivity when compared with the reaction system without CO_2.

Sierra *et al.* [52] studied the reason of deactivation, the role of metallic and acid functions on deactivation and the effect of operating conditions (temperature, pressure, and H_2/CO ratio in the feed) on the direct synthesis of DME synthesis over a CuO-ZnO-Al_2O_3/γ-Al_2O_3 bi-functional catalyst. Catalytic activity was conducted in an isothermal fixed bed reactor operating at 275 ^{0}C and 30 bar for the feed gas of H_2: CO=3/1. In their previous work [49], they observed coke formation on the metallic sites. Thus, they decided that four different water/syngas molar ratios (0, 0.08, 0.20, and 0.60) in the feed were used in order to understand the effect of water on the deactivation of the metallic component (CuO-ZnO-Al_2O_3). They observed that further increase in water content in the feed considerably declined both the amount of coke deposited on the metallic component and the yield of paraffins (undesired products), whereas a sharp decline of CO conversion and DME selectivity was obtained. The results showed that the equilibrium CO conversion for a water/syngas molar ratio of 0.20 decreased from 65.1 % for the feed without water to 24.8 % and the yield of DME also decreased from 61.2% for the feed without water to 20.4 %. They reported that the optimum water content in the feed would depend on reaction conditions and the study on the effect of co-feeding water should be enhanced.

.

Nie *et al.* [50] worked on a series of core-shell structured CuO-ZnO@H-ZSM-5 (CZ@H) catalysts via homogenous precipitation through urea hydrolysis for the single step DME synthesis. Activity tests were carried out in a stainless steel tubular, high pressure, fixed bed reactor operating at 220-280 ^{0}C, 20 bar, gas hourly space velocity (GHSV)= 1500-7500 ml/ (g_{-cat} h) for a molar feed gas composition of H_2/CO=2. Activity tests indicated that the highest CO conversion of 53.2% and 69.6% selectivity of DME was obtained at 260 ^{0}C, 20 bar and at a space velocity of 6000 ml/ (g_{-cat} h). They reported that this novel preparation method and excellent core-shell structure were contributed to the high Cu surface area as well as high Cu dispersion and these bi-functional CZ@H catalysts showed excellent catalytic performances.

Ereña *et al.* [48] investigated the effect of operating conditions (time on stream, temperature, pressure, and space time) on the conversion of CO and CO_2, selectivity to DME, yield of DME and product distribution over a CuO-ZnO-Al_2O_3/NaHZSM-5 bi-functional catalyst. The Autoclave Engineers' BTRS-Jr. reaction system that can handle reactor pressures up to 100 bar and up to 650 ^{0}C was used for activity tests. Activity tests were evaluated at 175-350 ^{0}C, 10-50 bar, and at four different space time values (8.33, 16.66, 33.33, and 66.66 (g of catalyst) h/ mol of reactants). They reported that deactivation was not important during the 6 h experimentation, whereas the coke content deposited on the porous structure of the catalyst became important in the 12 h experimentation. They observed that the highest amount of oxygenates (methanol and DME) was reached in the temperature ranges from 250 to 300 ^{0}C. The results show that hydrocracking reactions became dominating above 300 ^{0}C, namely, the synthesis of light paraffins (mostly methane) became important that caused a sharp decrease in the selectivity to DME. On the other hand, increased amount of CO_2 was observed above 275 ^{0}C resulted from the cracking of DME produced water. The optimum temperature, pressure, time on stream and space time were found as 275 ^{0}C, 40 bar, 6 h and 66.66 (g of catalyst) h/ mol of reactants, respectively at a feed ratio of H_2/CO=2/1. In addition, selectivity to DME and yield of DME were obtained as 80% and 78%, respectively.

Mao *et al.* [53] prepared DME synthesis catalysts by physically mixing CuO/ZnO/Al_2O_3 as methanol synthesis component and HZSM-5 zeolites modified with different contents of magnesium oxide (0-10wt %) as methanol dehydration component.

They focused on the effect of MgO modification of HZSM-5 on its catalytic activity for methanol dehydration. The reaction studies were conducted in a fixed bed continuous flow reactor operating at 40 bar, 260 ^{0}C and at a gas hourly space velocity of 1500 ml/ (h g_{cat}) with a feed gas mixture of CO:CO_2:H_2=30:4:66. They observed that with the addition of a suitable amount of magnesium oxide to HZSM-5, Brönsted acid sites (mostly the strong Brönsted acid sites) decreased, whereas Lewis acid sites increased. The results indicated that MgO loading up to 5 wt% decreased the formation of undesirable side products including hydrocarbons from enhancing DME to hydrocarbon reactions and CO_2 from favoring the water gas shift reaction, and led to an increase in DME selectivity from ca. 49% for the HZSM-5 without MgO to more than 64%. Moreover, they reported that the conversion of CO did not change when MgO-modified HZSM-5 was used as a dehydration catalyst. On the other hand, for MgO loading higher than 5 wt%, DME selectivity decreased dramatically due to a decrease in the acidity of the catalyst and the conversion of CO decreased as well.

Moradi *et al.* [4] prepared CuO-ZnO-Al_2O_3/γ-Al_2O_3 hybrid catalysts for the synthesis gas to dimethyl ether (STD) reaction by using seven different methods including co-precipitation by Na_2CO_3 and $NaAlO_2$, co-precipitation impregnation, co-precipitation sedimentation, sol-gel and novel sol-gel impregnation, and impregnation techniques and studied the effect of these catalysts on catalytic activity. In addition, different contents of alumina at a fixed CuO/ZnO ratio were prepared by sol-gel impregnation method to define the effect of alumina on the catalytic activity. Activity tests were carried out in a micro slurry reactor operating at 240 ^{0}C, 40 bar, and space velocity 1000 ml/g_{cat} h for a feed of H_2/CO/N_2= 64/32/4. The catalysts prepared by sol-gel impregnation and co-precipitation sedimentation exhibited the highest catalytic activity. The optimum weight percent of Al_2O_3 for CuO/ZnO/Al_2O_3 was found as 2:1:5.

Naik *et al.* [54] prepared CuO-ZnO-Al_2O_3/SiO_2-Al_2O_3 catalysts by using composite and hybrid catalyst synthesis strategies and focused on the effect of the methods of catalyst preparation for the CuO-ZnO-Al_2O_3 and SiO_2-Al_2O_3 (Si/Al = 2) systems on selectivity to DME and CO conversion. The activity tests were carried out in a high-pressure tubular stainless steel fixed-bed reactor operating at 260 °C, 50 bar, gas hourly space velocity of 5000 ml/ (h g_{cat}) with a feed gas mixture of CO:H_2:CO_2= 47:47:6. The results revealed that

hybrid catalysts prepared by a mechanical mixing of the two catalytic components showed better performance than composite catalysts prepared by mixing the catalyst precursors. They reported that DME, $HCOOCH_3$, CO_2, and CH_4 were formed as the reaction products and the selectivity to DME and CO conversion using hybrid catalysts were obtained as 96% and 20%, respectively.

Jiang *et al.* [55] worked direct DME synthesis over bi-functional mesoporous Cu– γ-Al_2O_3 type catalysts prepared with various copper contents by one-pot synthesis method. Catalytic activity was tested in a fixed bed stainless-steel reactor in which 1 g of catalyst was loaded in the middle section of the reactor operating at 50 bar and a temperature range of 280-325 ^{0}C with a feed gas mixture of H_2:CO:N_2= 60:30:10. The results showed that copper particles were developed as small particles spread around the whole crystalline γ-Al_2O_3 network with large surface area and high thermal stability, which made the material a bright future for DME synthesis catalysts. Activity tests indicated that a CO conversion of 72% and a DME selectivity of 69% were reached at 50 bar and 310 ^{0}C.

Song *et al.* [56] studied the direct synthesis of DME from biomass-derived syngas over bi-functional catalysts composed of Cu–ZnO–Al_2O_3/γ-Al_2O_3 with different ZrO_2 contents (0-10 mol%). The aim of this work was to investigate the effect of Zr-loading on the activity of the methanol synthesis component of hybrid catalyst. Catalytic activity was tested in a continuous flow-type fixed-bed reactor system evaluated at 270 ^{0}C, 50 bar for a feed gas of H_2/CO/CO_2/CH_4 = 52/24/23/1 during a 100 h reaction. Catalytic activity tests showed that a CO conversion of 79.3% and a DME selectivity of 85.8%, the highest catalytic activity and stability, were all obtained with 3 mol% ZrO_2 content. They reported that addition of a suitable amount ZrO_2 to the catalyst enhanced Cu dispersion which resulted in a high Cu surface area and good reducibility. A linear relationship between CO conversion and Cu surface area was also detected. With the further increase in Zr content (>5 mol %), the decrease in CO conversion and DME selectivity was observed due to the growth of Cu crystallites after catalyst reduction.

The one-step synthesis of dimethyl ether from syngas (STD process) over the hybrid catalysts including pure HMCM-22 zeolites with different SiO_2/Al_2O_3 contents was investigated by Mao *et al.* [57]. By mixing of a commercial methanol synthesis catalyst

(XNC-98, $CuO/ZnO/Al_2O_3$) with zeolite HMCM-22 with different SiO_2/Al_2O_3 ratios as a methanol dehydration catalyst, the hybrid catalysts were prepared. The prepared mixed catalysts were tested in a fixed-bed reactor operating at 40 bar and 260 ^{0}C with a feed gas mixture of H_2:CO=2:1 to which a small amount of CO_2 (2.2%) was also added. The SiO_2/Al_2O_3 ratio of the HMCM-22 zeolite was reported to be an important parameter for preventing the formation of by-products such as CO_2 and hydrocarbons. They reported that with the increase in the SiO_2/Al_2O_3 ratio of the HMCM-22 zeolite, the selectivity to DME increased steadily. The optimum DME selectivity at around 67.3% and CO conversion at around 93.6% were obtained with the value of SiO_2/Al_2O_3 ratio of 120 whereas the selectivity of CO_2 and hydrocarbons were about 29% and 0.1%, respectively. The high-silica HMCM-22 zeolite showed better performance, which can be attributed to decreasing of the strong Brønsted acid sites.

Celik *et al.* [58] studied direct DME synthesis over bi-functional catalyst by using the physical mixing of a commercial Cu-Zn catalyst (HIFUEL R120- Alfa Aesar) and a silicotungstic acid (STA) incorporated into mesoporous catalyst (TRC-75(L)). They tried to compare the catalytic performance of silicotungstic acid incorporated mesoporous TRC-75(L) catalyst with the conventional γ -alumina catalyst. They also investigated the effect of CO_2 on the feed stream. Catalytic activity tests carried out in a fixed bed tubular flow reactor operating at 50 bar and a temperature range of 250–400 ^{0}C with using two different gas mixtures (Mixture-1 and Mixture-2). Mixture-1 contained 50 % CO and 50 % H_2, whereas Mixture-2 contained 40 % CO, 10 % CO_2, and 50 % H_2. The experimental results showed that DME selectivity values were higher by using TRC-75(L), than commercial γ-alumina. They reported that presence of CO_2 in the feed stream led to significant improvement in DME selectivity. DME selectivity of about 0.85 was found in a temperature range 250-275 ^{0}C by using Mixture-2.

3. EXPERIMENTAL

3.1. Materials

3.1.1. Chemicals

The chemical reagents used for catalyst preparation are listed in Table 3.1. All chemicals used are research grade.

Table 3.1. Chemicals used for catalyst preparation.

Chemicals	**Formula**	**Source**	**Molecular weight g/mole**
Gamma Alumina	γ -alumina	Alfa Aesar	101.96
Copper (II) nitrate trihydrate	$Cu(NO_3)_2 \cdot 3H_2O$	Sigma Aldrich	241.60
Zinc nitrate hexahydrate	$Zn(NO_3)_2 \cdot 6H_2O$	Sigma Aldrich	297.49
Aluminum nitrate nonahydrate	$Al(NO_3)_3 \cdot 9H_2O$	Sigma Aldrich	375.13
HiFUEL R120	Copper based methanol reforming catalyst	Alfa Aesar	-
Sodium carbonate	Na_2CO_3	Merck	105.99
Zeolite	microporous, aluminosilicate	Sigma Aldrich	-
Aluminosilicate, mesostructured MCM-41	SiO_2/Al_2O_3	Sigma Aldrich	-
Phosphotungstic acid hydrate	$12WO_3 \cdot H_3PO_4 \cdot x H_2O$	Sigma Aldrich	2880.05
Cerium(III)nitrate hexahydrate	$Ce(NO_3)_3 \cdot 6H_2O$	Sigma Aldrich	434.22

3.1.2. Gases

All of the gases used in this research were supplied by Birleşik Oksijen Sanayi (BOS) A.Ş. and Linde Group, Istanbul. Table 3.2 and Table 3.3 list the specifications and applications of the liquids and gases employed in this research.

Table 3.2. Applications and specifications of the liquids used.

Liquid	**Specification**	**Application**
Water	Deionized (DI)	Aqueous solution

Table 3.3. Specifications and applications of the gases used in the study.

Gas	**Specification (%)**	**Application**
Helium	99.998 Linde	GC/MS Carrier Gas
Argon	99.995 BOS	GC Carrier Gas
Carbon monoxide	99.999 BOS	Reactant
Nitrogen	99.998 Linde	Inert
Hydrogen	99.995 BOS	Reactant, Reducing Agent
Carbon dioxide	99.995 Linde	Product, GC calibration
Methane	99.995 BOS	Product, GC calibration
Dry Air	78.4% N_2+21.5% O_2 Linde	Automated pneumatic valve operation

3.2. Experimental Systems

The experimental systems used in present work can be described in mainly four groups:

- Catalyst Preparation Systems: The system used in this part of the work consists of two different set-ups for catalyst preparation by both co-precipitation and incipient-to-wetness impregnation methods.

- Catalyst Characterization Systems: This group involves energy dispersive X-ray spectroscopy (EDX) and scanning electron microscopy (SEM) used and the systems used to characterize the chemical structure of the catalyst samples prepared and to examine the changes during and/or after reaction.

- Catalytic Reaction System: The Autoclave Engineers' BTRS-Jr-PC reaction system was used in the experiments. The system involves a tubular reactor with an internal diameter of 1/4 inch, mass flow controllers for automated delivery of reactants and a heated transfer line to the gas chromatograph. A computer equipped with Programmable Logic Controller (PLC) and HMI software performs data collection and allows for the remote control of system functions.

- Product Analysis System: Identification of the reaction products and the quantitative analysis of each component, both in the reactor effluent and feed stream, were performed by Shimadzu GC-2014 and Shimadzu GCMS-QP2010 that are connected on-line to the Autoclave Engineers' BTRS-Jr-PC reaction system. In addition, the liquid products are analyzed offline for determining their compositions by using Shimadzu GCMS-QP2010.

3.2.1. Catalyst Preparation Systems

3.2.1.1. Coprecipitation System. The system used for co-precipitation method, as shown in Figure 3.1, consists of a Nüve BS-302 water bath, a 400 ml beaker, a Heidolph impeller, a Mettler Toledo pH-meter and a MasterFlex computerized-drive peristaltic pump.

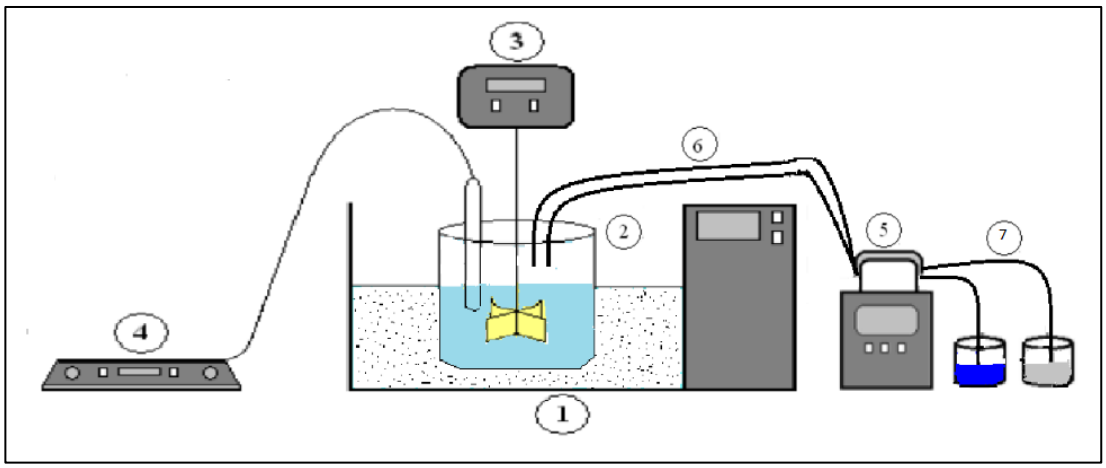

(1) Ultrasonic mixer or water bath, (2) Beaker, (3) Impeller, (4) pH-meter, (5) Peristaltic pump, (6) Silicone tubing, (7) Reactant Storage Tanks

Figure 3.1. Schematic diagram of co- precipitation system [59, 60].

3.2.1.2. Impregnation System. The system used for incipient-to-wetness impregnation, as shown in Figure 3.2., includes a Retsch UR1 ultrasonic mixer, a vacuum pump, a Büchner flask and a MasterFlex computerized-drive peristaltic pump.

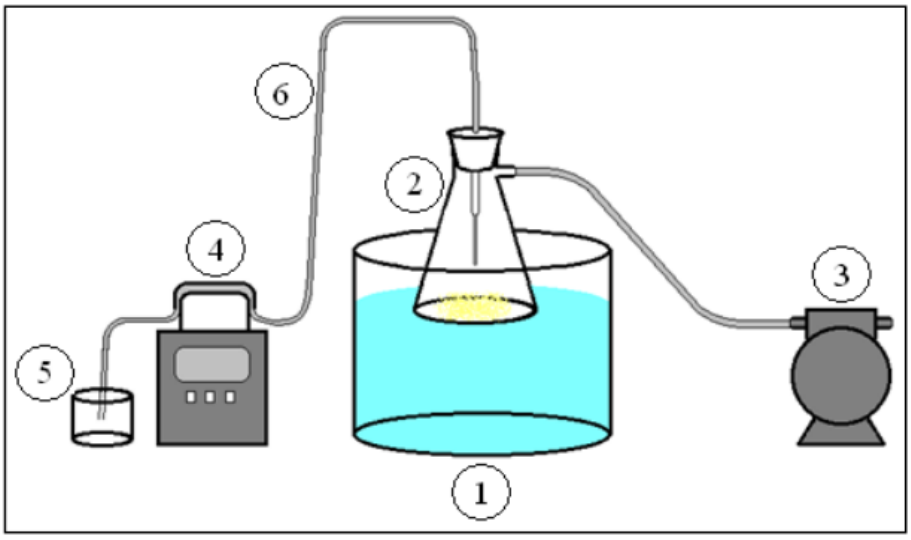

(1) Ultrasonic mixer, (2) Büchner flask, (3) Vacuum pump, (4) Peristaltic pump, (5) Precursor solution, (6) Silicone tubing.

Figure 3.2. Schematic diagram of the impregnation system [59].

3.2.2. Catalyst Characterization Systems

Synthesized catalysts were characterized by using several techniques to understand the chemical structure of the catalysts. In the scope of this study, energy dispersive X-ray spectroscopy (EDX) and scanning electron microscopy (SEM) were used. All experiments were performed at the Advanced Technologies Research and Development Center of Boğaziçi University.

3.2.2.1. Scanning Electron Microscopy (SEM). The microstructure, morphology and composition of freshly reduced and spent catalysts were studied by scanning electron microscopy (SEM). The tests were conducted in a Philips XL 30 ESEM-FEG system, having a maximum resolution of 2 nm.

3.2.2.2. Energy Dispersive X-ray Spectroscopy (EDX). For the energy dispersive X-ray spectroscopy (EDX), SEM instrument Philips XL 30 ESEM-FEG was used.

3.2.3. Catalytic Reaction System

The catalytic activity tests were conducted in a commercial high pressure set-up containing a 5 ml fixed-bed tubular continuous flow reactor (BTRS–Jr-PC, Autoclave Engineers Inc.). The AE BTRS-Jr-PC is a high temperature and high pressure laboratory system that can handle reactor pressures up to 100 bar and reactor temperatures up to 650 ^{0}C, as shown in Figure 3.3 and Figure 3.4 Schematic process diagram of this system is also depicted in Figure 3.5.

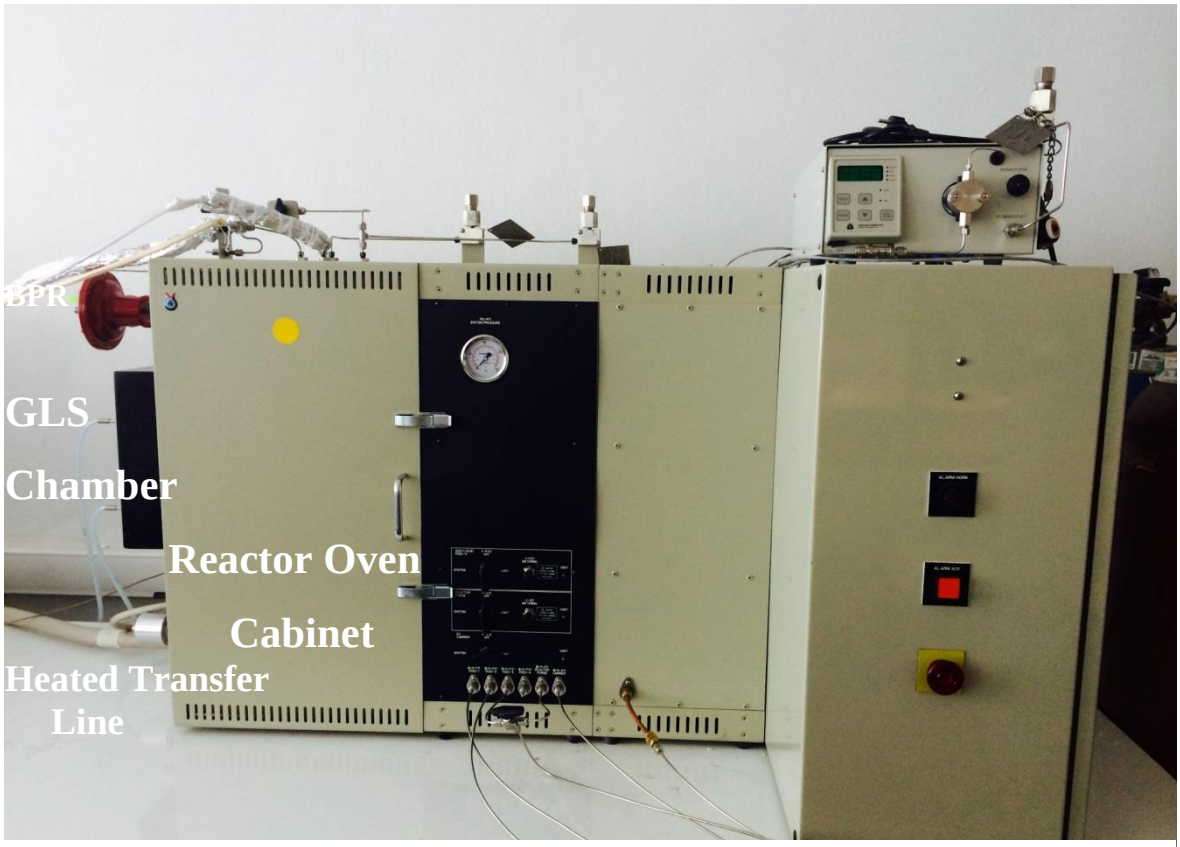

Figure 3.3. The AE BTRS-Jr-PC System.

The AE BTRS-Jr-PC reactor system is composed of three main parts:

- Reactant Preparation (feed mixing, heating and reactor status valve)
- Reactor
- Product Handling (gas liquid separation vessel, back pressure regulator, GC sampling valve and GC transfer line)

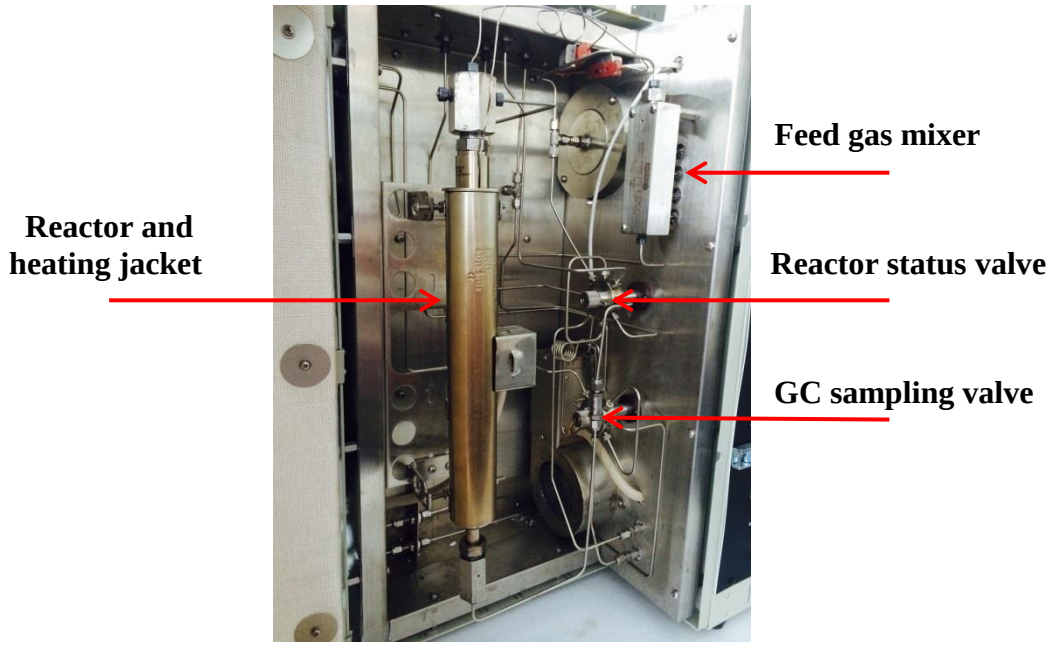

Figure 3.4. The AE BTRS-Jr-PC System oven cabinet.

Detailed description of these sub-systems is given in the following sections. The AE BTRS-Jr-PC reactor system is a bench-top reactor constructed entirely of 316 stainless - steel (SS). This system allows for accurate and automatic control of the process, including implementing set point changes (reactor temperature, pressure and reactant gas flow rates), switching valve positions for reactor status and sample valves, activating alarms and shutting down the system in the event of a dangerous operating condition by Programmable Logic Controller (PLC) and HMI software running on a standard desktop computer. The (PC) workstation (using Wonderware software HMI) acts as an interface between the operator and the system, facilitating manual entry of set point changes. The computer automatically starts the HMI software and establishes communications with the PLC in the BTRS-Jr-PC control panel. A screenshot of this software program is shown in Figure 3.6.

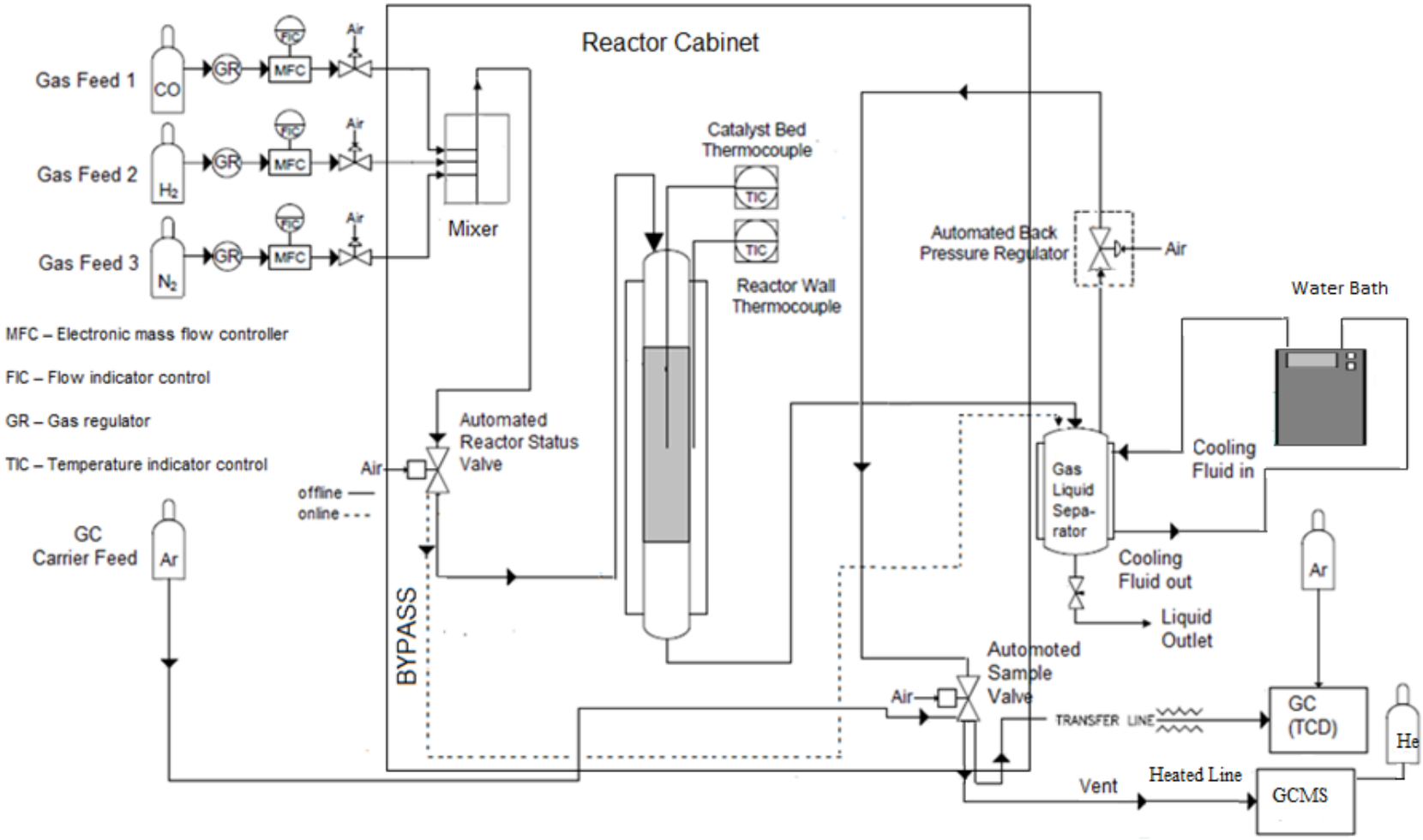

Figure 3.5. Schematic Diagram of the AE BTRS-Jr-PC (adapted from [61]).

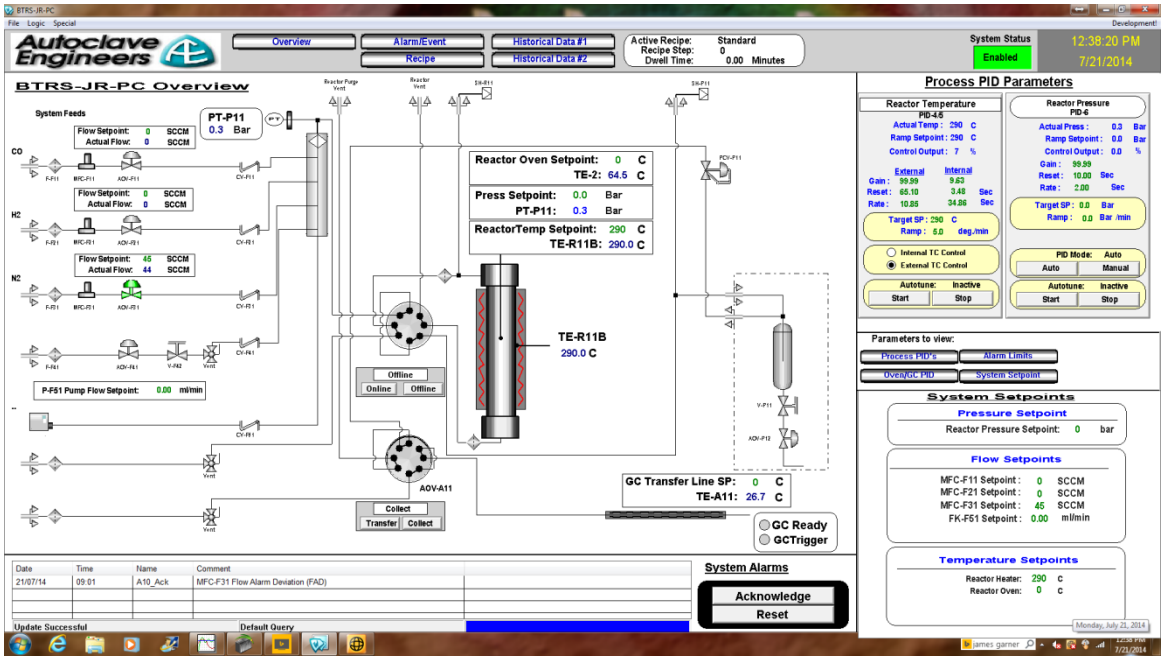

Figure 3.6. Screenshot of software program used for controlling the BTRS Jr-PC.

3.2.3.1. Reactant Preparation. The high purity gas inputs (hydrogen, carbon monoxide and nitrogen), GC sample carrier gas (argon), and air (for automated pneumatic valve operation in the reactor system) are supplied by pressurized cylinders and are passed through the gas flow regulators. The inputs are situated in the middle of the unit. Gas flow rates are metered by Brooks Instrument Model number 5850TRG mass flow controllers and their set points are adjusted by the programmable logic controller (PLC). Next, the feed gases enter the mixer-vaporizer where they are homogenously mixed and heated to the desired temperature. The mixer-vaporizer is located inside the reactor oven cabinet.

After being mixed and pre-heated, the homogenous feed passes through reactor status valve, a 2-position 8-port valve located in the reactor oven cabinet, facilitating the option of either diverting pre-mixed feed stream ‘off-line’ for feed analysis, or directing it to the reactor system for reaction. However, after detailed practising, it was found that reactor status valve display in the HMI screen was ‘off-line’ when reactor was actually ‘on-line’. Detailed description of the major challenges encountered during start-up of the AE BTRS-Jr-PC is given in Section 3.5.1.

3.2.3.2. Reactor. The AE BTRS-Jr-PC consists of one tubular reactor and one furnace assembly. The reactor assemblies include:

- A type 316 stainless steel tube (7.9 mm I.D. x 14.3 mm O.D. x 27.94 cm, V= 5 cm^3)
- A ceramic heating jacket
- An internal catalyst bed thermocouple
- An external reactor wall thermocouple

The electric resistance heater is located on the exterior of a metal jacket. The electric resistance heater zone has two thermocouples, which are connected to the PLC and are used to set and monitor reactor temperature. One of the thermocouples is Type "K" which is located within an axial 316 stainless steel thermowell, extending from the top of the reactor downward through the catalyst bed. The other is a Type "K" thermocouple located on the furnace wall. Both of them are located horizontally at the center of the furnace. The reactor temperature is controlled from the bed thermocouple.

3.2.3.3. Gas Liquid Separator. After leaving the reactor, the gases flow into the Gas Liquid Separator (GLS), which is a heat exchanger with 150 ml reactor. The GLS unit is located outside of the oven (Figure 3.3 and Figure 3.5). The product gases enter the GLS through a dip tube in the top and then exit through a tee in the top. The heat exchanger is equipped with copper coils for water cooling. Continuous supply and temperature of the cooling water is maintained by an external circulating water bath (Nüve BS-302) with cooling function. An air operated valve and a metering valve are connected to the bottom of GLS vessel to drain the condensed liquids.

3.2.3.4. Back Pressure Regulator. After the GLS section, the product stream passes through a back pressure regulator. This regulator is automatically controlled by the PLC to maintain the desired pressure set-point entered in the HMI overview screen. System pressure is monitored by an isolated pressure gauge/transducer. The back pressure regulator is located on the top left hand side of the unit (Figure 3.3 and Figure 3.5).

3.2.3.5. GC Sampling Valve (optional). After the back pressure regulator, the product stream then enters the GC Sampling Valve (Figure 3.3 and Figure 3.5). This valve is normally in the 'collect' position and the product stream passes through the sample loop with 1 ml volume and then flows through the vent. Simultaneously, the GC carrier feed gas (argon) flows through a heated transfer line connected to the on-line GC-2014, providing carrier gas flow for the installed Carboxen-1000 packed column. Alternatively, when the sample valve is in the 'transfer' position, the GC carrier feed gas (argon) pushes the sample trapped in the sample loop to the heated transfer line and on to the on-line GC-2014 for analysis. Concurrently, sample gases are directly vented from the system, as illustrated in Figure 3.7.

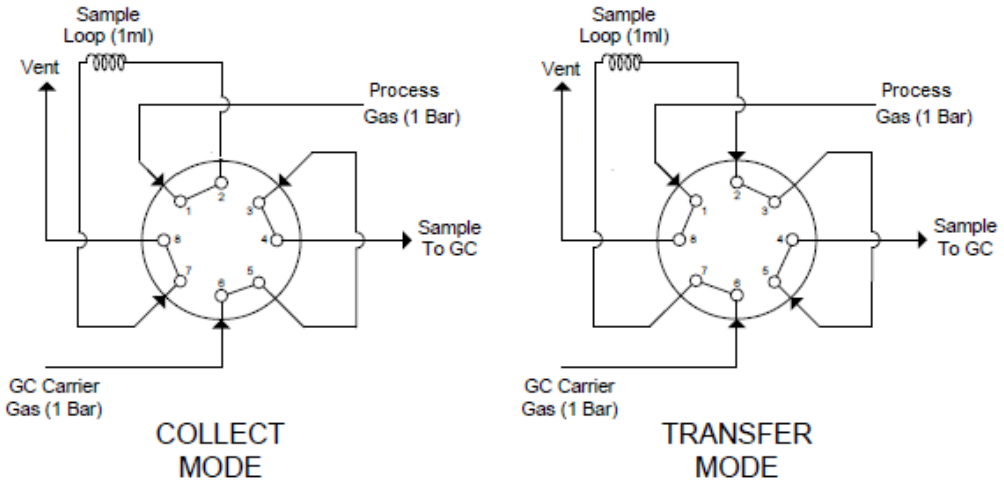

Figure 3.7. GC Sampling Valve Connections.

3.2.3.6. Transfer Line. The GC sampling valve directs the product gases to a heated transfer line (maximum T = 180ºC). This line is an insulated, stainless steel microbore tube about 3 meters long. The temperature of the transfer line (and of the product gases) is controlled by entering the desired set point in the HMI overview screen, as shown in Figure 3.6.

3.2.3.7. BTRS Oven. The reactor, mixer tubing, switching valves, and system tubing are all housed in a heated, insulated, stainless steel oven which allows for isothermal operation (maximum temperature of 250 ^{0}C). The oven temperature is controlled via the oven temperature set-point in the HMI screen, as shown in Figure 3.6.

3.2.4. Product Analysis System

Two types of analysis equipment are employed for the identification and quantification of feed and products; an online GC analyzer (Shimadzu GC-2014) for the analysis of permanent gases and an offline/online GC/MS analyzer (Shimadzu GCMS-QP2010) for the analysis of products including CO_2, CH_4, and DME. The gas sample leaving the reactor (permanent gases, including CO, H_2 and N_2) during each experiment was automatically injected every 45 minutes via a heated transfer line (at 150ºC) into the online GC equipped with Carboxen-1000 packed column and a thermal conductivity detector (TCD). Simultaneously, gas sample leaving the reactor vent (other gases, including CO_2, CH_4 and DME) was analyzed using the online GCMS-QP2010 gas chromatography via another heated line, whose temperature control is carried out by an external PID temperature controller. In addition, the liquid products condensed during the reaction in the GLS are analyzed offline for their compositions by injecting the liquid sample using a syringe into GCMS-QP2010 gas chromatography manually. Analysis conditions of the GC-2014 and GCMS-QP2010 are given in Table 3.4 and Table 3.5.

Table 3.4. Reactant and product gas analysis conditions for GC-2014.

GC Property	**Attribute/Value**
Detector type	TCD
Column temperature	40 ^{0}C for 14 min, 40 -150 ^{0}C at 55 ^{0}C/min, 150 ^{0}C for 16 min
Injector temperature	100 ^{0}C
Detector temperature	175 ^{0}C
Carrier gas	Argon
Detector current	50 μA
Carrier gas flow rate	25 ml/min
Column packing material	Carboxen-1000, 80-60 mesh
Column tubing material	Stainless steel
Column length & ID	6 m & 3 mm

Table 3.5. Product gas analysis conditions for GCMS-QP2010.

GC-MS Property	**Attribute/Value**
Detector type	Mass Spectrometer Detector
Column type	Rt-Q-Bond Capillar
Carrier gas	Helium
Column length, ID and thickness	30 m, 0.53 mm and 20 μm
GC part	
Column temperature	35 ^{0}C for 5 min 35 -150 ^{0}C at 50 ^{0}C/min 150 ^{0}C for 10 min
Injector temperature	220 ^{0}C
Injection mode	Split
Column flow	3 ml/min
Split Ratio	50
Total analysis time	17.30 min
MS part	
Ion source temperature	220 ^{0}C
Scan speed	769 m/z
Solvent cut time	0.6 min

3.3. Catalyst Preparation and Pretreatment

Catalyst mixtures composed of two methanol synthesis catalysts ($Cu/ZnO/Al_2O_3$, commercial Cu–Zn based HiFUEL R120 catalyst) and various methanol dehydration components (δ -Al_2O_3, zeolite, MCM-41 type SiO_2/Al_2O_3, phosphotungstic acid hydrate (PTA) and 20wt% ceria-modified δ -Al_2O_3) were used in the experiments. In the present study, catalysts used for direct synthesis of DME can be listed as follows:

- Bi-functional HiFUEL R120/ δ-Al_2O_3 catalyst
- Bi-functional CuO-ZnO-Al_2O_3/ δ-Al_2O_3 catalyst
- Bi-functional HiFUEL R120-SiO_2/Al_2O_3 catalyst
- Bi-functional HiFUEL R120/ Zeolite catalyst
- Bi-functional HiFUEL R120/Phosphotungstic acid hydrate (PTA) catalyst
- Bi-functional HiFUEL R120-20% CeO_2/δ-Al_2O_3 catalyst
- 2wt%Pd-20wt%CeO_2/ γ- Al_2O_3 catalyst

CuO-ZnO-Al_2O_3 and 20wt% ceria-modified γ-Al_2O_3 were synthesized in our laboratory. 2wt%Pd-20wt%CeO_2/ γ-Al_2O_3 catalyst was synthesized by Ertem [68] in our laboratory. The other components (γ- Al_2O_3, HiFUEL R120, zeolite and SiO_2/Al_2O_3) were supplied externally. Catalysts synthesized in our laboratory are explained in detail below. Moreover, bi-functional catalyst beds prepared by dry physical mixing are also described.

3.3.1. Preparation and Pretreatment of $CuO/ZnO/Al_2O_3$

Ternary $CuO/ZnO/Al_2O_3$ catalyst was prepared by modifying of co-precipitation method reported by Baltes *et al.* [62] and Schüth *et al.* [63] in the system described in Figure 3.1. A solution of metal nitrates [($Cu(NO_3)_2$ (0.6 mol/L), $Zn(NO_3)_2$ (0.3 mol/L), Al $(NO_3)_3$ (0.1 mol/L))] and a solution of Na_2CO_3 (1 mol/L) as a precipitant were pumped by MasterFlex computerized-drive peristaltic pump (at constant flow rate of 5 ml/min) into a stirred and heated glass reactor with a starting volume of 200 ml of deionized water. Precipitation of 1 M metal solutions was made with the 40 ml solution. Such a solution required the addition of 0.04 mole of metals to the solution. During the precipitation process, pH and temperature were kept constant at 70 ^{0}C and 7, respectively. While the

metal nitrate solution was being pumped continuously, the sodium carbonate solution was added to maintain a constant pH (±0.2 unit), controlled by a Mettler Toledo pH meter. The co-precipitation was stopped when 40 ml of metal nitrate solution has been added. The pH was kept constant at 7 also during the aging process through the controlled addition of metal nitrate or sodium carbonate solution.

After aging for 1 h, main solution was allowed to cool to room temperature. After that, the precipitates were filtered and washed three times with 150 ml of deionized water each. During the washing step, the precipitates were fed to the washer and resultant precipitant was accumulated on the filter. The precipitant was then dried overnight at 80 °C under vacuum and calcined with air in a muffle furnace at 350 °C for 4 h. This catalyst was named CZA. The schematic diagram of the procedure is also given in Figure 3.8.

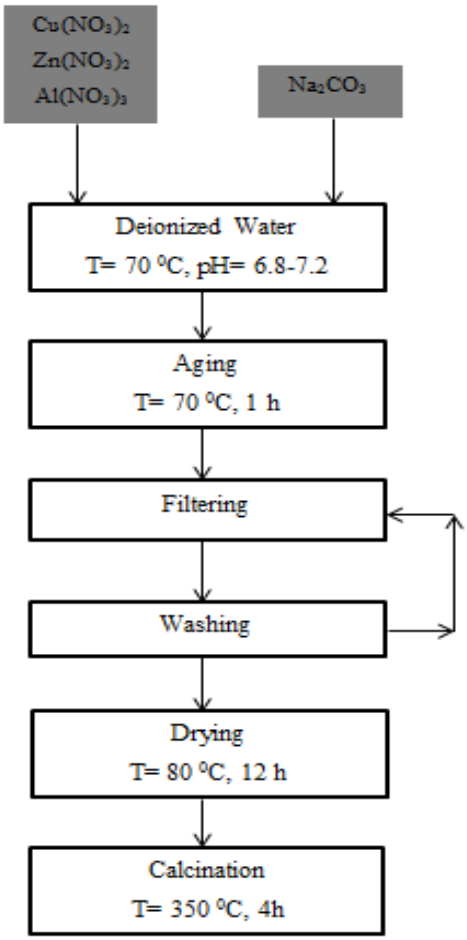

Figure 3.8. Schematic diagram of preparation recipe (adapted from Erena *et al.* [64]).

3.3.2. Preparation and Pretreatment of 20wt% ceria-modified δ -Al_2O_3 catalyst

γ-Al_2O_3 is a high surface area material. However, it is reported to have low stability and tends to facilitate carbon formation in the presence of steam due to its high acidity. The most thermally stable version of alumina is obtained when γ-phase is transformed into α-phase at temperatures greater than 1100 °C. However, its low surface area, which is less than 5 $m^2.g^{-1}$, is likely to end up with poor catalytic activities due to the low dispersion of active metals. Hence using a support such as δ-alumina – an intermediate phase between γ and α - having relatively low acidity and an acceptable surface area can be optimum in terms of obtaining an efficient catalytic performance [65, 66].

Commercial γ-Al_2O_3 (Alfa Aesar) was crushed and sieved into 45-60 mesh size (344-255 μm), and crushed particles were first dried at 200 °C for 2 hours followed by calcination at 900 °C for 4 hours. BET surface area of the δ-Al2O3 support obtained was found as 81.6 m^2 [67].

Ceria addition to alumina support was conducted via incipient to wetness impregnation method in the system described in Figure 3.2. A certain amount of alumina support was put in a vacuum flask and was kept under vacuum in the first step. The support material in the vacuum flask was mixed under vacuum with an ultrasonic mixer for 30 minutes before impregnation. The calculated amount of aqueous solution of $Ce(NO_3)_3$ hydrate was dissolved in deionized water on the basis of 1 g alumina/1.1 ml solution. Aqueous $Ce(NO_3)_3$ hydrate solution was fed to the vacuum flask at a flow rate of 0.5 $ml.min^{-1}$ via a silicone tubing using a Masterflex computerized-drive peristaltic pump. The slurry was mixed ultrasonically during impregnation to maintain uniform distribution of the aqueous $Ce(NO_3)_3$ hydrate solution. After all the solution was fed, the mixing was continued for an additional 1.5 h. The resulting slurry was dried at 120 °C overnight before being calcined in air at 325 °C for 4 h to obtain the 20wt%Ce modified δ-Al_2O_3 catalyst.

3.3.3. Dry-Physical Mixing Catalysts

In the direct synthesis of dimethyl ether, bi-functional catalysts containing methanol synthesis and dehydration components are needed. One function is to synthesize methanol

from the synthesis gas whereas the other function is to convert the synthesized methanol into the dimethyl ether. These components were synthesized separately during the preparation of catalysts process.

A commercial methanol reforming catalyst was used as methanol synthesis catalyst. A methanol reforming catalyst is represented by general formula $(CuO)_w(ZnO)_x(Al_2O_3)_yM_z$ where M indicates one of the oxides selected from the group of lanthanum oxide, gallium oxide, cerium oxide and chromium oxide. Since methanol synthesis reaction is favorable over the catalysts comprising copper, zinc and aluminum metals, this commercial methanol reforming catalyst was decided to use for the preparation of direct DME synthesis catalysts. Commercial catalysts were in the pellet form (5.2mm x 3.0mm) so that catalyst was crushed and sieved into 45-60 mesh size (344-255 μm) before reaction.

A hybrid bi-functional catalyst was formed by physical mixing methanol synthesis and methanol dehydration catalysts. For this reason, the synthesized methanol synthesis co-precipitated catalyst ($CuO/ZnO/Al_2O_3$) or methanol reforming catalyst (HiFUEL R120) were mixed with one of the methanol dehydration catalysts (δ -Al_2O_3, MCM- 41 type SiO_2/Al_2O_3, zeolite (microporous), phosphotungstic acid hydrate (PTA) and 20wt%ceria-modified δ-Al_2O_3). As reported in the literature, γ-Al_2O_3 tends to facilitate carbon formation in the presence of steam due to its high acidity. For this reason, when γ-Al_2O_3 was used for methanol dehydration component, it was transformed to δ-Al_2O_3 by drying γ-Al_2O_3 at 200°C 2 h and then calcining it at 900°C for 4 h in a muffle furnace to obtain high catalytic performance. Therefore, δ -Al_2O_3 was used as methanol dehydration function in the experiments.

3.4. Reactor Tube Catalyst Packing

In order to pack the 5 ml reactor, the reactor tube is removed from the furnace and both the old catalyst and packing material (glass wool) are removed, if any, from the tube. The tube is then cleaned with lab grade solvents and dried.

Firstly, a small amount of glass wool is inserted into adapter coupling in order not to block the flow path. Next, 2 mm borosilicate beads are dropped onto the glass wool and

following a layer of glass wool is again inserted and pushed the layer onto the glass beads. After filling the tube with glass beads, the tube is gently tapped on the bench top to settle the material. The glass bed layers aid holding the packing in place against high pressure effect. Next, the tube is filled with the required amount of catalyst and followed by inserting glass wool layer. The packing should not be squeezed, otherwise flow through the tube is impeded, leading to a problem when the system is pressurized. This devised packing method is illustrated in Figure 3.9.

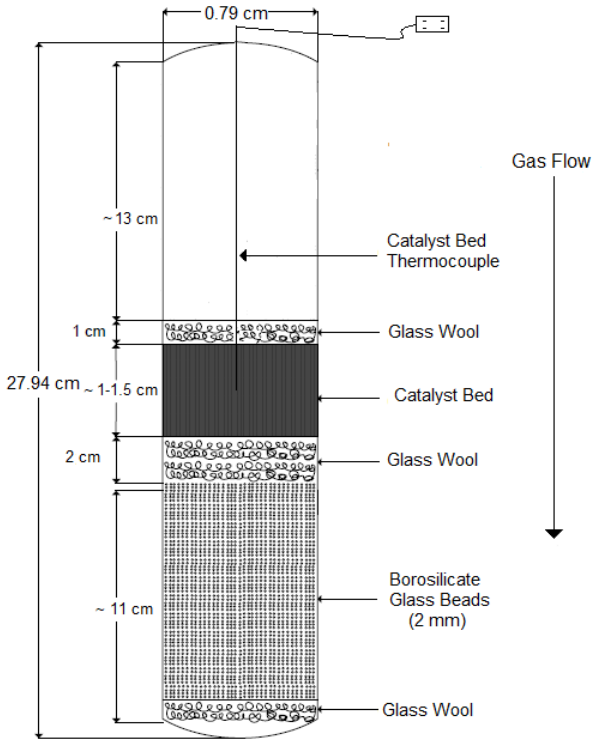

Figure 3.9. 5 ml reactor loading method.

The packed reactor is then reinstalled the furnace and re-connected to the automated reactor system, and is ready for the experiment.

3.5. Catalytic Activity Experiments

3.5.1. Preliminary Work

3.5.1.1. Commissioning of the BTRS-Jr-PC Reactor System. The BTRS-Jr-PC reactor system was installed on a lab bench top. However, a commissioning process was required

for the equipment. This commissioning process involved pressurizing the system with nitrogen to check for leaks, as well as checks for overall mechanical and electrical functionality. After all the installations were completed, numerous hardware challenges were faced during the operation phases of the equipment.

Firstly, the system was pressurized with nitrogen by inserting set value in the HMI overview screen. However, pressure test failed and resolution about the pressurizing problem was mediated with Autoclave Engineers (AE) personnel. The problem was resolved by modifying the fitting of the inlet liquid pump to the mixer. Then, all the flow paths of the system were checked for leaks by pressurizing the system about 3.5-4 bar and no leaks were detected.

Next, GC carrier gas flow rate was adjusted manually about 25 ml/min for the inlet flow of GC column since there is no mass flow controller for GC carrier gas. After that, a sample was sent to the on-line GC-2014 for analysis, but no peaks were observed. Technical service attempts were unsuccessful to define the problem at first. After nearly two weeks, the problem was resolved by modifying GC carrier gas flow rate for the exit flow of GC column via technical service.

Then, the system pressure was tried to perform higher pressure values such as 10-15 bar. After a long time, pressure tests failed due to the presence of severe leakage. Previously, leaks were checked under low pressure values (3-4 bar) so that their locations were not detected. This problem was also resolved with AE personnel consultation. Each connection was checked for leaks via a blind plug at high pressure values. After leaks were fixed, the system was pressurized successfully.

After the pressurizing problem was sorted out, the circuit breaker of the heater tripped. The circuit breaker was reset and then when the system energized, it tripped again. The root cause of the problem making the circuit breaker trip was found to be the wires in the heater connection (the part that screwed in to connect) that broke free. After this connection was fixed, the system was heated properly. Finally, the system was ready to begin experimental run.

After some experimental runs, a problem was found related to reactor status valve. According to BTRS-Jr-PC manual, if the reactor status valve is energized, namely in the *online* position, the reactant stream is diverted to the reactor for reaction whereas if the reactor status valve is not energized, namely in the *offline* position, reactor is placed in the bypass position. However, after some experimental runs were performed, data collected from gas chromotography were not logical. In order to understand the direction of flow paths through the reactor status valve, flow paths were checked using a soap bubble flow meter. As a result, it was found out that reactor status valve display in the HMI screen was *off-line* when reactor was actually *on-line*. The experiments were operated at *off-line* position.

3.5.1.2. Gas Chromatograph Calibration. Before starting the catalytic activity experiments, a Shimadzu GC-2014 was calibrated by injecting known amounts of each species (CO, H_2 and N_2) separately to the chromatographic column under the conditions given in Table 3.4. By recording the corresponding retention time and the area under the peak calculated by integration, micromole versus peak area graphs were constructed for each gas and the corresponding calibration factors were determined by linear regression.

Identification and quantification of DME, methane and carbon dioxide was performed by GCMS-QP2010. Methane and carbon dioxide were calibrated by injecting known amounts of each species separately to the chromatographic column under the conditions given in Table 3.5. By recording the corresponding retention time and the area under the peak calculated by integration, micromole versus peak area graphs were constructed for each gas and the corresponding calibration factors were determined by linear regression. The following expression was used to evaluate the molar percentage of DME via the ionization cross-section method using the following equation:

$$N_i = N_{ref} \frac{M_{ref}}{M_i} \frac{A_i}{A_{ref}} \frac{Q_{ref}}{Q_i} \tag{3.1}$$

where subscript “i” and “ref” correspond to the quantified species and reference compound, respectively. N is the number of moles of species, M is molecular weight and A

is the area under the peak obtained from GCMS-QP2010. For dimethyl ether, methane is taken as reference compound. Q is the total ionization cross section calculated using the method described by Fitch and Sauter *et al.* [68]:

$$Q = 0.943 + \sum a_j n_j \tag{3.2}$$

a_j is the contribution of atom j to the ionization cross-section while n_j is the number of j atoms in the molecule. The contributions of some of the atoms determined by Fitch and Sauter *et al.* [68] are given in Table 3.6.

Table 3.6. Contributions of Various Atoms to Total Ionization Cross Section [68].

Atom	Contribution (a)
C (sp^3)	2.12
C (sp^2)	1.70
C (sp)	0.85
H	0.38
O (sp^3)	1.26
O(sp^2)	0.62

Furthermore, the liquid products condensed during the reaction in the GLS are analyzed for their compositions on the offline GCMS-QP2010.

3.5.2. Reaction Tests

Prior to activity tests, the bi-functional catalysts were reduced *in situ* with 50 ml/min (10% H_2/N_2) at atmospheric pressure according to a specific heating program. First, the catalyst bed was heated from room temperature to 300 ^{0}C with heating rate 5 ^{0}C/ min under 45 ml/min N_2 flow. At 300 ^{0}C, 5 ml/min hydrogen was introduced in addition to N_2 flow. The temperature was kept constant at 300 ^{0}C for 2 h. After reduction, the system was

allowed to cool down or keep constant to the reaction temperature (250, 275 and 300 ^{0}C) under 45 ml/min N_2 flow for about 1 h.

Catalyst amount charged to the reactor was 0.4 gr and reactant gas flow rate was adjusted to 100 ml/min. Space time based on this flow rate at atmospheric pressure and temperature, and gas hourly space velocity (GHSV) were 0.24 g.s/ml and 15000 ml/(g_{-cat} h), respectively. A feed gas having the composition of H_2/CO/N_2= 64/32/4 volume ratio was used for most of the experiments. N_2 was added to the feed as an internal standard. The type of catalyst, reaction temperature and pressure, H_2/CO ratio and metal to acid weight ratio were changed in order to see the effects of different parameters on the catalyst activity. All the conditions in the reaction experiments are listed in Table 3.7.

Steady state was reached in usually 2 h for most of the experiments. Mostly six successive data points at steady state were taken and averages of these values were used in the conversion and selectivity calculations. Carbon monoxide and selectivity of the products were calculated.

The CO conversion (X_{CO}) was defined based on the molar flow rate of CO in the feed ($F_{CO,in}$) and in the outlet stream ($F_{CO,out}$), as follows:

$$Xco(\%) = \frac{Fco,in - Fco,out}{Fco,in} \times 100 \tag{3.3}$$

The product selectivities were defined as the ratio of moles of CO converted to a specific component to total moles of CO converted to the products. These were described as follows:

$$S_{DME}(\%) = \frac{2F_{DME}}{Fco,in - Fco,out} \times 100 \tag{3.4}$$

Table 3.7. The catalysts and the conditions used in the activity tests.

Exp., #	Catalyst	Temperature (^{0}C)	Pressure (bar)	Feed gas composition in N_2 as balance		(wt of metal catalyst/wt of acid catalyst)
				CO (vol%)	H_2 (vol%)	
1	HiFUEL R120/ δ-Al_2O_3	250	34	32	64	1:1
2		275	34	32	64	1:1
3		300	34	32	64	1:1
4		275	30	32	64	1:1
5		275	25	32	64	1:1
6		275	34	32	64	2:1
7		275	34	48	48	1:1
8	CZA/ δ-Al_2O_3	250	34	32	64	1:1
9		275	34	32	64	1:1
10		300	34	32	64	1:1
11	HiFUEL R120-SiO_2/Al_2O_3	250	34	32	64	1:1
12		275	34	32	64	1:1
13	HiFUELR120/ Zeolite	275	34	32	64	1:1
14	HiFUEL R120 /PTA	275	34	32	64	1:1
15	HiFUEL R120 - 20% CeO_2/δ-Al_2O_3	250	34	32	64	1:1
16		275	34	32	64	1:1
17	2wt%Pd-20wt%CeO_x/δ-Al_2O_3*	275	34	32	64	-

*Synthesized by Ertem [69].

$$Sco_2(\%) = \frac{Fco_2}{Fco,in - Fco,out} \times 100 \quad (3.5)$$

$$S_{CH4}(\%) = \frac{F_{CH4}}{Fco,in - Fco,out} \times 100 \quad (3.6)$$

Sample conversion and selectivity calculations are illustrated in the Appendix A.

4. RESULTS AND DISCUSSION

4.1. Catalyst Characterization Results

Freshly reduced HiFUEL R120/δ-Al_2O_3 and CZA/δ-Al_2O_3 were characterized by using scanning electron microscopy (SEM) coupled with energy dispersive X-ray spectroscopy (EDX) to obtain the microstructure, morphology and composition, and the amount of carbon deposit formed on their surface during reaction. Metal mapping studies were performed to understand the dispersion of metals and whether the agglomeration of metals occurs on the support surface during reaction. For commercial Cu–Zn based catalyst, HiFUEL R120 and CuO/ZnO/Al_2O_3 catalyst prepared by co-precipitation technique, referred to as CZA, a representative set of SEM-EDX test results, including bright area images of freshly reduced and spent samples, and metal mappings on their surface are given in Figures 4.1 and 4.2.

It can be seen from Figures 4.1a and 4.1b that very small particles were formed and much larger particles were also observed on HiFUEL R120. In these images, clusters are seen over the catalyst as white and shining spots. The metal mappings of the Cu and Zn (Figure 4.1c) confirm the well dispersion of Cu and Zn with a good homogeneity on freshly reduced sample whereas clustering over the catalyst was observed for alumina.

When it comes to the SEM micrographs of CZA catalyst shown in Figures 4.2a and 4.2b, it can be seen that very small particles were formed and much larger particles were also observed. The metal mappings of the Zn (Figure 4.2c) confirmed the well dispersion of Zn with a good homogeneity on freshly reduced sample whereas clustering over the catalyst was observed for both Cu and alumina particles (Figure 4.2c).

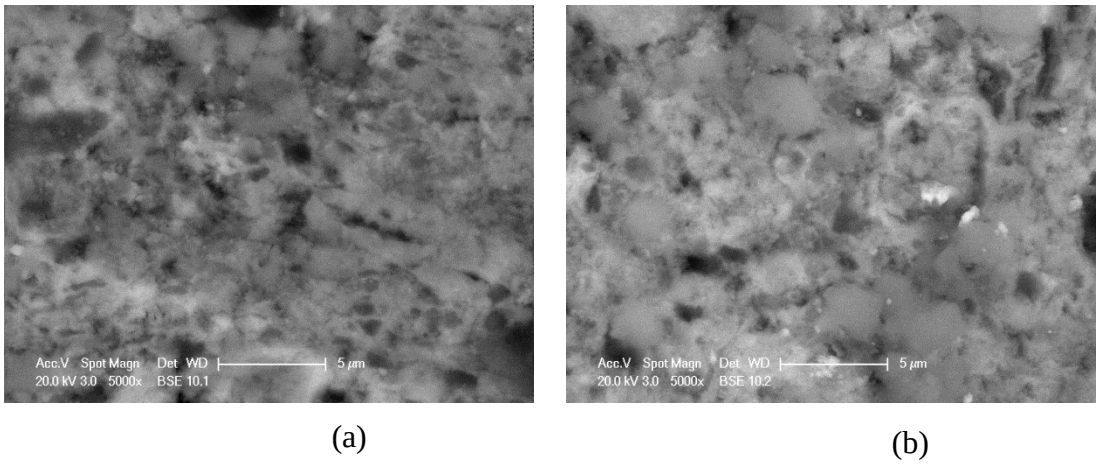

(a) (b)

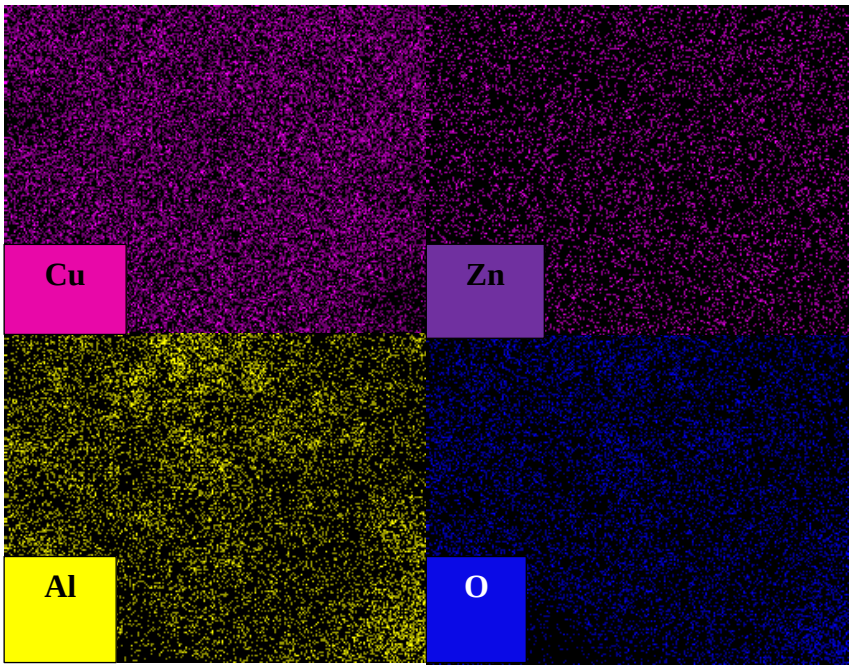

(c)

Figure 4.1. HiFUEL R120 catalyst (a) SEM bright area image of freshly reduced catalyst (b) SEM bright area image of the spent catalyst for feed stream: $CO/H_2/N_2$ =32/64/4, 34 bar, 275 ^{0}C (c) Cu-Zn-Al-O mapping of freshly reduced catalyst.

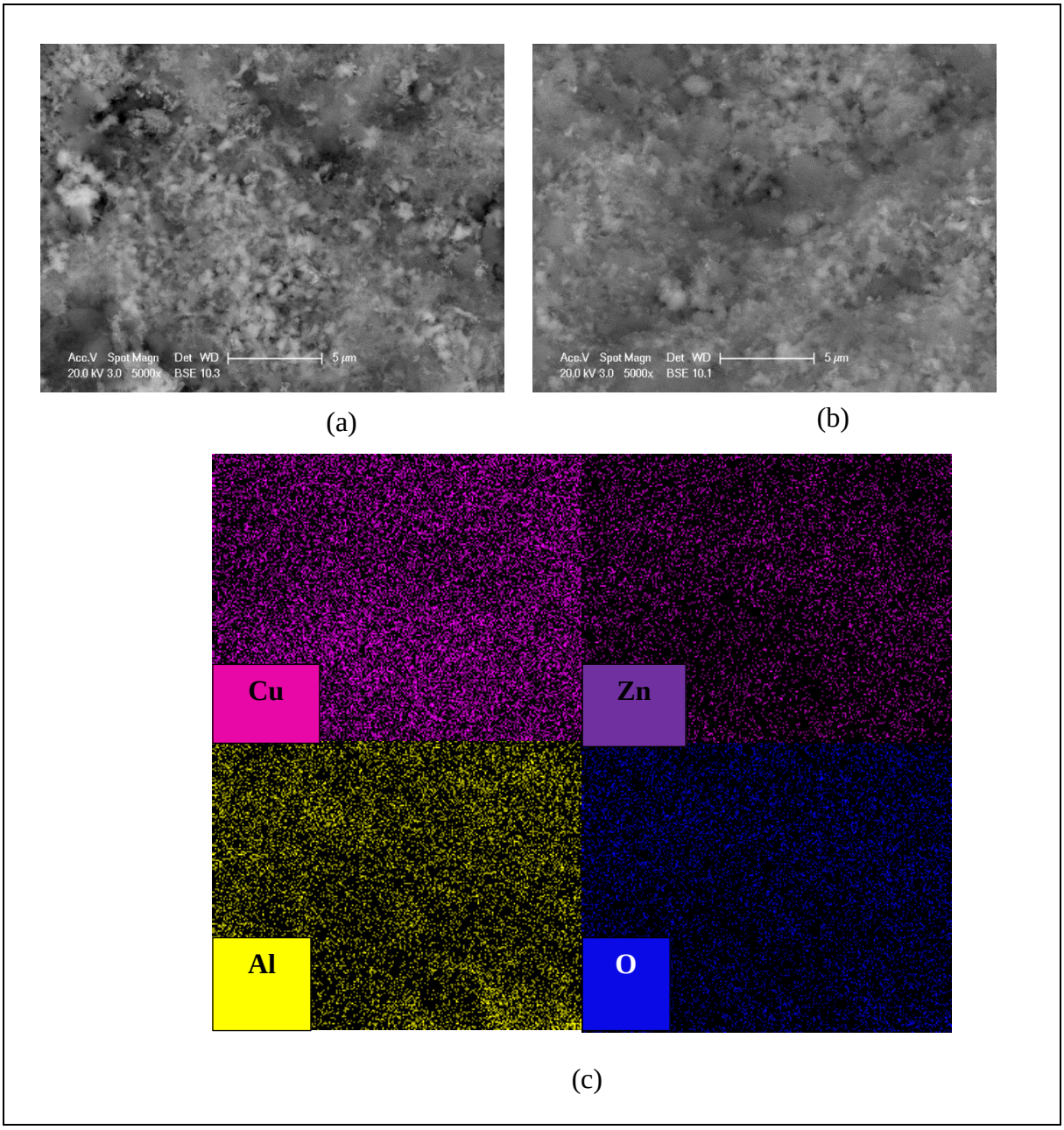

Figure 4.2. CZA catalyst (a) SEM bright area image of freshly reduced catalyst (b) SEM bright area image of the spent catalyst for $CO/H_2/N_2$ =32/64/4, 34 bar, 275 ^{0}C (c) Cu-Zn-Al-O mapping of freshly reduced catalyst.

It is well known that carbon deposition on the bi-functional catalyst during the direct synthesis of DME reaction plays a key role for catalyst deactivation. In order to estimate the amount of loadings and other surface species, EDX analysis was also conducted. When the HiFUEL R120 and CZA catalysts were compared, it was revealed that amount of carbon deposited over the surface of HiFUEL R120 catalyst was lower than that occurred

over the surface of CZA catalyst, which was confirmed by the EDX analyses, as shown in Table 4.1.

Table 4.1. EDX analysis results of HiFUEL and CZA catalysts.

Catalyst	Cu wt.%	Zn wt.%	Al wt.%	O wt.%	C wt.%
HiFUEL R120 (fresh)	51.2	21.9	13.7	13.2	-
HiFUEL R120 (spent)	50.7	19.9	13.4	12.9	3.3
CZA (fresh)	56.9	24.2	8.9	10.0	-
CZA(spent)	44.6	20.9	11.4	14.1	9.0

4.2. Catalyst Activity Results

In this section, the catalytic activity results of HiFUEL R120/ δ-Al_2O_3, CZA/δ-Al_2O_3, HiFUEL R120- SiO_2/Al_2O_3, HiFUEL R120/zeolite, HiFUEL R120/PTA, HiFUEL R120:20%wt.CeO_2/δ-Al_2O_3 and 2wt%Pd-20wt%CeO_2/γ-Al_2O_3 catalysts in direct synthesis of DME from synthesis gas are given. The carbon monoxide conversion and selectivity of the products are calculated for each catalyst and the results obtained are compared with respect to DME, CO_2 and CH_4 selectivities and carbon monoxide conversion for the same experimental conditions. The liquid products were usually comprised of a water phase (water plus soluble oxygenated compounds). When the oxygenated compounds were analyzed for their compositions offline in GCMS-QP2010, mostly methanol was observed. However, since the molar percentage of oxygenated compounds could not be calculated, the results of oxygenated compounds were not reported.

4.2.1. Catalytic Activity Results of HiFUEL R120/ δ-Al_2O_3

4.2.1.1. Effect of Temperature. The activity of HiFUEL R120/ δ-Al_2O_3 catalyst in direct synthesis of DME reaction was carried out in BTRS-Jr-PC operating at 34 bar and at three

different temperature values (250, 275 and 300 °C) for a feed gas composition of $CO/H_2/N_2$= 32/64/4. The bi-functional catalyst was prepared by dry physical mixing 0.2 gr of HiFUEL R120 and 0.2 gr of δ-Al_2O_3 catalyst. The stability of the activity of HiFUEL R120/ δ-Al_2O_3 under these conditions is presented in Figure 4.3.

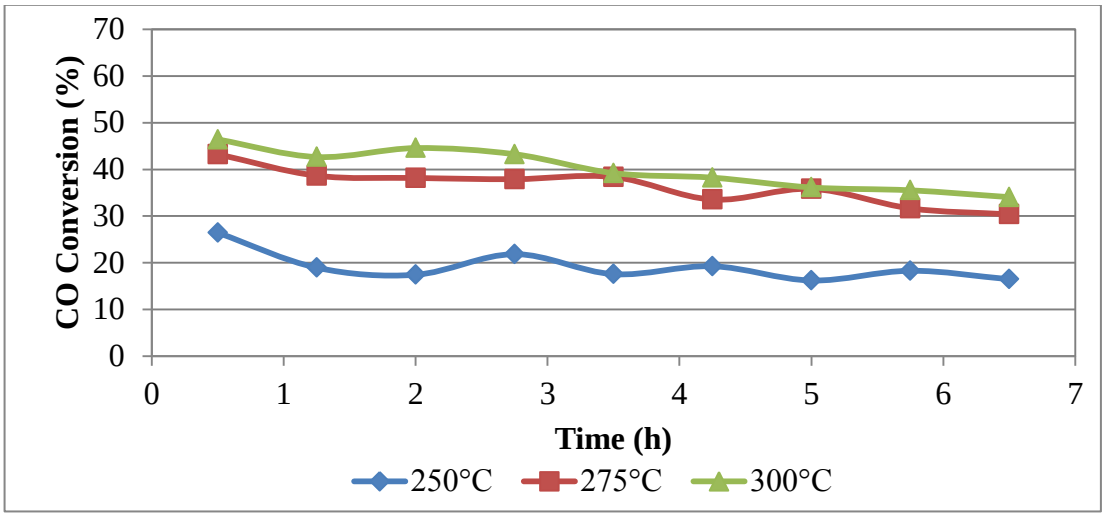

Figure 4.3. Evolution with time on stream of CO conversion for HiFUEL R120/ δ-Al_2O_3 ($CO/H_2/N_2$ =32/64/4, 34 bar, metal to acid ratio: 1/1).

As it can be seen from Figure 4.3, some decrease in activity was observed at all temperature values. These decreases with time on stream could be attributed to catalyst deactivation by coke formation and metal sintering via surface migration. This result is in line with the observations of Erena *et al.* [49]. They reported that coke was formed by degradation of intermediate oxygenates in methanol synthesis, which affected this reaction and favored the reaction of methanation, which was not affected by deactivation. In other words, methanation reaction occurs on Cu-ZnO-Al_2O_3 catalyst under conditions of high H_2 concentration. Methane is formed via the following reaction [49]:

$$CO + 3H_2 \leftrightarrow CH_4 + H_2O \quad (2.8)$$

Furthermore, water in the reaction medium may be responsible for the decrease in the activity of δ-Al_2O_3 acid function, given that it is adsorbed on these sites and competes with the reactants [47].

Steady state was reached in usually 2 h for most of the experiments. Mostly six successive data points at steady state were taken and averages of these values were used in the conversion and selectivity calculations. Carbon monoxide and selectivity of the products were calculated and the results are shown in Table 4.2. Sample conversion and selectivity calculations are illustrated in the Appendix A. The conversion of CO and selectivity of the products are presented in Figures 4.4 and 4.5, respectively.

Table 4.2. The results obtained with HiFUEL R120/ δ-Al_2O_3, which were calculated with respect to converted CO at temperature of 250, 275 and 300 °C for feed mixture of 32% CO, 64% H_2 and 4% N_2).

Temperature (^{0}C)	CO conversion (%)	DME selectivity (%)	CO_2 selectivity (%)	CH_4 selectivity (%)
250	18.1	27.5	16.9	3.8
275	35.1	34.0	12.3	4.1
300	38.7	22.5	13.1	15.0

As shown in Figure 4.4, when the temperature was increased from 250 to 275 ^{0}C, CO conversion increased significantly, whereas in the 275-300 ^{0}C range, the conversion of CO increased slightly. The slight increase in conversion as temperature was increased above 275 ^{0}C may be caused by the thermodynamic restrictions of the exothermic reaction (Reaction 2.2) and Cu sintering leading to partial loss of catalyst activity.

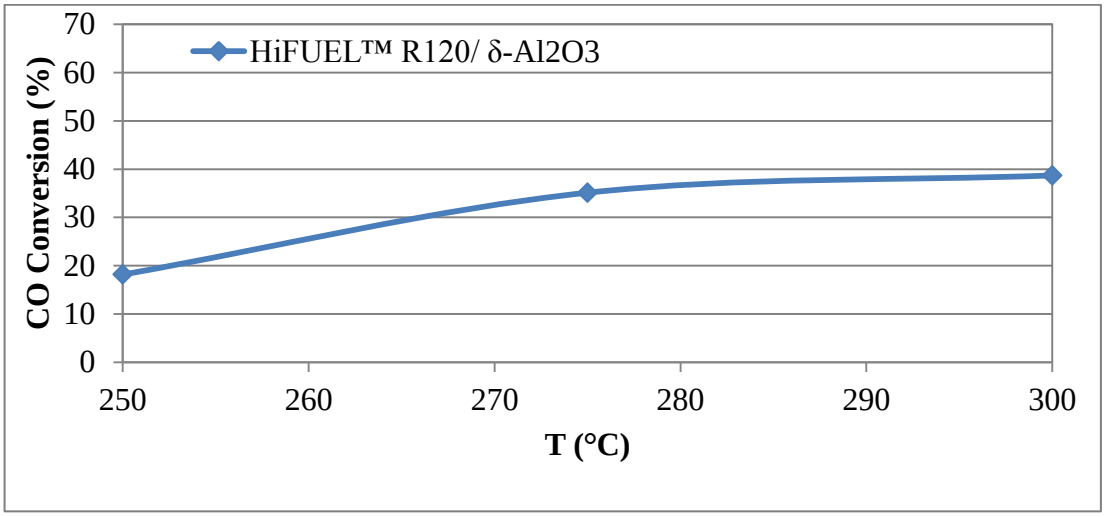

Figure 4.4. Effect of temperature on CO conversion over HiFUEL R120/ δ-Al_2O_3 ($CO/H_2/N_2$ =32/64/4, 34 bar, metal to acid ratio: 1/1).

When the product distribution obtained over the hybrid catalyst was examined, it was seen that the highest selectivity to DME was obtained as 34% at 275 ^{0}C, as shown in Figure 4.5. According to the experimental results, at 300 ^{0}C hydrocracking reactions are favored (Reaction 2.9) meaning that the production of hydrocarbons (mostly methane) becomes important, which provokes a sharp decrease in the selectivity to DME (22.5%). A considerable increase in the selectivity to CH_4 (from 3.8 to 15%) with increasing temperature was observed in the 250- 300 ^{0}C range. The reason of the further dehydration of the originally formed DME to hydrocarbons may be attributed to the strong acidic sites of methanol dehydration catalyst. The general reaction scheme given by Mao *et al.* [53] can be described as follows:

$$2CH_3OH \xrightarrow{-H_2O} CH_3OCH_3 \xrightarrow{-H_2O} \text{Hydrocarbons (mostly methane)} \qquad (2.9)$$

Formation of water was occurred by Reaction 2.6 and water reacted with carbon monoxide through water gas shift reaction (Reaction 2.4). The water-gas shift reaction is more favorable at 250 ^{0}C whereas above 275 ^{0}C, excess CO_2 formation may also take place through coke formation on the catalyst surface via Reaction 2.5. In view of these results, the temperature of 275 ^{0}C can be taken as optimum.

$CO + H_2O \leftrightarrow CO_2 + H_2$ (2.4)

$2CO \rightarrow CO_2 + C_{(s)}$ (2.5)

$2\ CH_3OH \leftrightarrow CH_3OCH_3 + H_2O$ (2.6)

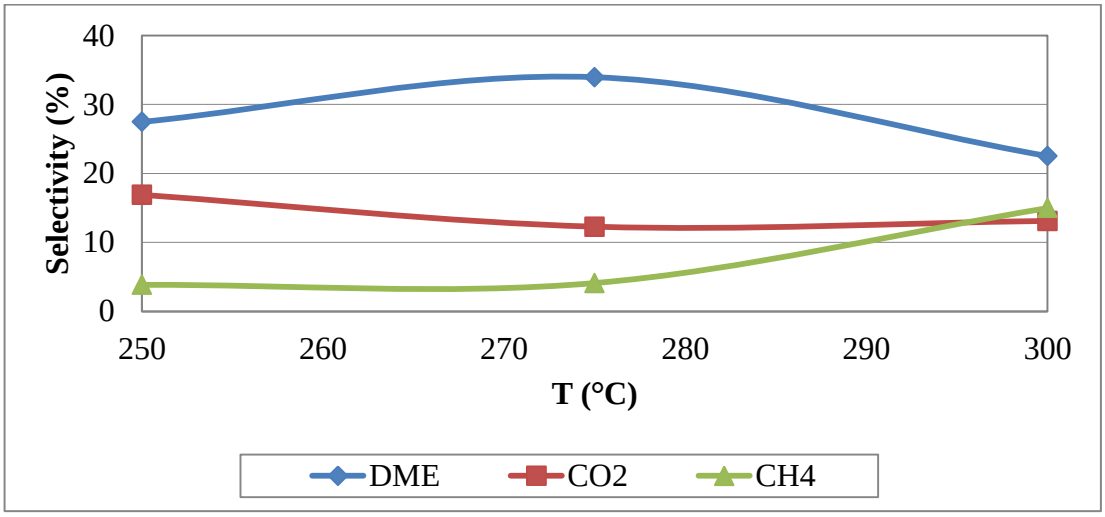

Figure 4.5. Effect of temperature on DME, CO_2 and CH_4 selectivities over HiFUEL R120/ δ-Al_2O_3 ($CO/H_2/N_2$ =32/64/4, 34 bar, metal to acid ratio: 1/1).

4.2.1.2. Effect of Pressure. HiFUEL R120/ δ-Al_2O_3 was tested in BTRS-Jr-PC operating at 275 °C in the pressure range of 25–34 bar for a feed gas composition of $CO/H_2/N_2$= 32/64/4. The bi-functional catalyst was prepared by dry physical mixing 0.2 gr of commercial catalyst which is responsible for methanol synthesis and 0.2 gr of δ-Al_2O_3 catalyst which is responsible for methanol dehydration. The stability of the activity of HiFUEL R120/ δ-Al_2O_3 under these conditions is presented in Figure 4.6 below.

As it can be seen from Figures 4.6 and 4.7 as well as Table 4.3, when pressure was increased in the range from 25 - 34 bar, the conversion of CO increased gradually. This is a consequence of thermodynamics, since methanol synthesis (Reaction 2.2), which is the limiting step of the overall process, is favored at high pressure [48].

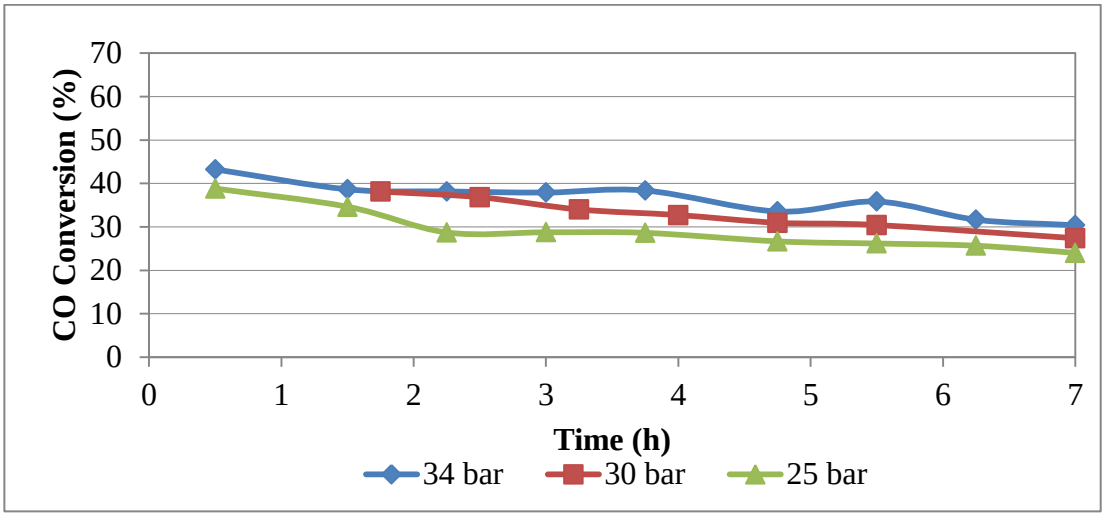

Figure 4.6. Effect of pressure in the evolution with time-on-stream of CO conversion for HiFUEL R120/ δ-Al_2O_3 (CO/H_2/N_2 =32/64/4, 275 ^{0}C metal to acid catalyst ratio: 1/1).

Table 4.3. The results obtained with HiFUEL R120/ δ-Al_2O_3, which were calculated with respect to converted CO at pressure of 25, 30 and 34 bar for feed mixture of 32% CO, 64% H_2 and 4% N_2).

Pressure (bar)	CO conversion (%)	DME selectivity (%)	CO_2 selectivity (%)	CH_4 selectivity (%)
25	26.9	24.1	15.2	5.4
30	32.1	27.8	13.4	4.7
34	35.1	34.0	12.3	4.1

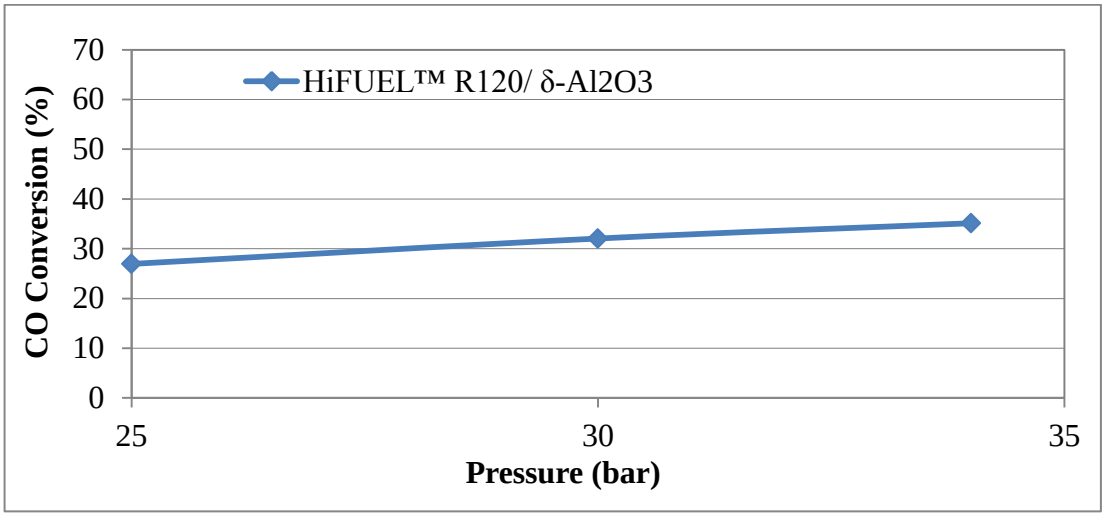

Figure 4.7. Effect of pressure on CO conversion over HiFUEL R120/ δ-Al_2O_3 ($CO/H_2/N_2$ =32/64/4, 275 ^{0}C, metal to acid catalyst ratio: 1/1).

When it comes to product distribution of HiFUEL R120/ δ-Al_2O_3, as pressure was increased the selectivities of CO_2 and CH_4 decreased whereas DME selectivity increased gradually as expected. Product distribution obtained over this catalyst is given in Figure 4.8 and in Table 4.3. As it can be seen from Reactions 2.1, 2.4 and 2.6, methanol synthesis reaction is stoichiometric-number-reducing reaction, but methanol dehydration and water gas shift reaction are equivalent-mole-number reactions. Therefore, pressure improvement is only favorable to the conversion of CO. On the other hand, since the direct synthesis of DME can be considered as the cascade reaction which consists of methanol synthesis and methanol dehydration, methanol as an intermediate species has adequate time for further transformation into DME. Thus, the selectivity of DME increases obviously with increasing pressure [48, 70]. Among the tested pressure values, the pressure of 34 bar can be taken as the optimum.

$$CO + 2\ H_2 \leftrightarrow CH_3OH \quad (2.1)$$

$$2\ CH_3OH \leftrightarrow CH_3OCH_3 + H_2O \quad (2.6)$$

$$CO + H_2O \leftrightarrow CO_2 + H_2 \quad (2.4)$$

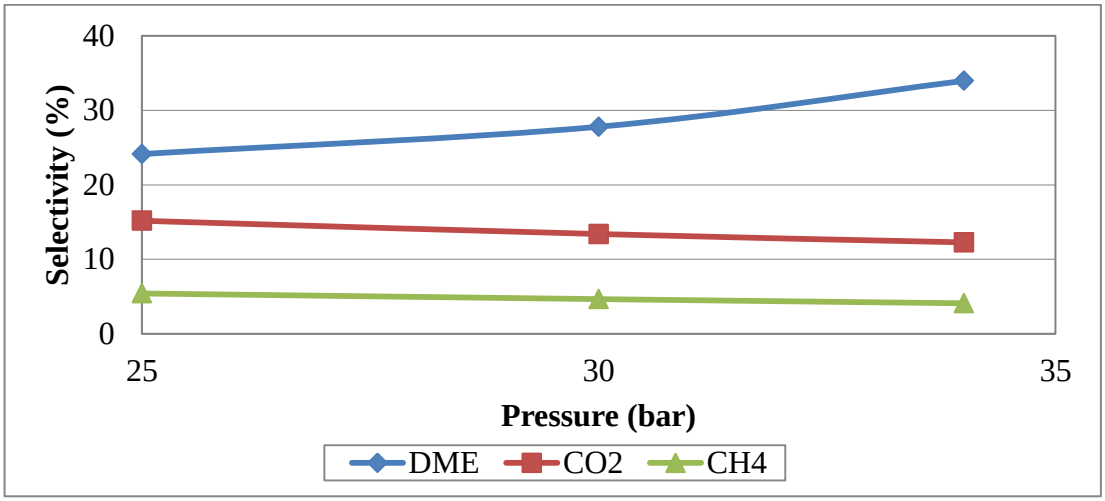

Figure 4.8. Effect of pressure on DME, CO_2 and CH_4 selectivities over HiFUEL R120/ δ-Al_2O_3 ($CO/H_2/N_2$ =32/64/4, 275 ^{0}C, metal to acid catalyst ratio: 1/1).

4.2.1.3. Effect of Feed Composition. HiFUEL R120/ δ-Al_2O_3 was also tested in BTRS-Jr-PC operating at 275 °C and 34 bar for a feed gas composition of $CO/H_2/N_2$= 48/48/4. 0.2 gr of commercial catalyst was mixed physically with 0.2 gr of methanol dehydration δ-Al_2O_3 catalyst. The stability and the activity of HiFUEL R120/ δ-Al_2O_3 under these conditions are presented in Figure 4.9. As shown in Figure 4.9, CO conversion increased with increasing of H_2/CO feed ratio. In other words, higher H_2/CO ratio leads to the higher CO conversion.

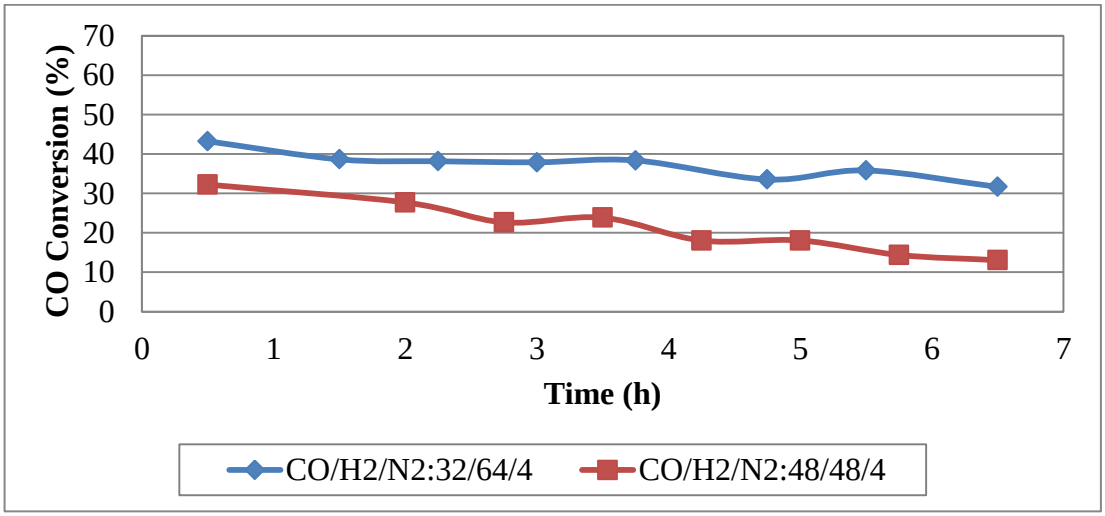

Figure 4.9. Effect of feed composition in the evolution with time-on-stream of CO conversion for HiFUEL R120/ δ-Al_2O_3 (275 ^{0}C, 34 bar, metal to acid catalyst ratio: 1/1).

When the product distribution of the hybrid catalyst was examined, the highest selectivity to DME was obtained as about 49.1% with CO-rich synthesis gas, as shown in Figure 4.10. As reported in the literature, high H_2/CO ratio suppresses the forward WGS (Reaction 2.4) and causes the amount of H_2O to increase. However, since H_2O is a product of the methanol dehydration, Reaction 2.6 can be shifted thermodynamically to the direction of DME consumption and methanol formation. Hence, DME selectivity decreased with increasing H_2 content in the feed mixture. On the other hand, CO-rich synthesis gas would favor the forward WGS by consuming H_2O, which favors the methanol dehydration (Reaction 2.6) in accordance with Le Chatelier's principle [71]. Comparison of carbon monoxide conversion and selectivity of the products values obtained for a feed gas composition of $CO/H_2/N_2$:32/64/4 and $CO/H_2/N_2$:48/48/4 is given in Table 4.4.

It can be seen that in addition to DME, relatively high amounts of by-products CH_4 and CO_2 were detected. Furthermore, the data in Table 4.4 show that methanation (Reaction 2.8) and WGS (Reaction 2.4) play important roles in the feed composition of $CO/H_2/N_2$:48/48/4. As mentioned previously, methane formation can be also attributed to catalyst deactivation by coke which was formed by the further conversion of the originally formed DME to hydrocarbons like methane. At the same time, water formed accelerates WGS, leading to the formation of larger quantities of CO_2.

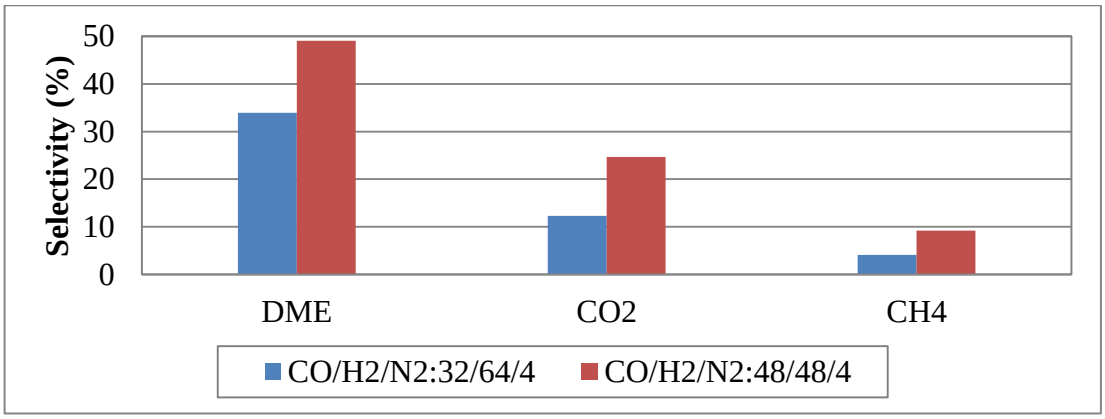

Figure 4.10. Comparison of product distributions obtained over HiFUEL R120/ δ-Al_2O_3 for CO/H2/N2= 32/64/4 and CO/H2/N2= 48/48/4 (275 ^{0}C, 34 bar)

Table 4.4. Comparison of CO conversion and selectivity of the products values obtained with a feed gas composition of $CO/H_2/N_2$:32/64/4 and $CO/H_2/N_2$:48/48/4.

Feed Gas Composition	CO conversion (%)	DME selectivity (%)	CO_2 selectivity (%)	CH_4 selectivity (%)
$CO/H_2/N_2$:32/64/4	35.1	34.0	12.3	4.1
$CO/H_2/N_2$:48/48/4	19.7	**49.1**	24.7	9.2

4.2.1.4. Effect of Metal to Acid Catalyst Weight Ratio. Up to now, the metal to acid ratio was kept at a constant value of 1 for all experiments involving HiFUEL R120/ δ-Al_2O_3 catalyst. In other words, the 0.2 gr of commercial Cu–Zn based catalyst was mixed physically with 0.2 gr of methanol dehydration δ-Al_2O_3 catalyst. In this section, the effect of metal to acid catalyst ratio was investigated by increasing the amount of the commercial Cu–Zn based catalyst. For this purpose, the bi-functional catalyst was prepared by physical mixing of the 0.27 gr of commercial Cu–Zn based catalyst and 0.13 gr of methanol dehydration catalyst. The stability and the activity of HiFUEL R120/ δ-Al_2O_3 under these conditions are presented in Figure 4.11.

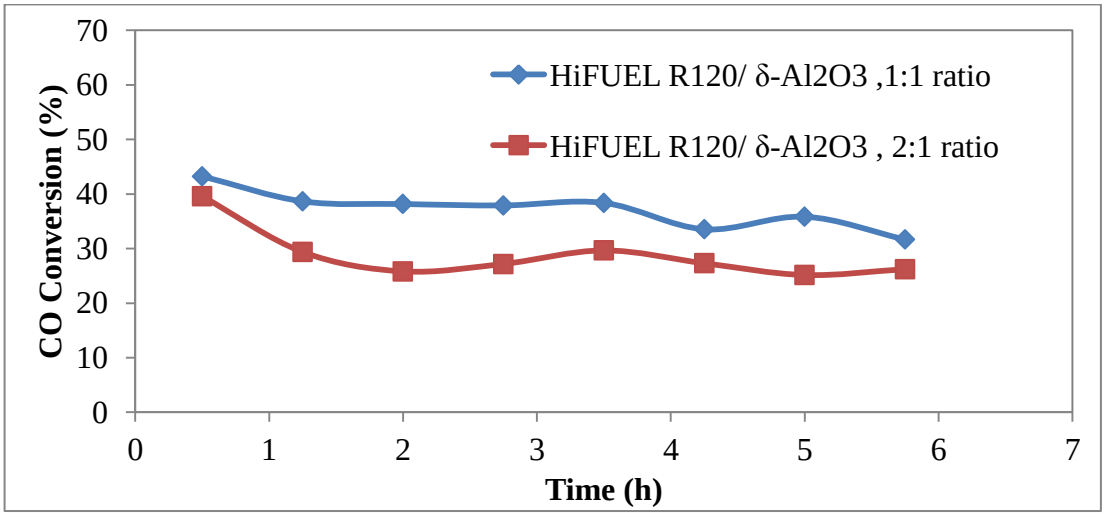

Figure 4.11. Effect of metal to acid catalyst weight ratio in the evolution with time-on-stream of CO conversion for HiFUEL R120/ δ-Al_2O_3 ($CO/H_2/N_2$ =32/64/4, 275 ^{0}C, 34 bar).

As can be seen from Figure 4.11, CO conversion decreased by increasing the weight of commercial Cu–Zn based catalyst. Since the methanol produced was not efficiently converted to DME, the direct synthesis of DME from syngas could not be completed, which led to the decrease in conversion of CO. According to the results, there are no benefits in increasing the metal catalyst weight for the bi-functional catalyst.

Comparison of product distributions obtained with HiFUEL R120/ δ-Al_2O_3 for 1:1 and 2:1 ratios are given in Figure 4.12. As shown in Figure 4.12, lower DME selectivity was observed with a 2:1 ratio, which means that the amount of acid catalyst is insufficient to convert the methanol formed to DME [72]. Comparison of carbon monoxide conversion and selectivity of the products values obtained for 1:1 and 2:1 ratios are given in Table 4.5.

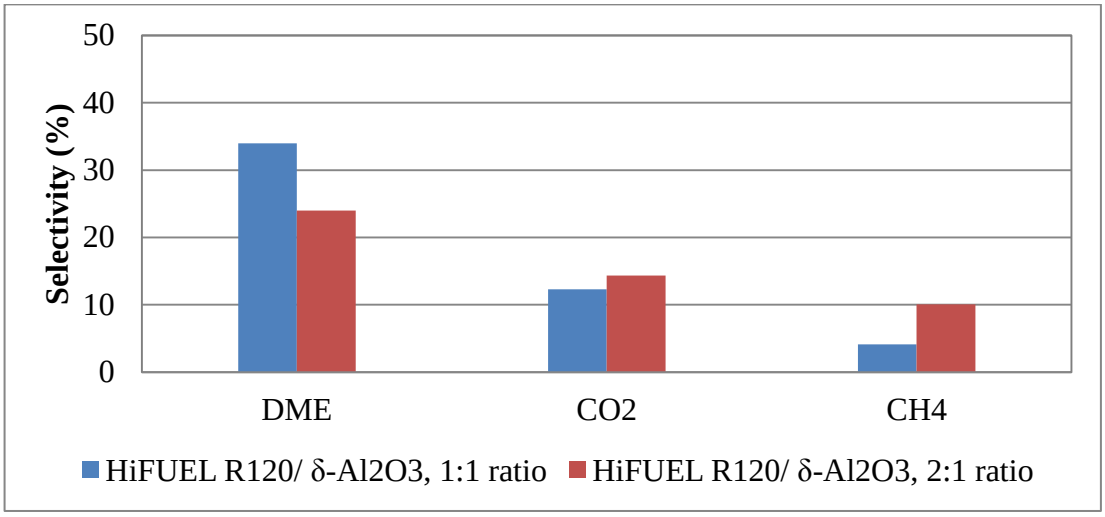

Figure 4.12. Comparison of product distributions obtained over HiFUEL R120/ δ-Al_2O_3 for 1:1 and 2:1 ratios ($CO/H_2/N_2$ =32/64/4, 275 ^{0}C, 34 bar).

Table 4.5. Comparison of CO conversion and selectivity of the products values obtained with different metal to acid weight ratio of HiFUEL R120/ δ-Al_2O_3 catalyst.

Metal to acid weight ratio	CO conversion (%)	DME selectivity (%)	CO_2 selectivity (%)	CH_4 selectivity (%)
1:1[a]	35.1	34.0	12.3	4.1
2:1[a]	26.9	24.0	14.4	10.1

[a] Metal to acid weight ratio of HiFUEL R120/ δ-Al_2O_3 catalyst.

4.2.2. Catalytic Activity Results of CZA/ δ-Al_2O_3

In the direct synthesis of DME from synthesis gas, another bed configuration involving physical mixture of the co-precipitated CuO/ZnO/Al_2O_3 in-house made catalysts (CZA) and δ-Al_2O_3 catalyst for synthesis and dehydration of methanol, respectively. The bed was prepared by physical mixing 0.2 gr of CZA and 0.2 gr of δ-Al_2O_3. Activity tests were conducted at 34 bar and in the temperature range of 250 - 300 °C for a feed gas composition of $CO/H_2/N_2$= 32/64/4. The stability and the activity of CZA/ δ-Al_2O_3 under these conditions are presented in Figure 4.13.

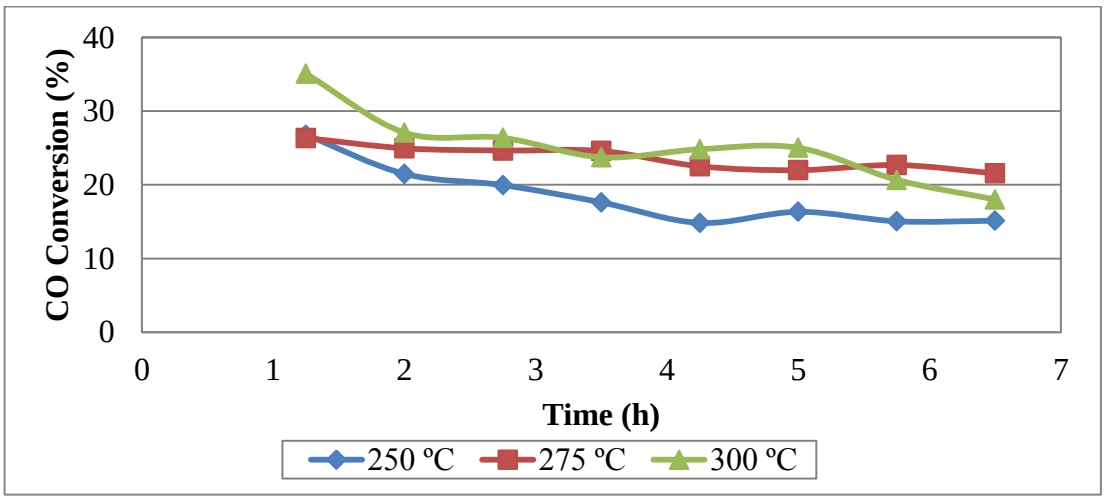

Figure 4.13. Effect of temperature in the evolution with time-on-stream of CO conversion for CZA/ δ-Al_2O_3 ($CO/H_2/N_2$ =32/64/4, 34 bar).

As can be seen from Figure 4.13, some decrease in activity was observed at all temperatures. Among the tested temperatures, the highest catalyst deactivation was observed at 300 ^{0}C. As mentioned previously, the decreasing trend could be attributed to catalyst deactivation by coke, as well as sintering of the metallic sites. Furthermore, water in the reaction medium may be responsible for the decrease in the activity of the active sites [47].

When the product distribution of the hybrid catalyst was examined, it was seen that the highest selectivity to DME was obtained as 29% at 275 ^{0}C. As shown in Figure 4.14, formation of CH_4 was not observed at 250 ^{0}C whereas above 250 ^{0}C, a small amount of CH_4 formation was detected. In addition to CH_4 formation, a small amount of CO_2 formation was also observed at all temperatures.

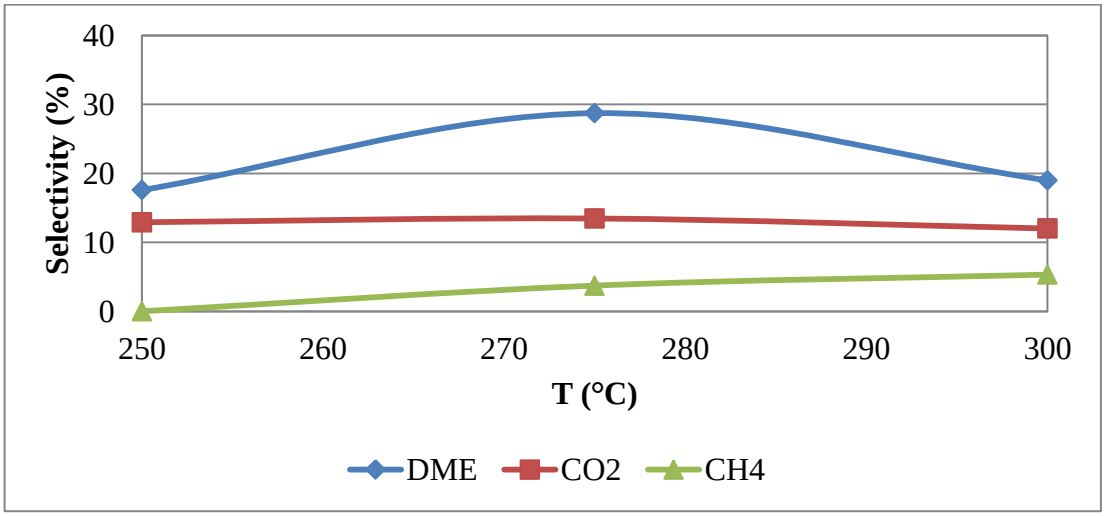

Figure 4.14. Effect of temperature on DME, CO_2 and CH_4 selectivities over CZA/ δ-Al_2O_3 ($CO/H_2/N_2$ =32/64/4, 34 bar, metal to acid ratio: 1/1).

CO conversion values of two mixed catalysts, one is HiFUEL R120/ δ-Al_2O_3 and the other is CZA/ δ-Al_2O_3, are plotted in comparison with respect to temperature, and shown in Figure 4.15. It was seen that for all temperatures, carbon monoxide conversion was lower over the CZA/ δ-Al_2O_3 catalyst.

When the product selectivities of HiFUEL R120/ δ-Al_2O_3 and CZA/ δ-Al_2O_3 are compared, it can be seen from Figure 4.16 that HiFUEL R120/ δ-Al_2O_3 catalyst showed higher catalytic activity. The reason of the low catalytic activity of CZA/ δ-Al_2O_3 is the deposition of coke on the metallic sites. Carbon deposition on CZA was proved by EDX analyses. According to the EDX result, 9.04 wt. % of carbon was detected over the spent CZA catalyst (see Section 4.1 for further details).

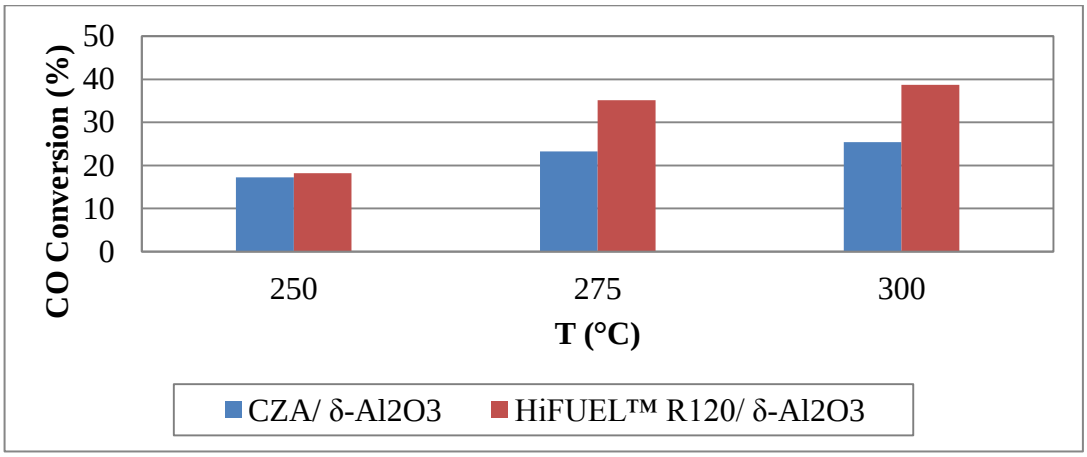

Figure 4.15. Comparison of carbon monoxide conversions obtained over CZA/ δ-Al_2O_3 and HiFUEL R120/ δ-Al_2O ($CO/H_2/N_2$ =32/64/4, 275 ^{0}C, 34 bar, metal to acid ratio: 1/1).

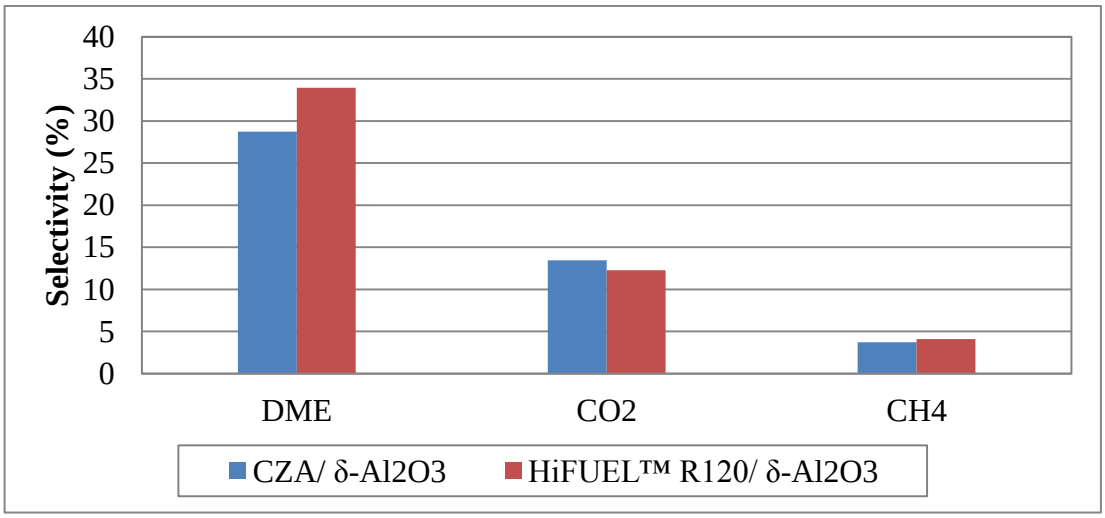

Figure 4.16. Comparison of selectivities of the products obtained over CZA/ δ-Al_2O_3 and HiFUEL R120/ δ-Al_2O ($CO/H_2/N_2$ =32/64/4, 275 ^{0}C, 34 bar, metal to acid ratio: 1/1).

4.2.3. Catalytic Activity Results of HiFUEL R120 with Different Acid Catalysts

The activity of bi-functional catalyst made by combining HiFUEL R120 and various solid acids including MCM-41 type SiO_2/Al_2O_3, zeolite, phosphotungstic acid (PTA) and 20 wt. % CeO_2/δ-Al_2O_3 was tested for direct synthesis of DME.

4.2.3.1. HiFUEL R120-SiO_2/Al_2O_3. Apart from δ-Al_2O_3, aluminosilicate which is a mesostructured MCM-41 type catalyst was used for methanol dehydration function. The hybrid catalyst was prepared by physical mixing 0.2 gr of HiFUEL R120 and 0.2 gr of SiO_2/Al_2O_3. Activity tests were conducted at 34 bar and at two different temperature values (250 and 275 °C) for a feed gas composition of $CO/H_2/N_2$= 32/64/4. The changes in the CO conversion as a function of time are depicted in Figure 4.17.

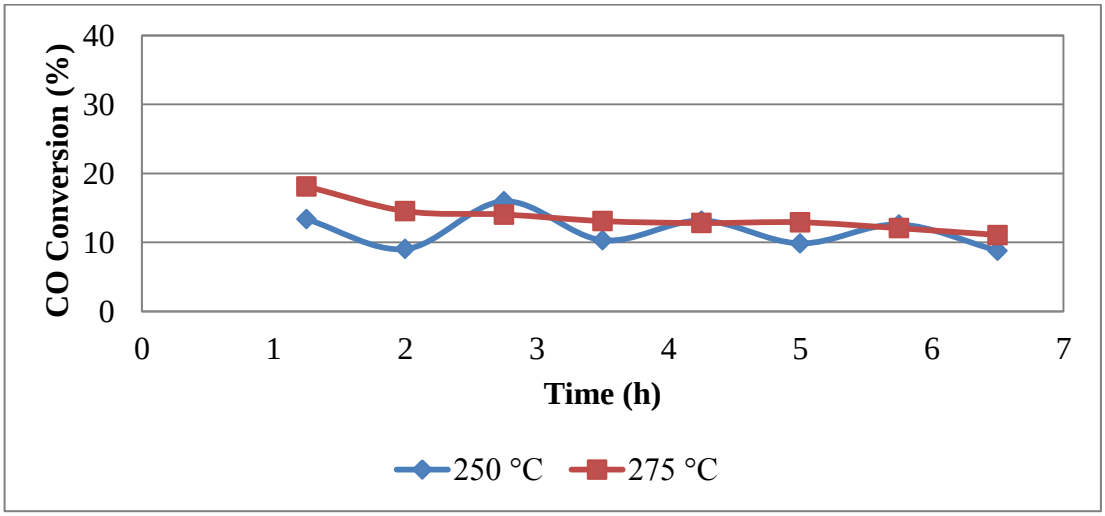

Figure 4.17. Effect of temperature in the evolution with time-on-stream of CO conversion for HiFUEL R120-SiO_2/Al_2O_3 ($CO/H_2/N_2$ =32/64/4, 34 bar).

As can be seen clearly in Figure 4.17, the conversion of CO remained essentially constant after the second hour at 275 ^{0}C, indicating that no noticeable deactivation of the bi-functional catalyst was observed during the 6.5 h experimentation. The conversion of CO was found as 11.8% and 13.2% at 250 ^{0}C and 275 ^{0}C, respectively.

When product distribution was investigated, mostly methane and carbon dioxide formation were observed at both temperatures. As mentioned previously, methanation (Reaction 2.8) over Cu-Zn based catalyst might have occurred. At 250 ^{0}C, selectivities of methane and carbon dioxide were about 14.3% and 20%, respectively whereas at 275 ^{0}C, selectivities were about 17.9% and 20.9%, respectively. In addition to formation of CO_2 and CH_4, DME selectivity was obtained as 12.6% and 20.1% at 250 ^{0}C and 275 ^{0}C, respectively.

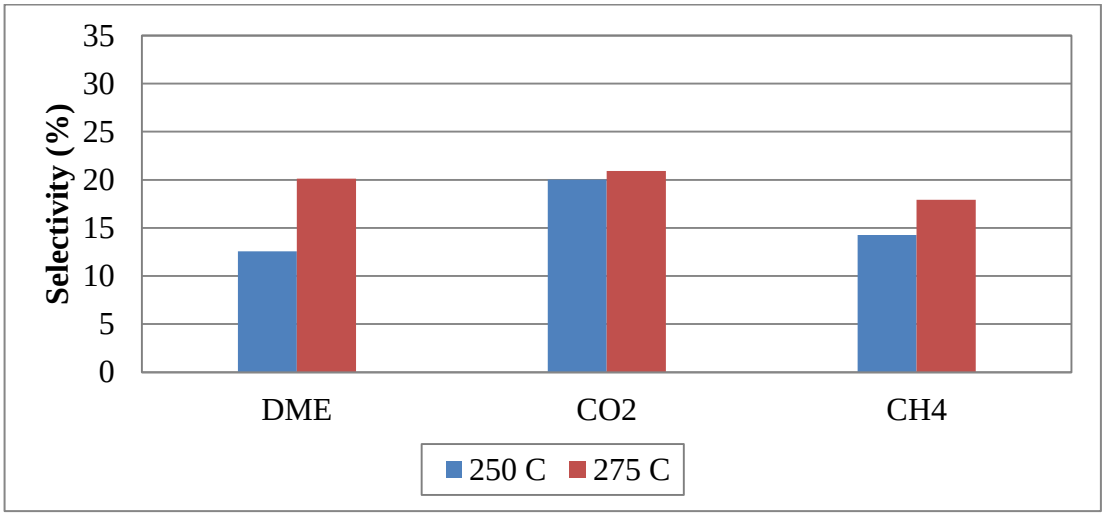

Figure 4.18. Effect of temperature on DME, CO_2 and CH_4 selectivities over HiFUEL R120-SiO_2/Al_2O_3 ($CO/H_2/N_2$ =32/64/4, 34 bar, metal to acid ratio: 1/1).

4.2.3.2. HiFUEL R120/Zeolite. Zeolite, a microporous, aluminosilicate mineral, was also investigated used for methanol dehydration function. The hybrid catalyst was prepared by physical mixing 0.2 gr of HiFUEL R120 and 0.2 gr of zeolite. Activity tests were conducted at 34 bar and 275 °C for a feed gas composition of $CO/H_2/N_2$= 32/64/4. The changes in the CO conversion as a function of time are depicted in Figure 4.19.

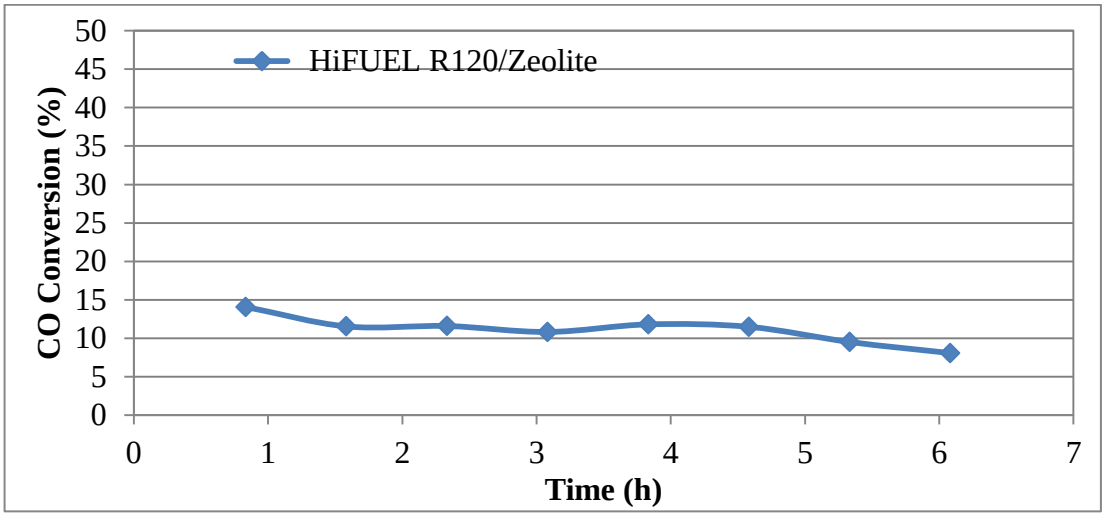

Figure 4.19. Evolution with time on stream of CO conversion for HiFUEL R120/Zeolite ($CO/H_2/N_2$ =32/64/4, 275 ^{0}C, 34 bar, metal to acid ratio: 1/1).

As can be seen in Figure 4.19, catalytic activity of HiFUEL R120/Zeolite catalyst was observed to decrease in time. This might be caused by coke formation. The conversion of CO was found as 11.4%.

When product distribution was investigated, mostly methane and carbon dioxide formation were observed. Selectivities of methane and carbon dioxide were about 37.9% and 25.2%, respectively. Formation of CH_4 and CO_2 was considered to be due to having too strong acid sites of zeolite and some of the formed CO_2 was expected to be produced in WGS (Reaction 2.4). In addition, the high concentration of CH_4 can be attributed to methanation (Reaction 2.8). DME selectivity was found as 4% for this catalyst, indicating low activity for direct synthesis of DME reaction.

4.2.3.3. HiFUEL R120/PTA. Phosphotungstic acid (PTA) or tungstophosphoric acid (TPA), is a Heteropoly acid with the chemical formula $H_3PW_{12}O_{40}$. Heteropoly acids have very strong acidity and they are preferred for dehydration reactions of alcohols [73]. For methanol dehydration function, phosphotungstic acid (PTA) was used because the dehydration of methanol to DME is a well-known acid catalyzed reaction. Activity tests were conducted at 34 bar and 275 °C for a feed gas composition of $CO/H_2/N_2$= 32/64/4. The changes in the CO conversion as a function of time are depicted in Figure 4.20.

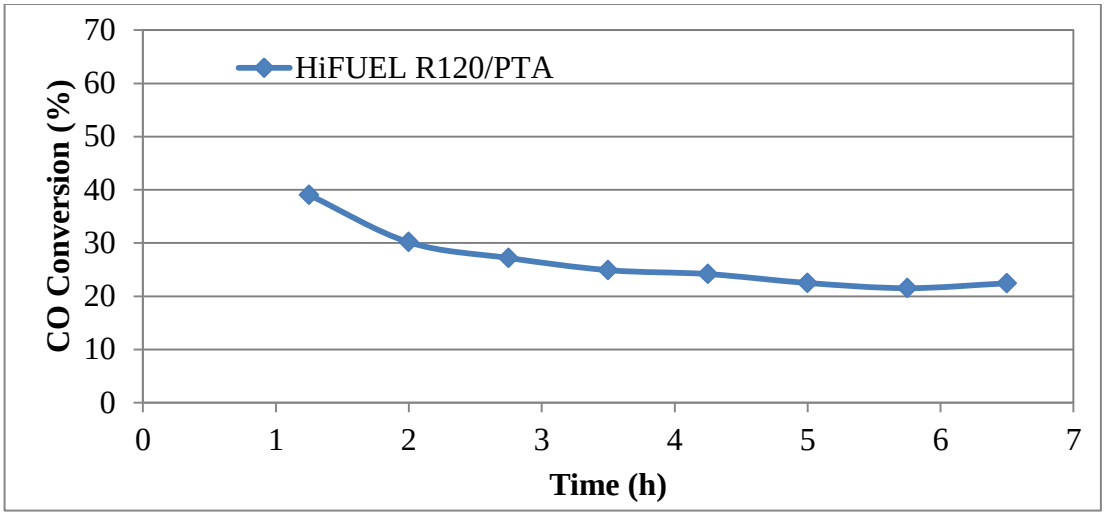

Figure 4.20. Evolution with time on stream of CO conversion for HiFUEL R120/PTA ($CO/H_2/N_2$ =32/64/4, 275 ^{0}C, 34 bar, metal to acid ratio: 1/1).

As can be seen in Figure 4.20, the conversion of CO decreased with time. The decrease in conversion of CO may similarly be explained by coke formation. The conversion value was about 24.7% at a reaction temperature of 275 ^{0}C.

When product distribution was investigated, the selectivity of DME was found as 27%. In addition to DME formation, mostly methane and carbon dioxide formation were observed. Selectivities of methane and carbon dioxide were about 16.7% and 20.1%, respectively. As reported in the literature, too strong acid sites favor the formation of larger amounts of by-products, methane and CO_2, leading to lower selectivity for DME. Furthermore, the presence of water in the product stream might have led to some decrease in the activity of PTA [74].

4.2.3.4. HiFUEL R120-20 wt%CeO_2/ δ-Al_2O_3. δ-Al_2O_3 modified with 20 wt. % of cerium oxide was prepared with an incipient to wetness impregnation technique. Cerium oxide was added to δ-Al_2O_3 in order to prevent the further conversion of the synthesized DME to hydrocarbons like methane and CO_2. The modified δ-Al_2O_3 catalyst was mixed physically with HiFUEL R120 to perform the direct synthesis of DME. Activity tests were conducted at 34 bar and two different temperature values (250 and 275 °C) for a feed gas composition

of $CO/H_2/N_2$= 32/64/4. The changes in the CO conversion as a function of time are depicted in Figure 4.21.

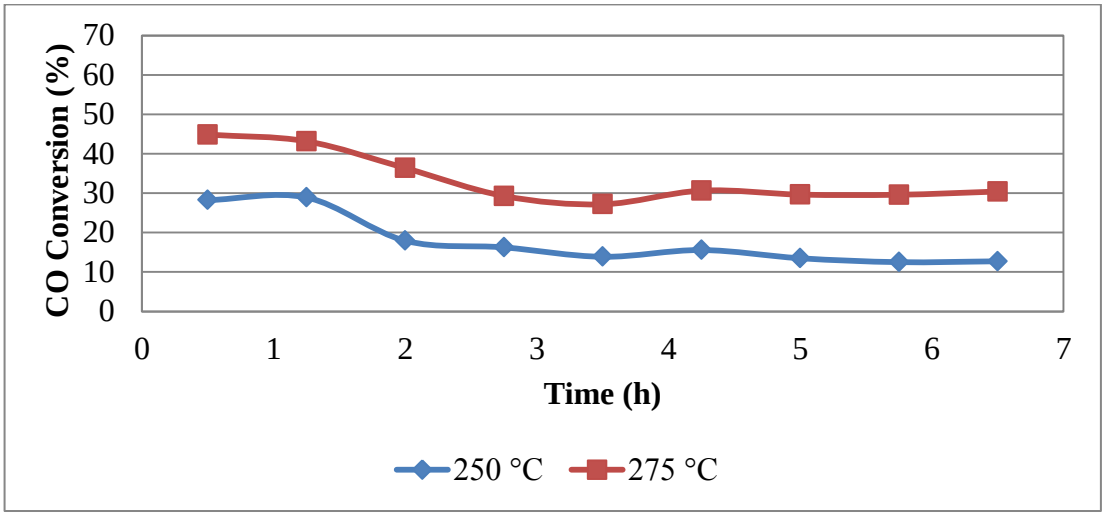

Figure 4.21. Effect of temperature in the evolution with time-on-stream of CO conversion for HiFUEL R120-20 wt. % CeO_2/ δ-Al_2O_3 ($CO/H_2/N_2$ =32/64/4, 34 bar).

As can be seen from Figure 4.21, some activity loss in CO conversion was observed. The conversion of CO was found as 15% and 29.5% at 250 ^{0}C and 275 ^{0}C, respectively. When the hybrid catalysts with unmodified and cerium oxide modified δ-Al_2O_3 were evaluated, lower conversion of CO was observed with δ-Al_2O_3 modified with cerium oxide.

When product distribution was investigated, the selectivities for DME were found as 15.6% and 20.5% at 250 ^{0}C and 275 ^{0}C, respectively. In addition to DME formation, methane and carbon dioxide formation were also observed. At 250 ^{0}C, selectivities of methane and carbon dioxide were about 2.4% and 13.7%, respectively whereas at 275 ^{0}C, these selectivities were about 6.2% and 11.6%, respectively. Product distribution is given in Figure 4.22. It was observed that methanation increased with increasing temperature which caused CO_2 formation to decrease. The aim of these experiments was to prevent the formation of by-products like methane and CO_2 by eliminating strong acid sites of δ-Al_2O_3 through cerium oxide modification. However, the addition of a larger amount of cerium oxide caused both lower DME selectivity and lower conversion of CO due to the lower

catalytic activity for methanol dehydration. The low activity of δ-Al_2O_3 modified with 20 wt. % cerium oxide for methanol dehydration may be attributed to its rather low acidity. This excessive amount of CeO_2 may cause the decrease in the number of acid sites responsible for methanol dehydration and irregular acidity distribution.

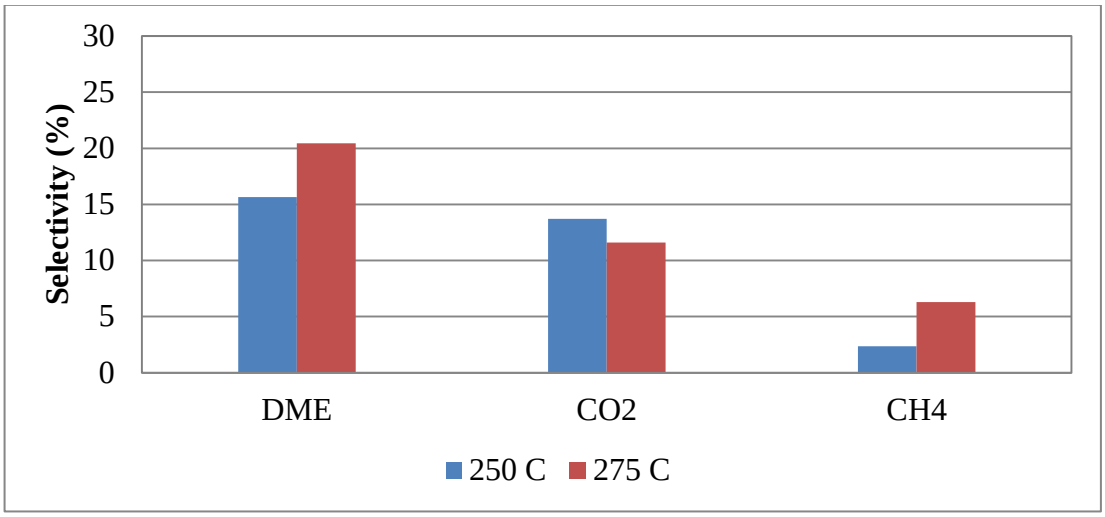

Figure 4.22. Effect of temperature on DME, CO_2 and CH_4 selectivities over HiFUEL R120-20 wt. % CeO_2/ δ-Al_2O_3 ($CO/H_2/N_2$ =32/64/4, 34 bar).

When the product selectivities of bi-functional catalyst made by combining HiFUEL R120 and various solid acid catalysts were compared, it was found that HiFUEL R120/ δ-Al_2O_3 catalyst showed the highest catalytic activity whereas HiFUEL R120/ zeolite showed the lowest DME selectivity. For the DME synthesis catalyst, the acidity of the methanol dehydration catalyst component is very important because it affects the selectivity of DME significantly. Methane and CO_2 formation were observed significantly over SiO_2/Al_2O_3, zeolite and PTA. It is well-known that formation of methane and CO_2 was attributed to the strong acidic sites. Therefore, among the tested solid acid catalyst, it was found that SiO_2/Al_2O_3, zeolite and PTA catalyst had strong acidic sites, which was responsible for the further conversion of the originally produced DME to by-products. At the same time, the produced water accelerated WGS (Reaction 2.4) that increased CO_2 formation. Furthermore, the modified δ-Al_2O_3 with cerium oxide showed lower catalytic activity due to its acidity.

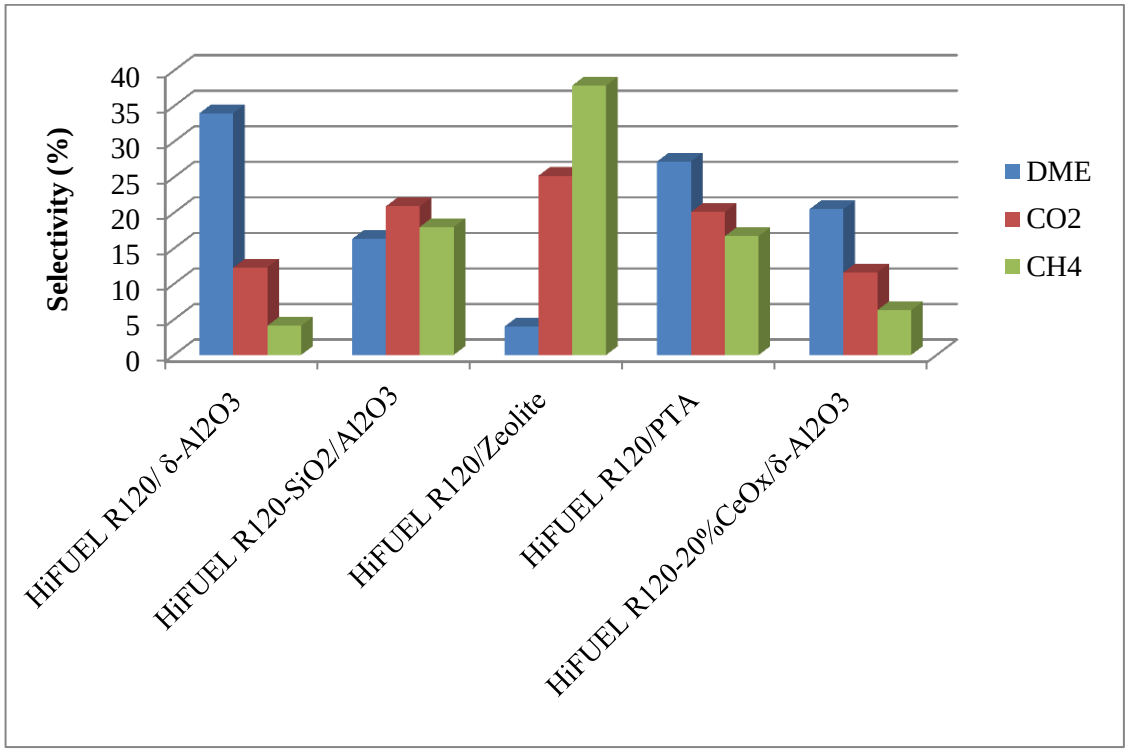

Figure 4.23. Comparison of selectivity of the products obtained over bi-functional catalyst made by combining HiFUEL R120 and various solid acid catalysts (275 ^{0}C, 34 bar, $CO/H_2/N_2$ =32/64/4, metal to acid ratio:1/1).

4.2.4. Catalytic Activity Results of 2wt%Pd-20wt%CeO_2/ γ-Al_2O_3

Up to now, the most common catalysts reported in the literature for direct synthesis of DME process involve the physical mixture of the methanol synthesis and the solid acid catalysts. The Cu/ZnO-based catalyst has been used mostly for methanol synthesis function. However, the conventional $Cu/ZnO/Al_2O_3$ catalyst used for methanol synthesis suffers from instability and deactivation at high temperatures. In the literature, Pd/CeO_2-type catalyst was found to be highly active for the methanol synthesis from carbon monoxide and hydrogen. Beyond methanol synthesis, Pd/CeO_2-type catalyst was also found to be very active for water gas shift reaction [69]. Hence, high stability of the Pd/CeO_2-type catalyst makes it a potential candidate for use in the synthesis of methanol from syngas. Shen *et al.* [29] also found that Pd/Al_2O_3 was observed to show specific selectivity for dimethyl ether. They reported that selectivity for DME was found as 50.2% at 250 ^{0}C and 20 bar for a feed gas composition of H_2/CO=2. In light of this information,

2wt%Pd-20wt%CeO_2/ γ-Al_2O_3 catalyst synthesized by Ertem [69] was decided to be used for direct synthesis of DME. Activity tests were conducted at 34 bar and 275 °C for a feed gas composition of $CO/H_2/N_2$= 32/64/4. The changes in the CO conversion as a function of time are depicted in Figure 4.24.

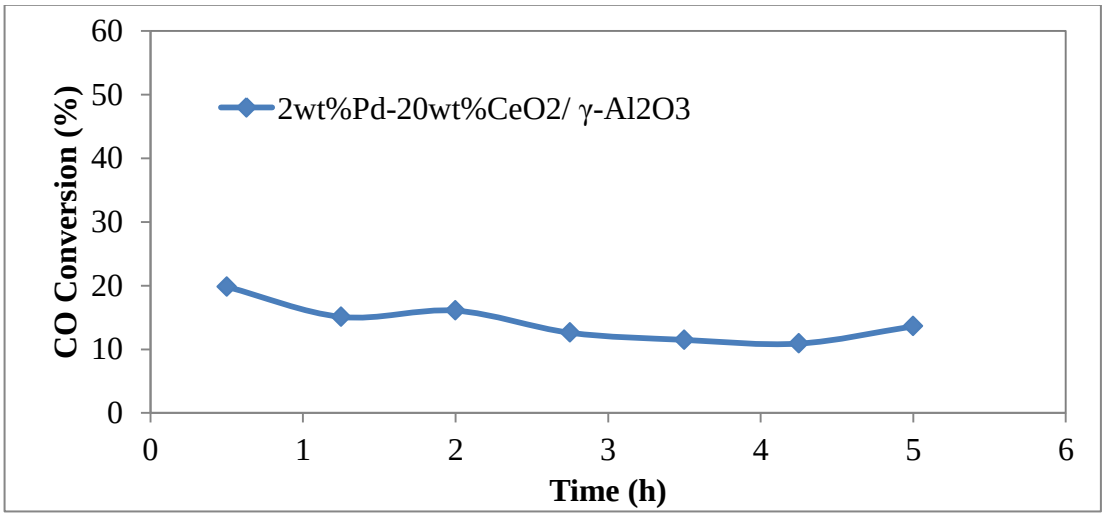

Figure 4.24. Evolution with time on stream of CO conversion for 2wt%Pd-20wt%CeO_2/ γ-Al_2O_3 ($CO/H_2/N_2$ =32/64/4, 275 ^{0}C, 34 bar, metal to acid ratio: 1/1).

Unlike the other catalysts explained in previous sections, 2wt%Pd-20wt%CeO_2/ γ-Al_2O_3 was reduced with pure hydrogen according to Ertem [69]. The conversion of CO was found as 13.3% for in the 5 h experimentation. When product distribution was investigated, mostly formation of methane and CO_2 was observed. The selectivities for methane and CO_2 were found as 26.3% and 12.1%, respectively. When it comes to DME selectivity, it was found as 8.1%. In order to consider Pd/CeO_2/Al_2O_3 as a catalyst for direct conversion of syngas to DME it will be necessary to further investigate the parameters that could favor methanol synthesis, decrease methane formation, and increase DME selectivity.

5. CONCLUSIONS AND RECOMMENDATIONS

5.1. Conclusions

In this study, bi-functional DME synthesis catalytic materials were synthesized by co-precipitation and incipient-to-wetness techniques. In addition to the synthesized ones, a commercial catalyst is also used in the studies. Catalyst beds were prepared by physical mixing of methanol synthesis with methanol dehydration catalysts.

The experimental work involved a parametric study of CO hydrogenation reaction as a function of time, temperature, pressure, feed composition and metal to acid catalyst weight ratio over HiFUEL R120/ δ-Al_2O_3 catalyst. A parametric study involving CZA/δ-Al_2O_3 catalyst was also performed. In addition to these bi-functional catalysts, the activity of bi-functional catalyst made by combining HiFUEL R120 and various solid acid catalysts including MCM-41 type SiO_2/Al_2O_3, microporous zeolite, phosphotungstic acid (PTA) and 20 wt. % CeO_2- δ-Al_2O_3 were tested at 34 bar, 275 ^{0}C and at a molar feed gas composition of $CO/H_2/N_2$ = 32/64/4. Moreover, the standalone 2wt%Pd-20wt%CeO_2/ γ-Al_2O_3 catalyst synthesized in our laboratory was tested for direct synthesis of DME from syngas. The major conclusions that can be drawn from current study can be given as follows:

- The results of HiFUEL R120/ δ-Al_2O_3 catalyst showed that there is a potential limitation for reaction temperature due to catalyst deactivation and sintering on the metallic sites. The optimum reaction temperature was found as 275 ^{0}C.

- With the increase in pressure, CO conversion and DME selectivity increased whereas formation of the by-products, methane and CO_2, decreased. The optimum reaction pressure was obtained at 34 bar for HiFUEL R120/ δ-Al_2O_3 catalyst.

- The optimum molar feed composition was found to be $CO/H_2/N_2$=48/48/4 for the HiFUEL R120/ δ-Al_2O_3 catalyst. The maximum DME selectivity of 49.1% was found for this feed composition.

- The most suitable ratio between the metal and acid functions was found as 1:1 for HiFUEL R120/ δ-Al_2O_3 catalyst.

- CZA/ δ-Al_2O_3 catalyst showed lower catalytic activity in comparison with HiFUEL R120/ δ-Al_2O_3 catalyst. The reason of the low catalytic activity of CZA/ δ-Al_2O_3 was the deposition of coke on the metallic sites. According to the EDX result, 9.04 wt. % of carbon deposition was detected over CZA catalyst.

- HiFUEL R120/ zeolite showed the lowest DME selectivity.

- Methane and CO_2 formation were observed significantly over SiO_2/Al_2O_3, zeolite and PTA catalysts. Among the tested solid acid catalyst, it was found that SiO_2/Al_2O_3, zeolite and PTA catalyst had strong acidic sites, which were responsible for the further conversion of the originally produced DME to by-products. At the same time, the produced water accelerated WGS that increased CO_2 production.

- The modified δ-Al_2O_3 with cerium oxide showed lower catalytic activity than unmodified one due to low acidity. This amount of CeO_2 added may cause the decrease in the number of acid sites responsible for methanol dehydration significantly.

- Among all the catalysts, HiFUEL R120/ δ-Al_2O_3 catalyst exhibited the highest catalytic activity operating at 34 bar and 275 ^{0}C for a feed gas composition of $CO/H_2/N_2$ =48/48/4. The highest DME selectivity was found as 49.1% under these reaction conditions.

5.2. Recommendations

Considering the results of the experimental study, following ideas are thought to be beneficial for future studies on direct synthesis of DME:

- In order to minimize carbon deposition on CZA catalyst during direct synthesis of DME, effect of promoters like Zr and Ce can be investigated.

- The effect of calcination and reduction temperatures on the CZA catalyst can be investigated.

- Pressure can be increased since methanol synthesis reaction is favored at high pressures.

- In order to the formation of carbon dioxide in the product stream, carbon dioxide could be added to the feed in small amounts.

- In order to enhance the catalytic activity of CZA/δ-Al_2O_3, the acidity of the bi-functional catalyst can be increased by increasing mass ratio of acidic function.

- The weight percent of CeO_2 on δ-Al_2O_3 may be changed to search for better catalytic activity.

- In order to consider Pd/CeO_2/Al_2O_3 as a catalyst for direct conversion of syngas to DME, it will be necessary to further investigate the parameters such as the per cent weight of Pd and CeO_2 that could favor lower methane formation.

APPENDIX A: SAMPLE CONVERSION AND SELECTIVITY CALCULATIONS

In the activity tests, products and unconverted gases were analyzed with an online GC 2014 and GCMS-QP2010 connected to experimental set-up. Details of experimental system are explained in Section 3.2. From GC analyses, peaks regarding to component(s) were obtained. In this Appendix, sample calculation for conversion and selectivity calculations are illustrated for activity Results of HiFUEL R120/ δ-Al_2O_3 for a feed composition of 32%CO, 64%H_2 and 4%N_2.

Activity test of HiFUEL R120/ δ-Al_2O_3 was made at a pressure of 34 bar and 275 ^{0}C. Reactant gas flow rate was 100 ml/min and 0.4 gr catalyst was loaded to reactor. Activity results were given in Section 4.2.1.1.

The CO conversion was calculated by Equation 3.3 at this temperature. CO conversion can be calculated by

$$Xco(\%) = \frac{Fco,in - Fco,out}{Fco,in} \times 100 \tag{3.3}$$

In experiments, steady state was reached at around 2 h. After steady state reached, mostly six successive runs were carried out and peak areas corresponding to any component was recorded. For conversion and selectivity calculations, average of them was taken.

According to average area value of CO obtained from GC analyses, the molar flow rate of CO in the feed ($F_{CO,in}$) and in the outlet stream ($F_{CO,out}$) were calculated as 9.3779 μmol/min and 6.08404 μmol/min, respectively. According to Equation 3.3, the CO conversion was calculated to be 35.1% at 275 ^{0}C.

$$Xco(\%) = \frac{9.3779 - 6.08404}{9.3779} \times 100 = 35.1\%$$

Product selectivities were defined as the ratio of moles of CO converted to a specific component to total moles of CO converted to the products. The selectivity of products was calculated by Equations 3.4, 3.5 and 3.6 at this temperature. The selectivities can be calculated by

$$S_{DME}(\%) = \frac{2F_{DME}}{Fco,in - Fco,out} \times 100 \tag{3.4}$$

$$Sco_2(\%) = \frac{Fco_2}{Fco,in - Fco,out} \times 100 \tag{3.5}$$

$$S_{CH4}(\%) = \frac{F_{CH4}}{Fco,in - Fco,out} \times 100 \tag{3.6}$$

As it can be noticed from chemical structure of chemicals, CH_4 and CO_2, contain only one carbon atom whereas DME contains two carbon atoms. For this reason, respective mole numbers of DME was multiplied by 2. CH_4 and CO_2 were calibrated by injecting known amounts of each species separately to the chromatographic column under the conditions given in Table 3.5. According to average area values of CH_4 and CO_2 obtained from GC analyses, the molar flow rates of CH_4 and CO_2 in the outlet stream (F_{CH4}) and (F_{CO2}) were calculated to be 0.135093 μmol/min and 0.404432 μmol/min, respectively. According to Equations 3.5 and 3.6, the selectivities of CO_2 and CH_4 were calculated to be 12.3% and 4.1% at 275 ^{0}C.

$$SCO_2(\%) = \frac{0.404432}{(9.3779 - 6.08404)} \times 100 = 12.3\%$$

$$SCH_4(\%) = \frac{0.135093}{(9.3779 - 6.08404)} \times 100 = 4.1\%$$

The following expression was used to evaluate the molar percentage of DME via the ionization cross-section method using the following equation:

$$N_i = N_{ref} \frac{M_{ref}}{M_i} \frac{A_i}{A_{ref}} \frac{Q_{ref}}{Q_i} \tag{3.1}$$

where subscript "i" and "ref" correspond to the quantified species and reference compound, respectively. N is the number of moles of species, M is molecular weight and A is the area under the peak obtained from GCMS-QP2010. For dimethyl ether, methane is taken as reference compound. Q is the total ionization cross section calculated using the method described by Fitch and Sauter *et al.* [68]:

$$Q = 0.943 + \sum a_j n_j \tag{3.2}$$

a_j is the contribution of atom j to the ionization cross-section while n_j is the number of j atoms in the molecule. The contributions of some of the atoms determined by Fitch and Sauter *et al.* [68] are given in Table 3.6.

$$Qref = 0.943 + (1 \times 2.12 + 4 \times 0.38) = 4.583$$
$$QDME = 0.943 + (2 \times 2.12 + 6 \times 0.38 + 1 \times 1.26) = 8.723$$
$$Nref = 0.01635792 \mu mol / \min$$
$$Mref = 16.042 g / mol$$
$$MDME = 46.07 g / mol$$
$$Aref = 1165521$$
$$ADME = 217826050$$

$$NDME = 0.01635792 \times \frac{16.042}{46.07} \times \frac{217826050}{1165521} \times \frac{4.583}{8.723} = 0.559$$
$$SDME = \frac{2 \times 0.559}{(9.3779 - 6.08404)} \times 100 = 33.96\%$$

REFERENCES

1. Fleisch, T.H., A. Basu, R.A. Sills, "Introduction and Advancement of a New Clean Global Fuel: The Status of DME Developments in China and Beyond", *Journal of Natural Gas Science and Engineering*, Vol. 9, pp. 94-107, 2012.

2. Dogu, T., D. Varisli, "Alcohols as Alternatives to Petroleum for Environmentally Clean Fuels and Petrochemicals", *Turkish Journal of Chemistry*, Vol. 31, pp. 551-567, 2007.

3. Wood, D.A., C. Nwaoha, B.F. Towler, "Gas-to-liquids (GTL): A Review of an Industry Offering Several Routes for Monetizing Natural Gas", *Journal of Natural Gas Science and Engineering*, Vol. 9, pp. 196-208, 2012.

4. Moradi, G.R., S. Nosrati, F. Yaripor, "Effect of the Hybrid Catalysts Preparation Method upon Direct Synthesis of Dimethyl Ether from Synthesis Gas", *Catalysis Communications*, Vol. 8, pp. 598–606, 2007.

5. Sierra, I., J. Erena, A.T. Aguayo, M. Olazar, J. Bilbao, "Deactivation Kinetics for Direct Dimethyl Ether Synthesis on a CuO-ZnO-Al_2O_3/ γ- Al_2O_3 Catalyst", *Industrial and Engineering Chemistry Research*, Vol. 49, pp. 481-489, 2010.

6. Olah, G.A., A. Goeppert, G.K.S Prakash, "Chemical Recycling of Carbon Dioxide to Methanol and Dimethyl Ether: From Greenhouse Gas to Renewable, Environmentally Carbon Neutral Fuels and Synthetic Hydrocarbons", *Journal of Organic Chemistry*, Vol. 74, pp. 487-498, 2009.

7. Semelsberger, T.A., R.L. Borup, H.L. Greene, "Dimethyl ether (DME) as an Alternative Fuel", *Journal of Power Sources*, Vol. 156, pp. 497-511, 2006.

8. Arcoumanis, C., C. Bae, R. Crookes, E. Kinoshita, "The Potential of Di-methyl Ether (DME) as an Alternative Fuel for Compression Ignition Engines", *Fuel*, Vol. 87, pp. 1014-1030, 2008.

9. Becker, P., J. Schröder, R. Ahmad, M. Zimmermann, T. Otto, M. Döring, U. Arnold, "Recent Patents on the Conversion of Biomass to Fuels via Synthesis Gas", *Recent Patents on Chemical Engineering*, Vol. 5, pp. 75-86, 2012.

10. Ohno, Y., M. Yoshida, T. Shikada, O. Inokoshi, T. Ogawa, N. Inoue, "New Direct Synthesis Technology for DME (Dimethyl Ether) and Its Application Technology", *JFE Technical Report*, Vol. 6, pp. 70-75, 2006.

11. Takeishi, K., "Dimethyl Ether (DME): A Clean Fuel of the 21st Century and Catalysts for It", *Proceedings of the 4th IASME / WSEAS International Conference on Energy & Environment*, 2009.

12. JFE Holdings Inc., "Production of DME", http://japan-dme.or.jp/english/dme/index.html, [accessed June 2014].

13. Ogawa, T., N. Inoue, T. Shikada, Y. Ohno, "Direct Dimethyl Ether Synthesis", *Journal of Natural Gas Chemistry*, vol. 12, pp. 219-227, 2003.

14. Nexant, "Dimethyl Ether Technology and Markets", *ChemSystems Process Evaluation/Research Planning Program Report*, December 2008.

15. Lee, S., J.G. Speight, S.K. Loyalka, *Handbook of Alternative Fuel Technologies*, CRC Press, Boca Raton, FL, pp. 297-321, 2007.

16. Tijm, P.J.A., F.J. Waller, D.M. Browna, "Methanol Technology Developments for the New Millennium", *Applied Catalysis A: General*, Vol. 221, pp. 275-282, 2001.

17. Meshkini, F., M. Taghizadeh, M. Bahmani, "Investigating the Effect of Metal Oxide Additives on the Properties of Cu/ZnO/Al_2O_3 Catalysts in Methanol Synthesis from Syngas Using Factorial Experimental Design", *Fuel*, Vol. 89, pp. 170-175, 2010.

18. Herman, R.G., "Advances in Catalytic Synthesis and Utilization of Higher Alcohols", *Catalysis Today*, Vol. 55, pp. 233-245, 2000.

19. Suh, Y., S. Moon, H. Rheea, "Active Sites in Cu/ZnO/ZrO_2 Catalysts for Methanol Synthesis from CO/H_2", *Catalysis Today*, Vol. 63, pp. 47-452, 2000.

20. Arena, F., G. Italiano, K. Barbera, G. Bonura, L. Spadaro, F. Frusteri, "Basic Evidences for Methanol-Synthesis Catalyst Design", *Catalysis Today*, Vol. 143, pp. 80-85, 2009.

21. Shen, W.J., Y. Ichihashi, Y. Matsumura, "Low Temperature Methanol Synthesis from Carbon Monoxide and Hydrogen Over Ceria Supported Copper Catalyst", *Applied Catalysis A: General*, Vol. 282, pp. 221-226, 2005.

22. Pokrovski, K.A., A.T. Bell, "An Investigation of the Factors Influencing the Activity of Cu/$Ce_xZr_{1-x}O_2$ for Methanol Synthesis via CO Hydrogenation", *Journal of Catalysis*, Vol. 241, pp. 276-286, 2006a.

23. Pokrovski, K.A., A.T. Bell, "Effect of Dopants on the Activity of Cu/$M_{0.3}Zr_{0.7}O_2$ (M = Ce, Mn, and Pr) for CO Hydrogenation to Methanol", *Journal of Catalysis*, Vol. 244, pp. 43-51, 2006b.

24. Słoczynski, J., R. Grabowski, P. Olszewski, A. Kozłowska, J. Stoch, M. Lachowska, J. Skrzypek, "Effect of Metal Oxide Additives on the Activity and Stability of Cu/ZnO/ZrO_2 Catalysts in the Synthesis of Methanol from CO_2 and H_2", *Applied Catalysis: A General*, Vol. 310, pp. 127-137, 2006.

25. Gao, P., F. Lia, N. Zhao, F. Xiaoa, W. Wei, L. Zhongd, Y. Suna, "Influence of Modifier (Mn, La, Ce, Zr and Y) on the Performance of Cu/Zn/Al Catalysts via Hydrotalcite-like Precursors for CO_2 Hydrogenation to Methanol", *Applied Catalysis A: General*, Vol. 468, pp. 442-452, 2013.

26. Zhang, L., Y. Zhang, S. Chen, "Effect of Promoter TiO_2 on the Performance of CuO–ZnO–Al_2O_3 Catalyst for CO_2 Catalytic Hydrogenation to Methanol", *Journal of Fuel Chemistry and Technology*, Vol. 39, pp. 912-917, 2011.

27. Lmamura, S., K. Denpo, K. Utani, Y. Matsnmura, H. Kanai, "Synthesis of Methanol over Pd Promoted By Ceria", *Reaction Kinetics and Catalysis Letters*, Vol. 67, pp. 163-168, 1999.

28. Shen, W.J., Y. Ichihashi, M. Okumura, Y. Matsumura, "Methanol Synthesis from Carbon Monoxide and Hydrogen Catalyzed over Pd/CeO_2 Prepared by the Deposition–precipitation Method", *Catalysis Letters*, Vol. 64, pp. 23-25, 2000.

29. Shen, W.J., M. Okumura, Y. Matsumura, M. Haruta, "The Influence of the Support on the Activity and Selectivity of Pd in CO Hydrogenation", *Applied Catalysis A: General*, Vol. 213, pp. 225-232, 2001.

30. Yaripour, F., F. Baghaei, I. Schmidt, J. Perregaard, "Catalytic Dehydration of Methanol to Dimethyl Ether (DME) over Solid-Acid Catalysts", *Catalysis Communications*, Vol. 6, pp. 147-152, 2005.

31. Topp-Jorgensen, J. U.S. Patent 4,536,485 to Haldor Topsoe A/S, Denmark, 1985.

32. Hassanpour, S., F. Yaripour, M. Taghizadeh, "Performance of Modified H-ZSM-5 Zeolite for Dehydration of Methanol to Dimethyl Ether", *Fuel Processing Technology*, Vol. 91, pp. 1212-1221, 2010.

33. Kim, S.D., S.C. Baek, Y. Lee, K. Jun, M.J. Kim, I.S. Yoo, "Effect of γ-alumina Content on Catalytic Performance of Modified ZSM-5 for Dehydration of Crude Methanol to Dimethyl Ether", *Applied Catalysis A: General*, Vol. 309, pp. 139-143, 2006.

34. Vishwanathan, V., K.W. Jun, J.W. Kim, H.S. Roh, "Vapour Phase Dehydration of Crude Methanol to Dimethyl Ether Over Na-modified H-ZSM-5 Catalysts", *Applied Catalysis A: General*, Vol. 276, pp. 251-255, 2004.

35. Moradi, G.R., F. Yaripour, P. Vale-Sheyda, "Catalytic Dehydration of Methanol to Dimethyl Ether over Mordenite Catalysts", *Fuel Processing Technology*, Vol. 91, pp. 461-468, 2010.

36. Naik, S.P., V. Bui, T. Ryu, J.D. Miller, W. Zmierczak, "Al-MCM-41 as Methanol Dehydration Catalyst", *Applied Catalysis A: General*, Vol. 381, pp. 183-190, 2010.

37. Tokay, K.C., T. Dogu, G. Dogu, "Dimethyl Ether Synthesis Over Alumina Based Catalyst", *Chemical Engineering Journal*, Vol. 184, pp. 278-285, 2012.

38. Fu, Y., T. Hong, J. Chen, A. Auroux, J. Shen, "Surface Acidity and the Dehydration of Methanol to Dimethyl Ether", *Thermochimica Acta*, Vol. 434, pp. 22-26, 2005.

39. Ciftci, A., D. Varisli, K.C. Tokay, N.A. Sezgi, T. Dogu, "Dimethyl Ether, Diethyl Ether & Ethylene from Alcohols over Tungstophosphoric Acid Based Mesoporous Catalysts", *Chemical Engineering Journal*, Vol. 207-208, pp. 85-93, 2012.

40. Ahmad, R., M. Hellinger, M. Buchholz, H. Sezen, L. Gharnati, C. Wöll, J. Sauer, M. Döring, J. Grunwaldt, U. Arnold, "Flame-made $Cu/ZnO/Al_2O_3$ Catalyst for Dimethyl Ether Production", *Catalysis Communications*, Vol. 43, pp. 52-56, 2014a.

41. Ahmad, R., D. Schrempp, S. Behrens, J. Sauer, M. Döring, U. Arnold, "Zeolite-based Bifunctional Catalysts for the Single Step Synthesis of Dimethyl Ether from CO-rich Synthesis Gas", *Fuel Processing Technology*, Vol. 121, pp. 38-46, 2014b.

42. Shi, R.M., G.Y. Cai, Z.U. Liu, C.L. Sun, "Development of Catalysts for Synthesizing Dimethyl Ether from Synthesis Gas", *Journal of Natural Gas Chemistry*, Vol. 5, pp. 287-295, 1996.

43. Peng, X. D., A.W. Wang, B.A. Toseland, P.J.A. Tijm, "Single-step Syngas-to Dimethyl Ether Processes for Optimal Productivity, Minimal Emissions, and Natural Gas-derived Syngas", *Industrial and Engineering Chemistry Research*, Vol. 38, pp. 4381-4388, 1999.

44. Mao, D., W. Yang, J. Xia, B. Zhang, G. Lu, "The Direct Synthesis of Dimethyl Ether from Syngas over Hybrid Catalysts with Sulfate-modified γ-alumina as Methanol Dehydration Components", *Journal of Molecular Catalysis A: Chemical*, Vol. 250, pp. 138-144, 2006.

45. Ng, K.L., D. Chadwick, B.A. Toseland, "Kinetics and Modeling of Dimethyl Ether Synthesis from Synthesis Gas", *Chemical Engineering Science*, Vol. 54, pp. 3587-3592, 1999.

46. Stiefel, M., R. Ahmad, U. Arnold, M. Döring, "Direct Synthesis of Dimethyl Ether from Carbon-monoxide-rich Synthesis Gas: Influence of Dehydration Catalysts and Operating Conditions", *Fuel Processing Technology*, Vol. 92, pp.1466-1474, 2011.

47. Aguayo, A.T., J. Ereña, I. Sierra, M. Olazar, J. Bilbao, "Deactivation and Regeneration of Hybrid Catalysts in the Single-step Synthesis of Dimethyl Ether from Syngas and CO_2", *Catalysis Today*, Vol. 106, pp. 265-270, 2005.

48. Ereña, J., R. Garoña, J.M. Arandes, A.T. Aguayo, J. Bilbao, "Effect of Operating Conditions on the Synthesis of Dimethyl Ether over a CuO-ZnO-Al_2O_3/NaHZSM-5 Bifunctional Catalyst", *Catalysis Today*, Vol. 107-108, pp. 467-473, 2005.

49. Ereña, J., I. Sierra, M. Olazar, A.G. Gayubo, A.T. Aguayo, "Deactivation of a CuO-ZnO-Al_2O_3/ γ-Al_2O_3 Catalyst in the Synthesis of Dimethyl Ether", *Industrial and Engineering Chemistry Research*, Vol. 47, pp. 2238-2247, 2008.

50. Nie, R., H. Lei, S. Pan, L. Wang, J. Fei, Z. Hou, "Core–shell Structured CuO–ZnO@H-ZSM-5 Catalysts for CO Hydrogenation to Dimethyl Ether", *Fuel* , Vol. 96, pp. 419-425, 2012.

51. Khoshbin, R., M. Haghighia, "Direct Syngas to DME as a Clean Fuel: The Beneficial Use of Ultrasound for the Preparation of CuO–ZnO–Al_2O_3/HZSM-5 Nanocatalyst", *Chemical Engineering Research and Design*, Vol. 91, pp. 1111-1122, 2013.

52. Sierra, I., J. Ereña, A.T. Aguayo, J.M. Arandes, M. Olazar, J. Bilbao, "Co-feeding Water to Attenuate Deactivation of the Catalyst Metallic Function (CuO–ZnO–Al_2O_3) by Coke in the Direct Synthesis of Dimethyl Ether", *Applied Catalysis B: Environmental*, Vol. 106, pp. 167–173, 2011.

53. Mao, D., W. Yang, J. Xia, B. Zhang, Q. Song, Q. Chen, "Highly Effective Hybrid Catalyst for the Direct Synthesis of Dimethyl Ether from Syngas with Magnesium Oxide-modified HZSM-5 as a Dehydration Component", *Journal of Catalysis*, Vol. 230, pp. 140–149, 2005.

54. Naik, S.P., H. Du, H. Wan, V. Bui, J.D. Miller, W.W. Zmierczak, "Comparative Study of ZnO-CuO-Al_2O_3/SiO_2-Al_2O_3 Composite and Hybrid Catalysts for Direct Synthesis of Dimethyl Ether from Syngas", *Industrial and Engineering Chemistry Research*, Vol. 47, pp. 9791-9794, 2008.

55. Jiang, H., H. Bongard, W. Schmidt, F. Schüth, "One-pot Synthesis of Mesoporous Cu– γ-Al_2O_3 as Bifunctional Catalyst for Direct Dimethyl Ether Synthesis", *Microporous and Mesoporous Materials*, Vol. 164, pp. 3-8, 2012.

56. Song, F., Y. Tan, H. Xie, Q. Zhang, Y. Hana, "Direct Synthesis of Dimethyl Ether from Biomass-derived Syngas over Cu–ZnO–Al_2O_3–ZrO_2(x)/γ-Al_2O_3 Bifunctional Catalysts: Effect of Zr-loading", *Fuel Processing Technology*, Vol. 126, pp. 88-94, 2014.

57. Mao, D., J. Xia, Q. Chen, G. Lu, "Highly Effective Conversion of Syngas to Dimethyl Ether over the Hybrid Catalysts Containing High-silica HMCM-22 Zeolites", *Catalysis Communications*, Vol. 10, pp. 620-624, 2009.

58. Celik, G., A. Arinan, A. Bayat, H.O. Ozbelge, T. Dogu, D. Varisli, "Performance of Silicotungstic Acid Incorporated Mesoporous Catalyst in Direct Synthesis of Dimethyl Ether from Syngas in the Presence and Absence of CO_2", *Topics in Catalysis*, Vol. 56, pp. 1764-1774, 2013.

59. Yoğurtçu, B., *An Experimental Study on the Effect of Metal Loading on WGS Performance of Au-Re System*, M.S. Thesis, Boğaziçi University, 2012.

60. Akın, A. N., *Development of Coprecipitated Cobalt-Alumina Catalysts for the Production of C1-C4 Hydrocarbons by Carbon Monoxide Hydrogenation*, Ph. D. Dissertation, Boğaziçi University, 1996.

61. Doss, T.P., *Low Severity Fischer-Tropsch Synthesis for the Production of Synthetic Hydrocarbon Fuels*, Ph.D. Dissertation, Aston University, 2012.

62. Baltes, C., S. Vukojevi, F. Schüth, "Correlations between Synthesis, Precursor, and Catalyst Structure and Activity of a Large Set of CuO/ZnO/Al_2O_3 Catalysts for Methanol Synthesis", *Journal of Catalysis*, Vol. 258, pp. 334-344, 2008.

63. Schüth, F., M. Hesse, K.K. Unger, *Handbook of Heterogeneous Catalysis*, Wiley-VCH, Ruhr, Germany, pp. 100–119, 2008.

64. Ereña, J., J.M. Arandes, R. Garona, A.G. Gayubo, J. Bilbao, "Study of the Preparation and Composition of the Metallic Function for the Selective Hydrogenation of CO_2 to Gasoline Over Bifunctional Catalysts", *Journal of Chemical Technology and Biotechnology*, Vol. 78, pp. 161-166, 2003.

65. Ma, L., *Hydrogen Production from Steam Reforming of Light Hydrocarbons in an Autothermic System*, Ph.D. Dissertation, University of South Wales, 1995.

66. Selen, B., *Production of Hydrogen from Light Hydrocarbons via Indirect Partial Oxidation on Bimetallic Catalysts*, M.S. Thesis, Boğaziçi University, 2003.

67. Avci, A. K., *Computational and Experimental Investigation of Catalytic Hydrocarbon Fuel Processing for Autothermal Hydrogen Production*, Ph.D. Dissertation, Boğaziçi University, 2003.

68. Fitch, W.L., A.D Sauter, "Calculation of Relative Electron Impact Total Ionization Cross Section for Organic Molecules", *Analytical Chemistry*, Vol. 55, pp. 832-835, 1983.

69. Ertem, Ö., *Parametric Investigation of Water Gas Shift Over Pd Based Catalysts*, M.S. Thesis, Boğaziçi University, June 2014.

70. Chen, Z., H. Zhang, W. Ying, D. Fang, "Global Kinetics of Direct Dimethyl Ether Synthesis Process from Syngas in Slurry Reactor over a Novel Cu-Zn-Al-Zr Slurry Catalyst", *World Academy of Science, Engineering and Technology*, Vol. 4, pp. 08-23, 2010.

71. Hayer, F., H. Bakhtiary-Davijany, R. Myrstad, A. Holmen, P. Pfeifer, H.J. Venvik, "Synthesis of Dimethyl Ether from Syngas in a Microchannel Reactor-Simulation and Experimental Study", *Chemical Engineering Journal*, Vol. 167, pp. 610-615, 2011.

72. Abu-Dahrieh, J., D. Rooney, A. Goguet, Y. Saih, "Activity and Deactivation studies for Direct Dimethyl Ether Synthesis using CuO-ZnO-Al_2O_3 with NH_4ZSM-5, HZSM-5, or γ-Al_2O_3", *Chemical Engineering Journal,* Vol. 203, pp. 201-211, 2012.

73. Kozhevnikov, I.V., "Catalysis by Heteropoly Acids and Multicomponent Polyoxometalates in Liquid-Phase Reactions", *Chemical Reviews,* Vol. 98, pp. 171-198, 1998.

74. Ivanova, S., X. Nitsch, F. Romero-Sarria, B. Louis, M.A. Centeno, A.C. Roger, J.A. Odriozola, "New Class of Acid Catalysts for Methanol Dehydration", *10th International Symposium Scientific Bases for the Preparation of Heterogeneous Catalysts,* 2010.